CONTROL LAW SYNTHESIS FOR AUTOMATIC CONTROL OF THE DHC-2 "BEAVER", USING CLASSICAL METHODS OF DESIGN

SYMMETRIC MOTIONS

P. Lammertse

april 1985

SUMMARY

A survey has been made of practical control laws and simple, classical methods of control law synthesis using root locus analysis in reduced order models. For flight path angle and altitude control via the elevator, a comparison has been made between the usual θ-based solution and the use of direct feedback of measured flight path angle and normal acceleration, as found in some recent literature. For the autothrottle, the usual feedback of perturbations in speed has been compared with feedback of perturbations in total energy (potential and kinetic). The full order root loci used to check the reduced order analyses have been drawn by computer for five linearizations of a non-linear model of the DHC-2 "Beaver" aircraft, for varying speeds and centre of gravity positions.

CONTENTS

0. NOTATIONS AND DEFINITIONS

0.1 List of symbols

a_n	acceleration in negative Z-direction
$\underline{a}_i$	i-th column in $\underline{A}$
$\underline{b}_i$	i-th column in $\underline{B}$
A_x	specific force in positive X-direction
A_z	specific force in positive Z-direction
$\underline{A}$	system matrix
$\underline{B}$	input matrix
c	mean aerodynamic chord
$\underline{C}$	output matrix
$\underline{D}$	throughput matrix
e	perturbation in specific total energy
E	total energy
g	acceleration due to gravity
h	altitude
H_{ab}	transfer function from a to b
I_{xx}	aircraft moment of inertia
I_{yy}	aircraft moment of inertia
J_{xz}	aircraft inertia cross product
K_{ab}	feedback gain (negative feedback) of a on b
m	aircraft mass
m_a	derivative in abbreviated notation (see appendix A)
n	normal load factor
$\underline{N}$	transformation matrix
p_z	perturbation in inlet manifold pressure
$\underline{P}$	transformation matrix
$\underline{Q}$	transformation matrix
q	pitch rate
R	transformation matrix
s	complex frequency
u	perturbation in speed in X-direction
$\hat{u}$	u/V
$\underline{u}$	input vector
V	airspeed
w	perturbation in speed in Y-direction
x_a	derivative in abbreviated notation (see appendix A)
x_{cg}	distance of centre of gravity behind leading edge of wing
$\underline{x}$	state vector
z_a	derivative in abbreviated notation (see appendix A)
z_{cg}	distance of centre of gravity below wing chord

α (perturbation in) angle of attack
α_g gust angle of attack
γ (perturbation in) flight path angle
δ_e (change in) elevator angle, or equivalent input signal
δ_f flap angle
δ_{p_t} (change in) total head rise in propeller wake
δ_t (change in) throttle input signal
λ variable in characteristic equation
ρ air density
τ_i time constant for integration

subscripts and superscripts:

a dummy for subscript
b dummy for subscript
ss steady state solution to the short period approximation
* fully dimensional and in body axes
o reference condition

0.2 Frames of reference

In this report, two frames of reference have been used:

1. The "stability axes": an aircraft-fixed right-handed reference frame XYZ. The origin lies in the aircraft's centre of gravity, the positive X-axis lies in the plane of symmetry and points forward. In the undisturbed symmetric flight condition the X-axis coincides with the velocity vector of the centre of gravity relative to the undisturbed air. The positive Y-axis points to the right, the positive Z-axis points downward.

2. The aircraft "body axes", an aircraft-fixed right-handed reference frame $X^* Y^* Z^*$. This reference frame is identical to the XYZ reference-frame with the exception of the orientation of the X^*-axis, which lies along the fuselage reference-line.

The systems have their Y-axis in common. The relationship between their X- and Z-axes is illustrated in figure 0.1.

0.3 Specific forces

The specific force A is defined as the external force F acting on a body, divided by the mass of the body:

$$\bar{A} = \bar{F}/m \qquad (0.1)$$

where $\bar{A}$ and $\bar{F}$ are vectors.
The relation between the acceleration $\bar{a}$ of a body and the specific force $\bar{A}$ acting on the body in the gravitational field of the earth can be derived from the following relation:

$$m.\bar{a} = \bar{F} + \bar{W} \qquad (0.2)$$

and

$$\bar{a} = \bar{F}/m + \bar{g} \qquad (0.3)$$

where $\bar{W}$ is the weight vector. Substitution of $\bar{A}$ leads to:

$$\bar{a} = \bar{A} + \bar{g} \qquad (0.4)$$

Since "accelerometers" basically measure the extension of a spring attaching a mass to the airframe, they are really specific force meters that would measure zero force only in a free fall, with no aerodynamic forces present. In steady horizontal flight, it would be better to say that they measure the specific wing lift, than to say that they measure the "acceleration" due to gravity, since the first line of reasoning is extended far more easily to the dynamic case, and to coordinated turns.

1. INTRODUCTION

The current research project DVB (Digital Flight Control) at Delft Technical University is aimed at flying the laboratory aircraft, a DHC-2 "Beaver", under full digital control. Practical control laws are needed, both for stabilising the aircraft and for manoeuvering it, and these will initially be designed using classical methods.The present study looks into suitable structures and parameters, and especially into simple and straightforward methods of synthesis of such control laws for the symmetric motions of the aircraft. A companion study is available on the asymmetric motions (ref.1).

The classical method of root locus analysis in reduced order models has been used wherever possible, but all actual root loci have been computed in the full order system as an extra check on the validity of the approximations used. It might be supposed, that aircraft control law synthesis by these methods has by now matured to the point of being a trivial textbook exercise; this is not quite true, however. Recent developments in instrumentation and state reconstruction techniques have made in-flight information available on state variables such as flight path angle and angle of attack, with an accuracy and reliability that brings their actual feedback into the realm of possibilities. Recent literature indicates that the use of these state variables, e.g. by replacing the traditional θ-based control systems by systems based on feedback of γ or $\dot{h}$ has the potential of creating systems of simplified structure and improved performance (refs.5-7). Therefore, direct flight path angle control has been considered in this report, in order to investigate what advantages, if any, could be gained if the associated problems of accuracy and robustness of the measurements and state reconstruction techniques can be satisfactorily solved.

2. MODELS AND FLIGHT CONDITIONS USED

2.1 Linearizing the basic non-linear model

The numerical values for the models used in this report have been obtained by linearizing, for a number of flight conditions, a non-linear model of the DHC-2 "Beaver" aircraft. Two versions of this non-linear model, a 1968 version and a 1982 version, are contained in the program package "CASPAR", developed by the Delft Disciplinary Group for Aircraft Stability and Control. A third, updated version may be available in the near future. The 1982 version has been used throughout, unless specifically noted otherwise.

The five linearizations were all for horizontal flight at an altitude of 1800 metres in standard atmosphere, and near maximum weight. Three of these were for flight at an average c.g. position (default c.g. in CASPAR), with speeds of 35 m/s (near minimum airspeed), 50 m/s and 80 m/s (near maximum permissible airspeed). The remaining two were for 50 m/s, with the c.g. at the forward and aft limits, respectively. More details are given in table 2.1, and with each model in tables 2.2 (a) through (e).

On linearizing the model with the CASPAR option LINMAIN, horizontal flight has to be achieved by a trial and error procedure for the power setting. At the 80 m/s speed, a slightly descending flight could not be avoided despite maximum power setting.

The models obtained are formulated in "body axes" (cf. paragraph 0.2), and fully dimensional; the state vector is $(u\ w\ \theta\ q)^T$. This state vector, and the system matrices associated with it, are distinguished by an asterisk to avoid confusion with the more usual non-dimensional state in stability axes, which will be used in the rest of this report, after transforming the present models in the next paragraph.

2.2 Transformation to non-dimensional state in stability axes

Body axes are less convenient to work with in control system design work than stability axes, since the physically important variables such as changes in airspeed and in angle of attack are state variables only in stability axes. In body axes they are linear combinations of state variables, creating extra terms in the system matrix and in feedback schemes.

We will therefore transform the models to stability axes, making the state vector non-dimensional in the process, but keeping the dimension of time. From the description of the frames of reference in 0.2 it is obvious, that the perturbations in θ and q are identical in both body axes and stability axes. Figure 2.1, on the other hand, illustrates the angular transformation needed for the speed perturbations u and w. Adding scaling factors to non-dimensionalize the state vector produces a linear transformation for state vector and system matrices of the form:

$$\dot{\underline{x}} = \underline{T}.\underline{x}^{*} \qquad (2.1)$$

where $\underline{x}^{*} = (u\ w\ \theta\ q)$ in body axes

$\underline{x} = (\hat{u}\ \alpha\ \theta\ qc/V)$ in stability axes

$$T = \begin{pmatrix} \cos\alpha_o/V & \sin\alpha_o/V & 0 & 0 \\ \sin\alpha_o/V & \cos\alpha_o/V & 0 & 0 \\ 0 & 0 & 1 & 0 \\ 0 & 0 & 0 & \bar{c}/V \end{pmatrix} \qquad T^{-1} = \begin{pmatrix} V.\cos\alpha_o & -V.\sin\alpha_o & 0 & 0 \\ V.\sin\alpha_o & V.\cos\alpha_o & 0 & 0 \\ 0 & 0 & 1 & 0 \\ 0 & 0 & 1 & V/\bar{c} \end{pmatrix}$$

The transformation of the system matrices is easily derived:

$\dot{\underline{x}}^{*} = \underline{A}^{*}.\underline{x}^{*} + \underline{B}^{*}.\underline{u}$ in body axes

$\dot{\underline{x}}^{*} = \underline{A}^{*}.\underline{T}^{-1}.\underline{x} + \underline{B}^{*}.\underline{u}$

$\dot{\underline{x}} = \underline{T}.\dot{\underline{x}}^{*} = \underline{T}.\underline{A}^{*}.\underline{T}^{-1}.\underline{x} + \underline{T}.\underline{B}^{*}.\underline{u}$ (2.2)

$\dot{\underline{x}} = \underline{A}.\underline{x} + \underline{B}.\underline{u}$ in stability axes

$\underline{A} = \underline{T}.\underline{A}^{*}.\underline{T}^{-1} \qquad \underline{B} = \underline{T}.\underline{B}^{*}$

The resulting system description is identical to the format used in ref.2, and we will use the same notation for the elements of the matrices $\underline{A}$ and $\underline{B}$ (the symbols are expressed in non-dimensional stability derivatives in appendix A):

$$\begin{pmatrix} \dot{\hat{u}} \\ \dot{\alpha} \\ \dot{\theta} \\ \dot{q}\bar{c}/V \end{pmatrix} = \begin{pmatrix} x_u & x_\alpha & x_\theta & x_q \\ z_u & z_\alpha & z_\theta & z_q \\ 0 & 0 & 0 & V/\bar{c} \\ m_u & m_\alpha & m_\theta & m_q \end{pmatrix} \begin{pmatrix} \hat{u} \\ \alpha \\ \theta \\ q\bar{c}/V \end{pmatrix} + \begin{pmatrix} 0 & x_{\delta t} \\ z_{\delta e} & z_{\delta t} \\ 0 & 0 \\ m_{\delta e} & m_{\delta t} \end{pmatrix} \begin{pmatrix} \delta_e \\ \delta_t \end{pmatrix} \qquad (2.3)$$

The term by term transformation of the nonzero elements of $\underline{A}$ and $\underline{B}$ is given in table 2.4. The resulting numerical models are given in tables 2.5 (a) through (e). From the transformations, an $x_{\delta e}$ arises which will be neglected in the reduced order analysis, but which is implicitly present in the full order root loci, because these have been computed in the original CASPAR format, with the state in stability axes defined as an output (cf.appendix B for examples of CASPAR data sets).

output transformation for specific forces

The CASPAR linearization procedure LINMAIN also produces an output matrix for the specific forces in body axes:

$$\begin{pmatrix} A_x^* \\ A_z^* \end{pmatrix} = \underline{C}^* . \underline{x}^* + \underline{D}^* \underline{u}$$

This can be transformed to stability axes and non-dimensional form using the same angular transformation, which we shall call $\underline{N}$, given in figure 2.1 for u and w. This yields:

$$\begin{pmatrix} A_x/g \\ A_z/g \end{pmatrix} = \frac{1}{g}.\underline{N} \begin{pmatrix} A_x^* \\ A_z^* \end{pmatrix} = \frac{1}{g}.\underline{N}.\underline{C}^* .\underline{I}^{-1}.\underline{x} + \frac{1}{g}.\underline{N}.\underline{D}^* .\underline{u} \qquad (2.4)$$

The results have been added to tables 2.5. They can be used as a partial numerical check on the transformations, since they can also be found directly from the two top rows of the system matrix. By following the derivation from the Euler equations in refs.2 and 3, it can be seen that (if there is no aerodynamic force due to $\dot{\alpha}$, which seems to be the case here) this requires subtracting the geometrical component $V/\bar{c}$ from z_q, eliminating the gravity components x_θ and z_θ, and multiplying by V/g:

$$\begin{pmatrix} A_x/g \\ A_z/g \end{pmatrix} = V/g \cdot \begin{pmatrix} x_u & x_\alpha & 0 & x_q \\ z_u & z_\alpha & 0 & z_q - V/\bar{c} \end{pmatrix} \begin{pmatrix} \hat{u} \\ \alpha \\ \theta \\ q\bar{c}/V \end{pmatrix} \qquad (2.5)$$

2.3 Using γ instead of θ as a state variable

It will sometimes be convenient to have the flight path angle as a state variable, instead of the pitch attitude θ. This can be arranged by a simple transformation $\underline{Q}$ similar to the one in the previous paragraph:

$$(\hat{u}\ \gamma\ \alpha\ q\bar{c}/V)^T = \underline{Q}.(\hat{u}\ \alpha\ \theta\ q\bar{c}/V)^T \qquad (2.6)$$

where

$$\underline{Q} = \begin{pmatrix} 1 & 0 & 0 & 0 \\ 0 & -1 & 1 & 0 \\ 0 & 1 & 0 & 0 \\ 0 & 0 & 0 & 1 \end{pmatrix} \qquad \underline{Q}^{-1} = \begin{pmatrix} 1 & 0 & 0 & 0 \\ 0 & 0 & 1 & 0 \\ 0 & 1 & 1 & 0 \\ 0 & 0 & 0 & 1 \end{pmatrix}$$

The transformation yields (for horizontal flight, with $z_\theta = 0$):

$$\begin{pmatrix} \dot{\hat{u}} \\ \dot{\gamma} \\ \dot{\alpha} \\ \dot{q}\bar{c}/V \end{pmatrix} = \begin{pmatrix} x_u & x_\theta & x_\alpha + x_\theta & x_q \\ -z_u & 0 & -z_\alpha & -z_q + V/\bar{c} \\ z_u & 0 & z_\alpha & z_q \\ m_u & 0 & m_\alpha & m_q \end{pmatrix} \begin{pmatrix} \hat{u} \\ \gamma \\ \alpha \\ q\bar{c}/V \end{pmatrix} + \begin{pmatrix} 0 & x_{\delta t} \\ -z_{\delta e} & -z_{\delta t} \\ z_{\delta e} & z_{\delta t} \\ m_{\delta e} & m_{\delta t} \end{pmatrix} \begin{pmatrix} \delta_e \\ \delta_t \end{pmatrix} \qquad (2.7)$$

The reason why γ and α have been rearranged will become obvious in the next paragraph. For easier comparison, the more usual θ-based system is also repeated below in rearranged form:

$$\begin{pmatrix} \dot{\hat{u}} \\ \dot{\theta} \\ \dot{\alpha} \\ \dot{q}\bar{c}/V \end{pmatrix} = \begin{pmatrix} x_u & x_\theta & x_\alpha & x_q \\ 0 & 0 & 0 & V/\bar{c} \\ z_u & 0 & z_\alpha & z_q \\ m_u & 0 & m_\alpha & m_q \end{pmatrix} \begin{pmatrix} \hat{u} \\ \gamma \\ \alpha \\ q\bar{c}/V \end{pmatrix} + \begin{pmatrix} 0 & x_{\delta t} \\ 0 & 0 \\ z_{\delta e} & z_{\delta t} \\ m_{\delta e} & m_{\delta t} \end{pmatrix} \begin{pmatrix} \delta_e \\ \delta_t \end{pmatrix} \qquad (2.8)$$

PL 2025 Shouldn't the second state be θ here ?

2.4 Reduced order models

It has been customary in control system design to use reduced order models extensively, for both conceptual and computational reasons. The computational advantage has lost most of its importance with the advent of widespread digital computing, but the reduced order model still has great value as a conceptual tool.

The basic model for most control system design work is the so-called short period approximation, based mainly on the assumption of constant speed and horizontal flight, either as a reference condition or also including perturbations (in which case $\theta = \alpha$). These approximations produce a second order model in α and $q\bar{c}/V$. The model can be augmented by the equations $\dot{\theta} = q$ and $\dot{h} = \theta - \alpha$. If velocity control is assumed, either manual or automatic, this analysis of flight path control may be perfectly valid, and it will be used in part of this report. A short derivation will be given.

The phugoid mode, however can never be represented by such a system description. A reduced order model for the phugoid is also available. This so-called phugoid approximation is usually based on the assumptions that $\dot{q} = 0$ and $\alpha = 0$. This leads to a second order model in $\hat{u}$ and θ. This approximation predicts the phugoid period and damping satisfactorily, but due to the deletion of the moment equation the elevator effectiveness is not adequately modelled. For this reason the model is not used for control applications.

A more refined version of the phugoid model is based on the assumptions that $\dot{q} = 0$ and $\dot{\alpha} = 0$, but does not require that α be zero; roughly, the inertia terms in the Z- and moment equations are neglected, but the equations as such are maintained. This method is applied in ref.3 to a system matrix for the state vector $(\hat{u}\ \alpha\ \theta\ q\bar{c}/V)^T$. A slightly different result will be obtained here by applying the method to the system matrix for the state vector $(\hat{u}\ \gamma\ \alpha\ q\bar{c}/V)^T$. The difference between the two methods is discussed in appendix A. A derivation for the latter method and the short period approximation will now be given.

(a) the short period approximation

The short period approximation is based on the assumption that $\hat{u} = 0$. This means, that in horizontal flight ,where $z_\theta = 0$ and $m_\theta = 0$ (as in systems (2.7) and (2.8)), there is no longer any influence of $\hat{u}$, γ or θ on the last two rows of the rearranged system matrix. These now form a reduced order model:

$$\begin{pmatrix} \dot{\alpha} \\ \dot{q}\bar{c}/V \end{pmatrix} = \begin{pmatrix} z_\alpha & z_q \\ m_\alpha & m_q \end{pmatrix} \begin{pmatrix} \alpha \\ q\bar{c}/V \end{pmatrix} + \begin{pmatrix} z_{\delta e} & z_{\delta t} \\ m_{\delta e} & m_{\delta t} \end{pmatrix} \begin{pmatrix} \delta_e \\ \delta_t \end{pmatrix} \qquad (2.9)$$

with characteristic equation:

$$\lambda^2 + \lambda(- z_\alpha - m_q) + (z_\alpha m_q - m_\alpha z_q) = 0$$

We will return to the steady state solution of this reduced order system when discussing the phugoid approximation. A further simplification can be achieved by also assuming the flight path in the short period oscillation to be a straight line, making $\gamma = 0$ and $\theta = \alpha$. Since $\theta' = q$, this would also make $\dot{\alpha} = q = (V/\bar{c}).q\bar{c}/V$. Dropping the Z-equation in favour of this new equation, we have:

$$\begin{pmatrix} \dot{\alpha} \\ \dot{q}\bar{c}/V \end{pmatrix} = \begin{pmatrix} 0 & V/\bar{c} \\ m_\alpha & m_q \end{pmatrix} \begin{pmatrix} \alpha \\ q\bar{c}/V \end{pmatrix} + \begin{pmatrix} 0 & 0 \\ m_{\delta e} & m_{\delta t} \end{pmatrix} \begin{pmatrix} \delta_e \\ \delta_t \end{pmatrix} \qquad (2.10)$$

Even this much simplified model gives results that are essentially correct, though not always very accurate. It amounts to setting $z_q = V/\bar{c}$, which is reasonable, and $z_\alpha = 0$, which is a definite simplification. The characteristic equation is:

$$\lambda^2 - \lambda \, . \, m_q - m_\alpha . V/\bar{c} = 0$$

(b) the phugoid approximation

The simple phugoid approximation is based on the assumptions, that in the phugoid mode $\alpha = 0$, and also that x_q and $V/\bar{c}-z_q$ are negligible. Under these conditions the two top rows of the γ-based system (2.7) are no longer influenced by α and $q\bar{c}/V$, and form a reduced order model:

$$\begin{pmatrix} \dot{\hat{u}} \\ \dot{\gamma} \end{pmatrix} = \begin{pmatrix} x_u & x_\theta \\ -z_u & 0 \end{pmatrix} \begin{pmatrix} \hat{u} \\ \gamma \end{pmatrix} + \begin{pmatrix} 0 & x_{\delta e} \\ -z_{\delta e} & -z_{\delta t} \end{pmatrix} \begin{pmatrix} \delta e \\ \delta t \end{pmatrix} \qquad (2.11)$$

with characteristic equation:

$$\lambda^2 - \lambda \cdot x_u + x_\theta z_u = 0$$

The more usual θ-based formulation gives a somewhat less elegant derivation. Arbitrarily neglecting the moment equation in the fourth row of (2.8), we have from the third row with $\alpha = 0$ and $\dot{\alpha} = 0$:

$$z_u.\hat{u} + z_q.q\bar{c}/V + z_{\delta e}.\delta e + z_{\delta t}.\delta t = 0 \longrightarrow$$

$$q\bar{c}/V = -\frac{z_u}{z_q}.\hat{u} - \frac{z_{\delta e}}{z_q}\delta e - \frac{z_{\delta t}}{z_q}.\delta t \qquad (2.12)$$

Assuming once again that $x_q = 0$ and $z_q = V/\bar{c}$, this reduces the two top rows of the rearranged system (2.8) to:

$$\begin{pmatrix} \dot{\hat{u}} \\ \dot{\theta} \end{pmatrix} = \begin{pmatrix} x_u & x_\theta \\ -z_u & 0 \end{pmatrix} \begin{pmatrix} \hat{u} \\ \gamma \end{pmatrix} + \begin{pmatrix} 0 & x_{\delta e} \\ -z_{\delta e} & -z_{\delta t} \end{pmatrix} \begin{pmatrix} \delta e \\ \delta t \end{pmatrix} \qquad (2.13)$$

The result is identical to (2.11), as it should be, since $\gamma = \theta$ under the assumption used that $\alpha = 0$. This simple approximation predicts the period and damping of the phugoid quite well, but due to neglecting the change in α caused by elevator deflection, the elevator effectiveness in this model is completely erroneous, even to the point of having the wrong sign.

A second, more refined version of the phugoid approximation does not require that $\alpha = 0$. Instead, the (mainly inertia) terms in $\dot{\alpha}$ and $\dot{q}$ are neglected, giving in the two last rows of the rearranged system matrix what can be considered as the steady state solution of the short period oscillation:

$$\begin{pmatrix} \dot{\hat{u}} \\ \dot{\gamma} \\ 0 \\ 0 \end{pmatrix} = \begin{pmatrix} x_u & x_\theta & x_\alpha + x_\theta & x_q \\ -z_u & 0 & -z_\alpha & V/\bar{c} - z_q \\ z_u & 0 & z_\alpha & z_q \\ m_u & 0 & m_\alpha & m_q \end{pmatrix} \begin{pmatrix} \hat{u} \\ \gamma \\ \alpha \\ q\bar{c}/V \end{pmatrix} + \begin{pmatrix} 0 & x_{\delta t} \\ -z_{\delta e} & -z_{\delta t} \\ z_{\delta e} & z_{\delta t} \\ m_{\delta e} & m_{\delta t} \end{pmatrix} \begin{pmatrix} \delta e \\ \delta t \end{pmatrix} \qquad (2.14)$$

The right hand side of the third equation, being equal to zero, can be added to the second, to yield:

$$\begin{pmatrix} \dot{\hat{u}} \\ \dot{\gamma} \\ 0 \\ 0 \end{pmatrix} = \begin{pmatrix} x_u & x_\theta & x_\alpha + x_\theta & x_q \\ 0 & 0 & & V/\bar{c} \\ z_u & 0 & z_\alpha & z_q \\ m_u & 0 & m_\alpha & m_q \end{pmatrix} \begin{pmatrix} \hat{u} \\ \gamma \\ \alpha \\ q\bar{c}/V \end{pmatrix} + \begin{pmatrix} 0 & x_{\delta t} \\ 0 & 0 \\ z_{\delta e} & z_{\delta t} \\ m_{\delta e} & m_{\delta t} \end{pmatrix} \begin{pmatrix} \delta e \\ \delta t \end{pmatrix} \qquad (2.15)$$

From the two final rows, steady state solutions tot the short period oscillation can be found by the usual methods of solving linear equations:

$$H_{\alpha uss} = \frac{-z_u m_q + m_u z_q}{z_\alpha m_q - m_\alpha z_q}$$

$$H_{quss} = \frac{z_u m_\alpha - m_u z_\alpha}{z_\alpha m_q - m_\alpha z_q} \qquad (2.16)$$

$$H_{\alpha\delta ess} = \frac{-z_{\delta e} m_q + m_{\delta e} z_q}{z_\alpha m_q - m_a z_q}$$

$$H_{q\delta ess} = \frac{z_{\delta e} m_\alpha - m_{\delta e} z_\alpha}{z_\alpha m_q - m_\alpha z_q} \qquad (2.17)$$

The steady state elevator effectivess (2.17) is identical to that found in ref.2 for the short period approximation. Some idea of the numerical values involved can be gained from table 2.6 , giving the results of substituting the numerical values of the models used in this report.

The value of $H_{q\delta ess}$ is closely related to the elevator angle per "g". In horizontal flight, we have with (2.15) and neglecting z_u:

$$a_n = \dot{h}' = V.\dot{\gamma}$$

$$\frac{\dot{\gamma}}{\delta e} = \frac{(V/\bar{c}).q\bar{c}/V}{\delta e} = (V/\bar{c}).H_{q\delta ess} \qquad (2.18)$$

It follows, that the steady state solution to the short period approximation transfer function of elevator angle to normal acceleration is:

$$H_{a_n\delta ess} = (V^2/\bar{c}).H_{q\delta ess} \qquad (2.19)$$

When divided by g, $H_{a_n\delta ess}$ is the inverse of the elevator angle per "g", $d\delta e/dn$, in a symmetrical pull-up manoeuvre at the point of horizontal flight. The centripetal force in this q-motion is of course supplied almost exclusively by a steady perturbation in angle of attack. For $z_{\delta e} = 0$ and $z_q \sim V/\bar{c}$ (i.e., no direct aerodynamic lift effect due to q itself), we have from (2.17) and (2.19):

$$\frac{H_{a_n\delta ess}}{H_{\alpha\delta ess}} = -V^2/\bar{c}.\frac{z_\alpha}{z_q} = -V.z_\alpha \qquad (2.20)$$

Although the effect of $q\bar{c}/V$ on the total lift is relatively small in conventional aircraft, the same is not true of the moment equation, and the term $z_\alpha m_q$ cannot be neglected in the denominators of (2.17)

Substituting (2.16) into the two top rows of (2.14) and neglecting $z_{\delta t}$ and $m_{\delta t}$ for the moment yields:

$$\begin{pmatrix} \hat{u}' \\ \dot{\gamma} \end{pmatrix} = \begin{pmatrix} x_u + H_{\alpha uss}.(x_\theta + x_\alpha) + H_{\alpha uss}.x_q & x_\theta \\ H_{quss}.V/\bar{c} & 0 \end{pmatrix} \begin{pmatrix} \hat{u} \\ \gamma \end{pmatrix} +$$

$$+ \begin{pmatrix} H_{\alpha\delta ess}.(x_\alpha + x_\theta) + H_{q\delta ess}.x_q & x_{\delta t} \\ H_{q\delta ess}.V/\bar{c} & 0 \end{pmatrix} . \begin{pmatrix} \delta e \\ \delta t \end{pmatrix} \qquad (2.21)$$

Neglecting x_q, the characteristic equation is:

$$\lambda^2.(z_\alpha m_q - m_\alpha z_q) + \lambda.(-x_u(z_\alpha m_q - m_\alpha z_q) - (x_\alpha + x_\theta)(-z_u m_q + m_u z_q)) - (x_\theta.V/\bar{c}.(z_u m_\alpha - m_u z_\alpha) = 0$$

By inspection, this equation reduces to (2.1) for $z_q = V/\bar{c}$ and $m_\alpha \longrightarrow \infty$. It should be noted, that this characteristic equation is not quite equivalent tot the one sometimes derived from a θ-based system (ref.3). The difference is, that we have $(x_\alpha + x_\theta)$, which partly cancel, instead of x_α only, in two places. The two methods are compared in appendix A.

A third phugoid model of intermediate complexity results by setting not only $\dot{q} = 0$ and $\dot{\alpha} = 0$ in the short period, but also neglecting the influence of speed in the short period approximation, effectively cancelling z_u and m_u from the two bottom rows of (2.14). Once again adding the right hand side of the third row, which equals zero, to the second row, we now find:

$$\begin{pmatrix} \dot{\hat{u}} \\ \dot{\gamma} \\ 0 \\ 0 \end{pmatrix} = \begin{pmatrix} x_u & x_\theta & x_\alpha + x_\theta & x_q \\ -z_u & 0 & & V/\bar{c} \\ 0 & 0 & z_\alpha & z_q \\ 0 & 0 & m_\alpha & m_q \end{pmatrix} \begin{pmatrix} \hat{u} \\ \gamma \\ \alpha \\ q\bar{c}/V \end{pmatrix} + \begin{pmatrix} 0 & x_{\delta t} \\ 0 & 0 \\ z_{\delta e} & z_{\delta t} \\ m_{\delta e} & m_{\delta t} \end{pmatrix} \begin{pmatrix} \delta e \\ \delta t \end{pmatrix} \qquad (2.22)$$

This intermediate version of the phugoid approximation combines the characteristic equation of the simple approximation (2.11) with the elevator effectiveness (2.17) of the refined model, to give:

$$\begin{pmatrix} \dot{\hat{u}} \\ \dot{\gamma} \end{pmatrix} = \begin{pmatrix} x_u & x_\theta \\ -z_u & 0 \end{pmatrix} \begin{pmatrix} \hat{u} \\ \gamma \end{pmatrix} + \begin{pmatrix} H_{\alpha\delta ess}.(x_\alpha + x_\theta) + H_{q\delta ess}.x_q & x_{\delta t} \\ H_{q\delta ess}.V/\bar{c} & 0 \end{pmatrix} \begin{pmatrix} \delta e \\ \delta t \end{pmatrix}$$

(2.23)

(c) the extended short period approximation

If speed control is assumed, either manual or automatic, it is customary in control system design work to assume that speed no longer influences the rest of the system. This reduces equations (2.24) to:

$$\dot{\gamma} = H_{q\delta ess} . (V/\bar{c}) . \delta e = (H_{a_n \delta ess}/V) . \delta_e \qquad (2.25)$$

In this case, there is no longer any difference between derivation in a θ-based or in a γ-based system; this is simply the short period approximation extended with the equation $\dot{h} = V.\gamma$.

3.1 FEEDBACK OF THE PITCH ATTITUDE

3. Phugoid damping

On most aircraft the phugoid mode has low damping, and the DHC-2 "Beaver" aircraft is no exception. Providing adequate damping for all modes of the aircraft can be considered as the most basic task of an automatic control system. The classical solution is, to use feedback of the pitch attitude θ on the elevator. We will be using the notation $K_{\theta\delta e}$ for the feedback gain, with the usual sign convention:

$$\delta e = -K_{\theta\delta e}.\theta \qquad (3.1)$$

This will make $K_{\theta\delta e}$ a negative number in all practical applications. Full order root loci are given in figure 3.1 (a) through (e) for a number of flight conditions. As might be expected, θ feedback affects both the short period mode and the phugoid mode. For modest feedback gains, it appears that the phugoid mode can be adequately damped without unduly increasing the frequency of the short period oscillation; with the exception perhaps of flight at the slowest speed examined, of 35 m/s. The feedback gains needed for a given damping of the phugoid, however vary considerably with c.g. position.

With larger feedback gains, the short period oscillation is visibly affected, and the phugoid mode degenerates into two separate modes, represented by two zeroes on the negative real axis, again with the exception of the slowest speed examined, where the zeroes form a complex pair. The location of the zeroes does not vary much with the c.g. position. Somewhat unexpectedly, the feedback gains needed for a given relative damping vary widely with speed. Even making the gains proportional to $1/V^2$ still gives relatively much more damping at higher speeds. We will try and explain in the next few paragraphs some of the facts observed here in the full order computations, using the reduced order models given in chapter 2.

The actual choice of a feedback gain will depend on the criteria to be met. If phugoid damping only is required, very modest feedback gains could be used, of the order indicated in the full order root loci of figures 3.1. If stiffness against external disturbances is required, then these will have to be studied separately. If a specific dynamic response is required when manoeuvering through the automatic control system (control wheel steering), then there is a choice between tailoring the actual response of the degenerated phugoid poles to this requirement, or of adding compensation (a prefilter) in the transfer function from the controller to the elevator channel.

3.2 The short period approximation

(a) pitch attitude feedback

We will consider the use of θ feedback in a constant speed reduced order model of the form (2.9). We will limit ourselves to the case of horizontal flight, making $z_\theta = 0$ and $m_\theta = 0$. The reduced order model (2.9) can be thought of as derived from the θ-based full order system description (2.8); in this case we will have to require that $\theta = \alpha$, or $\gamma = 0$ in order to bring $K_{\theta\delta e}$ into the reduced order system. Alternatively, the feedback of θ can be seen as simultaneous feedback of γ and α on elevator, both with gain $K_{\theta\delta e}$, in the γ-based system description. In this case, the condition that the perturbation in γ be zero is not needed. The system equations are:

$$\begin{pmatrix} \dot{\alpha} \\ \dot{q}\bar{c}/V \end{pmatrix} = \begin{pmatrix} z_\alpha - K_{\theta\delta e}.z_{\delta e} & z_q \\ m_\alpha - K_{\theta\delta e}.m_{\delta e} & m_q \end{pmatrix} \begin{pmatrix} \alpha \\ q\bar{c}/V \end{pmatrix} + \begin{pmatrix} z_{\delta e} & z_{\delta t} \\ m_{\delta e} & m_{\delta t} \end{pmatrix} \begin{pmatrix} \delta_e \\ \delta_t \end{pmatrix} \tag{3.2}$$

with characteristic equation:

$$\lambda^2 + \lambda.(-m_q - z_\alpha + K_{\theta\delta e}.z_\delta) + (m_q.(z_\alpha - K_{\theta\delta e}.z_{\delta e}) - z_q.(m_\alpha - K_{\theta\delta e}.m_{\delta e}))$$

The input can no longer be considered as an elevator angle a such, but rather as an input signal to be added tot the feedback signal.

Since the practical influence of $z_{\delta e}$ is small relative to that of $m_{\delta e}$, there is relatively not much influence on the trace of the matrix and hence on the sum of the eigenvalues. The main effect on the short period, and this is confirmed by the full order root loci in figure 3.1, is an increase in frequency. There is, however a small but not unimportant decrease in damping. It can be seen from equations (2.3) or (2.8), that bringing θ feedback into the system matrix does not alter the trace of the full order matrix, hence the sum of the eigenvalues. The decrease in damping of the short period therefore means, that this damping is transferred to the phugoid mode.

(b) pitch rate feedback

If there is insufficient damping in the short period mode, the natural solution is to add feedback of $q\bar{c}/V$. In keeping with the notation of ref.2, the feedback gain will be defined relative to q, not $q\bar{c}/V$:

$$\delta_e = - K_{q\delta e}.q = -K_{q\delta e}.(V/\bar{c}).q\bar{c}/V$$

The main effect of this feedback falls on the diagonal of the system matrix both in the full order model and in the short period approximation. This makes it ideally suited for adding damping to the system. In the short period approximation, the system becomes:

$$\begin{pmatrix} \dot{\alpha} \\ \dot{q}\bar{c}/V \end{pmatrix} = \begin{pmatrix} z_\alpha - K_{\theta\delta e}.z_{\delta e} & z_q - K_{q\delta e}.V/\bar{c}.z_{\delta e} \\ m_\alpha - K_{\theta\delta e}.m_{\delta e} & m_q - K_{q\delta e}.V/\bar{c}.m_{\delta e} \end{pmatrix} \begin{pmatrix} \alpha \\ q\bar{c}/V \end{pmatrix} + \begin{pmatrix} z_{\delta e} & z_{\delta t} \\ m_{\delta e} & m_{\delta t} \end{pmatrix} \begin{pmatrix} \delta_e \\ \delta_t \end{pmatrix} \qquad (3.3)$$

with characteristic equation:

$$\lambda^2 + \lambda.(-z_\alpha - m_q + K_{\theta\delta e}.z_{\delta e} + K_{q\delta e}.(V/\bar{c}).m_{\delta e}) + ((m_q - K_{q\delta e}.(V/\bar{c}).m_{\delta e}).(z_\alpha - K_{\theta\delta e}.z_{\delta e}) - z_q - K_{q\delta e}.(V/\bar{c}).m_{\delta e}).(m_\alpha - K_{\theta\delta e}.m_\delta)) = 0$$

In the straight-line flight approximation of (2.10), where $z_{\delta e} = 0$, $z_\alpha = 0$ and $z_q = V/\bar{c}$, this reduces to:

$$\lambda^2 + \lambda.(-m_q + K_{q\delta e}.(V/\bar{c}).m_{\delta e}) + (V/\bar{c}).(-m_\alpha + K_{\theta\delta e}.m_{\delta e}) = 0 \qquad (3.4)$$

Using this approximation, the feedback gain $K_{q\delta e}$ to produce a relative damping of $\zeta = 0.7$ in the full order root loci of figure 3.2 can be predicted to within $\pm 10\%$.

(c) steady state solution of the short period approximation

The steady state elevator effectiveness of equations (2.17) is modified when using feedback of θ and $q\bar{c}/V$, because all of the derivatives involved (except $z_{\delta e}$ and $m_{\dot{\delta e}}$) are effectively changed by the feedback, as can be seen in (3.3). Neglecting $z_{\delta e}$, we have:

$$H_{\alpha\delta ess} = \frac{m_{\delta e} z_q}{z_\alpha.(m_q - K_{q\delta e}.(V/\bar{c}).m_{\dot{\delta e}}) - z_q.(m_\alpha - K_{\theta\delta e}.m_{\dot{\delta e}})}$$

$$H_{q\delta ess} = \frac{-m_{\delta e} z_\alpha}{z_\alpha.(m_q - K_{q\delta e}.(V/\bar{c}).m_{\dot{\delta e}}) - z_q.(m_\alpha - K_{\theta\delta e}.m_{\dot{\delta e}})} \qquad (3.5)$$

It is useful to note, that the following approximations hold for extremely large $K_{\theta\delta e}$ and $z_{\delta e} m_q << m_{\delta e} z_q$:

$$H_{\alpha\delta ess} \longrightarrow \frac{1}{K_{\theta\delta e}}$$

$$H_{q\delta ess} \longrightarrow -\frac{z_\alpha}{z_q} \cdot \frac{1}{K_{\theta\delta e}} \qquad (3.6)$$

3.3 The phugoid approximation

The effect of θ feedback on the phugoid can be discussed in the reduced order model (2.23), using the elevator effectiveness (3.5). Neglecting x_q, we have:

$$\begin{pmatrix} \dot{\hat{u}} \\ \dot{\gamma} \end{pmatrix} = \begin{pmatrix} x_u & x_\theta - K_{\theta\delta e}.H_{\alpha\delta ess}.(x_\alpha + x_\theta) \\ -z_u & -K_{\theta\delta e}.H_{q\delta ess}.V/\bar{c} \end{pmatrix} \begin{pmatrix} \hat{u} \\ \gamma \end{pmatrix} \qquad (3.7)$$

with characteristic equation:

$$\lambda^2 + \lambda.(-x_u + K_{\theta\delta e}.H_{q\delta ess}.V/\bar{c}) + (x_\theta z_u + K_{\theta\delta e}.(-x_u.H_{q\delta ess}.V/\bar{c} - z_u.H_{\alpha\delta ess}.(x_\alpha + x_\theta)) = 0$$

From these equations, a number of conclusions can be drawn.

- for modest feedback gain $K_{\theta\delta e}$, the influence of $K_{\theta\delta e}$ on the "stiffness" of the short period mode will be small, according to equations (3.5). The effect on the phugoid mode will then be almost the same for feedback of θ as for feedback of the flight path angle γ.

- for larger values of $K_{\theta\delta e}$, the stiffness in the short period oscillation will be increased noticeably. This makes itself felt in the phugoid as a reduced effectiveness of the elevator feedback in (3.7), compared to feedback of γ alone.

- for extremely large values of $K_{\theta\delta e}$, the phugoid poles converge to zeroes which can be found directly from the full order calculation. These zeroes can be approximated by making $K_{\theta\delta e} \longrightarrow -\infty$, using the limits for the elevator effectiveness as given in (3.6), and setting $z_q = V/\bar{c}$ in the characteristic equation of (3.7), to find:

$$\lambda^2 + \lambda.(-x_u - z_\alpha) + (x_u z_\alpha - z_u x_\alpha) = 0 \qquad (3.8)$$

This is the same result obtained in the full order derivation of ref.2, for $K_{\theta\delta e} \longrightarrow -\infty$ and $z_{\delta e} = 0$. Since $(x_u z_\alpha - z_u x_\alpha)$ is much smaller than $(-x_u - z_\alpha)$, two zeroes should be found, one near $-(-x_u - z_\alpha)$, which in practice means near z_α, and the other near the origin. These zeroes can be seen in the full order root loci in figures 3.1, for 50 m/s and 80 m/s; but they unexpectedly form a complex pair at 35 m/s. No explanation for this departure from simplified theory has been found.

3.4 Adding altitude feedback

Having established phugoid damping and pitch attitude control, the next step in an aircraft control system is altitude control. In order to analyse this the state has to be expanded to include the altitude as a state variable. In horizontal flight, we have:

$$h' = V.\gamma = V.(\theta - \alpha) \qquad (3.9)$$

If there is no feedback of h, this merely adds a pole in the origin to the system, representing the fact that in an aircraft (apart from air density variations) altitude in itself is not stable or unstable, but indifferent.

Altitude can be controlled by elevator alone, although this is not necessarily the optimal solution. Feedback of altitude on elevator does not add any damping to the system, since there is clearly no effect on the trace of the system matrix (elevator does not have a direct effect on h'). The feedback stabilizes the indifferent h-pole, drawing its damping from the phugoid poles and sending these unstable almost at once, if no artificial phugoid damping is present. Therefore, altitude feedback without phugoid damping is futile. When phugoid damping is present, there is no problem in controlling the altitude as such. Figures 3.3 (a) through (c) give full order root loci for the feedback of h on elevator in the presence of phugoid damping by θ-feedback. The short period oscillation is not affected, and the h-pole in the origin can be thought of as forming a second order system with one of the degenerate phugoid poles. There is, of course a problem with the remaining pole near the origin, which is "passed" by the h pole through role transformation. This pole, loosely termed the "energy mode", will have to be discussed separately in chapter 6, on the use of autothrottle, before a more serious attempt at an altitude hold mode can be made in chapter 7.

Certain observations can be made at this stage, however. The full order root loci of figure 3.3 show, that apart from the energy mode, an altitude control can be created of reasonably constant frequency and damping, by using a feedback of the altitude proportional to that of θ, when gain scheduling both feedback gains to vary with $1/V^2$. This is rather an ad hoc result that will not be duplicated for the feedbacks of γ yet to be discussed. The root loci also indicate that the feedback of α contained in feedback of θ tends to mitigate the effects of centre of gravity variations.

Another point that can be made here is, that for θ feedback a reference value θ_i is required. If this reference value is incorrect for level flight at the chosen speed, a bias in the altitude will result. Probably the only practical way of obtaining this reference value is by a washout circuit, or by adding integration to the altitude feedback, which amounts to the same thing. To the credit side of θ feedback, it must be mentioned that θ can be reliably and accurately measured quite easily, and that the h-θ setup is traditionally the way in which a human pilot operates.

4. FEEDBACK OF THE FLIGHT PATH ANGLE

4.1 Introduction

It has been stated before, that there is a tendency in modern literature on aircraft control systems to prefer feedback of γ or $h^{\cdot}$ to that of θ, now that these signals are becoming available with the required accuracy and reliability. We will therefore have a look at feedback of the flight path angle γ. Figures 4.1 (a) through (e) give full order root loci for this feedback, with gains directly comparable to those marked in figures 3.1 for the feedback of θ. The differences and similarities will be discussed along the lines of the preceding chapter.

Having treated θ feedback basically as a combination of α feedback and γ feedback, the analysis of feedback of γ alone is clearly very simple. Since γ does not feature in the short period approximation, equations (2.9) and (2.17) can be used as though no feedback was present, and used in equations (2.23) for the phugoid, to give the following system for feedback of γ (neglecting x_q):

$$\begin{pmatrix} \hat{u}^{\cdot} \\ \dot{\gamma} \end{pmatrix} = \begin{pmatrix} x_u & x_\theta - K_{\gamma\delta e}.H_{\alpha\delta ess}.(x_\alpha + x_\theta) \\ -z_u & -K_{\gamma\delta e}.H_{q\delta ess}.V/\bar{c} \end{pmatrix} \begin{pmatrix} \hat{u} \\ \gamma \end{pmatrix} \qquad (4.1)$$

with characteristic equation:

$$\lambda^2 + \lambda.(-x_u + K_{\gamma\delta e}.H_{q\delta ess}.V/\bar{c}) + (x_\theta z_u + K_{\gamma\delta e}.(-x_u.H_{q\delta ess}.V/\bar{c} - z_u.H_{\alpha\delta ess}.(x_\alpha + x_\theta)) = 0$$

Comparing this to (3.9), we find that γ feedback is identical to θ feedback except that there is, to a first approximation, no effect on the frequency or the "stiffness" of the short period oscillation. Referring back to (2.7), for instance, it can be seen that unlike in θ feedback, there is now a genuine increase in total damping because the effect of $-K_{\gamma\delta e}.z_{\delta e}$ falls on the diagonal of the full order matrix.

The zeroes of the $H_{\gamma\delta e}$ transfer function are different to those for $H_{\theta\delta e}$ as found in (3.9). Making $K_{\gamma\delta e} > -\infty$ in (4.1), the only zero found is:

$$\lambda = \frac{-H_{\alpha\delta ess}.z_u.(x_\theta + x_\alpha) + H_{q\delta ess}.x_u.V/\bar{c}}{H_{q\delta ess}.V/\bar{c}} \qquad (4.2)$$

For $z_{\delta e} = 0$ and $z_q = V/\bar{c}$ in (2.17), this amounts to:

$$\lambda = \frac{x_u z_\alpha - z_u . (x_\theta + x_\alpha)}{z_\alpha} \qquad (4.3)$$

which is the same zero found in ref.2 for the full order derivation under the same conditions. In a complete full order analysis, two more zeroes appear which are also present in the figures 4.1. These zeroes are so far from the origin as to make their influence felt only for very large feedback gains. For practical purposes, it might be said that compared to the case of θ feedback the zero near the origin has moved to the location given in (4.3). This is the familiar zero for flight path angle control, which is also seen in altitude feedback, and which is stable or unstable depending on whether the aircraft is flying above or below the speed for minimum power required (in propeller aircraft), respectively.

4.2 Adding feedback of altitude

Since γ feedback, like θ feedback, provides adequate phugoid damping, it can be used as a basis for altitude control. In figures 4.2, full order root loci are given for an altitude feedback based on flight path angle damping, comparable in results to that in figures 3.3 for pitch attitude damping. There are certain differences, however.The first difference is, that for a speed of 50 m/s, the feedback gains for γ and h are roughly half those used for θ and h to give almost the same frequency and damping; this is much as expected, since the θ-feedback used more than doubles the stiffness the short period oscillation, indicating that the stiffness of these first attempts at altitude control may be excessive.

When varying speed,it becomes apparent that the feedback gain for the altitude should not be proportional to that of γ, as was the case with θ feedback; but that it should rather have an extra gain scheduling with 1/V relative to it. This will make the total gain scheduling for altitude with speed proportional to $1/V^3$, to produce eigenvalues that are reasonably independent of speed, since $K_{\gamma\delta e}$ already had been made proportional to $1/V^2$.

A third difference is, that for this altitude control based on γ, the dependence of the result on centre of gravity location is much stronger than in the case of θ feedback. This is due to the fact, that in θ feedback with the rather high gains used here, the α component in the feedback accounts for part of the effective static stability.

The reference value for γ in an altitude hold mode has the natural value of zero, eliminating a possible source of error relative to θ feedback, especially when engaging the mode. On the other hand, the actual value of γ is far more dificult to measure than θ, excluding its use for feedback altogether until fairly recently.

5. FEEDBACK OF NORMAL ACCELERATION

5.1 Introduction

In the preceding chapters, it has been shown that θ feedback and γ feedback both have their virtues and shortcomings. We will now make an effort to combine some of their advantages, notably the relative centre of gravity independence of θ-based feedback and the more natural reference values of γ-based feedback, by adding feedback of the normal acceleration a_n to the flight path angle feedback.

With $a_n = V.\dot{\gamma}$, we have from the full order equations in (2.3):

$$a_n = -V.z_u.\hat{u} - V.z_\alpha.\alpha - V.z_\theta.\theta - V.z_q.(V/\bar{c}) - V.z_{\delta e}.\delta e - V.z_{\delta t}.\delta t \qquad (5.1)$$

In the short period approximation $\hat{u} = 0$, and for the assumptions $z_q = V/\bar{c}$, $z_{\delta e} = 0$ and $z_{\delta t} = 0$ and horizontal flight that are often made, we have:

$$a_n = -V.z_\alpha.\alpha \qquad (5.2)$$

This can also be compared to (2.20) for the elevator effectiveness in the short period approximation. It might be concluded, that feedback of normal acceleration is almost equal to feedback of angle of attack. Taking this one step further, it could be argued that, say, feedback of $\gamma + a_n/(V.z_\alpha)$ is merely a complicated way of defining a feedback of θ. There is a number of differences, however. First of all, there is the trivial difference that by measuring and feeding back γ and a_n separately, we are not confined to precisely the combination equivalent to θ given here. We can therefore separate our design goals in the short period mode and in the phugoid mode. This could, of course also be achieved by feedback of γ and α instead of γ and a_n. The differences between feedback of a_n and α are more important. The first of these is, that there is a factor $-V.z_\alpha$ between the two. Since z_α is proportional to ρV for constant C_{Z_α} (see appendix A), a constant feedback gain for α on δe, corresponding to a constant increase in equivalent static stability, requires that any feedback of normal acceleration, in order to have the same effect should be made proportional to $\frac{1}{2}\rho V^2$; this has been done for the points marked in the full order root loci of figures 5.1. Even then, if C_{Z_α} is not a constant for all flight conditions, which it is not, a difference between the two feedbacks will remain.

The second difference between feedback of a_n and α is, that there is a natural reference value for a_n; viz. that of zero, in any symmetrical steady state flight. This does require, of course that this zero can be measured. The same does not apply to the specific normal force, for which the reference depends on the steady state flight path angle. A related difference between the specific force and the normal acceleration is that the gravity component z_θ appears in the one and not in the other, as can be seen by comparing equations (5.1) and (2.5).

The final and probably most important difference between feedback of a_n and α is not apparent in a root locus analysis of the system used so far (which points to the fact that root locus analysis alone is not sufficient to design a satisfactory control system). It is in the response to external disturbances, such as gusts. It should be realised, that θ and γ are defined and measured relative to an inertial reference, such as the earth's surface, and this applies to our definition of α too. The α in (5.1) and (5.2), however governs an aerodynamic force; it is really the angle of attack relative to the surrounding air. To a first approximation *), it can be said that if only vertical turbulence is considered:

$$a_n = -V.z_\alpha.(\alpha + \alpha_g) \qquad (5.3)$$

where α_g is the disturbance in vertical airspeed, w_g experienced due to atmospheric turbulence by the aircraft, divided by V. If we use feedback of θ or γ, this feedback does not contain any direct throughput from atmospheric turbulence. The signal from the specific force measurement used to find the normal acceleration, however does contain the throughput $A_z \approx V.z_\alpha.\alpha_g$. It can be concluded, that there is an essential difference between the behaviour in turbulence of a system having strong θ feedback, and a system having the equivalent feedbacks of γ and a_n. The stiff θ feedback will hold the aircraft in a fixed attitude relative to the ground, preventing any alleviating effect on the normal acceleration due to gusts that the aircraft might have due to natural static stability. The normal acceleration feedback, on the other hand enhances the static stability relative to the air, counteracting the normal acceleration due to gusts (apart from the effects of $z_{\delta e}$, and of being behind the location of the centre of gravity in the aircraft). Also, the flight path angle feedback reacts to any flight path angle deviation incurred, to which the θ feedback is neutral.

---

*) Penetration effect (ref.4) has been neglected here. Equation (5.3) is an approximation that can be obtained by setting $\hat{u} = 0$, $\hat{u}_g = 0$ and $z_q = 1$ in the final equation of ref.4, appendix 2. In ref.4, time has been non-dimensionalized, changing the scale of z_q by $\bar{c}/V$ relative to the notation used here.

Although the importance of these effects, and the frequencies at which our simplified discussion applies, can only be judged by a more serious treatment, there is evidence in recent literature that a decided improvement in response to turbulence results from replacing the traditional θ-based feedback schemes by those based on feedback of γ and a_n. Reference (7) reports how modifying a pitch attitude-based automatic carrier deck landing system into an $\dot{h}$-based system gave a 2.5 to 1 reduction in the dispersion in touch down point on the deck in simulation of three US Navy aircraft, the results being borne out in practice by flight test of an F4J on the carrier Independence. Also, Boeing have been working at a flight path angle-based control system for several years already and claim many advantages for the system, especially as regards ease of synthesis and modular implementation, as well as a superior performance in wind shear (refs.5 and 6). Airbus have chosen to fly the A-320 not by attitude, but by a control law "integrating rate of change of pitch attitude with normal load factor", the so-called C^* system (ref.8). It would certainly be worthwile to study these systems in more detail.

We will now turn to a simple discussion of these feedbacks in reduced order systems.

5.2 The short period approximation

As mentioned in the introduction to this chapter, feedback of a_n in the short period approximation with the usual simplifying assumptions is equal to feedback of $-V.z_\alpha.\alpha$. Feedback of the angle of attack α in the short period approximation has already been discussed in paragraph 3.2, including the feedback of $q\bar{c}/V$ that should accompany it if the damping of the short period oscillation leaves something to be desired. The results can be used as found there, by the proper substitution for $K_{\theta\delta e}$:

$$K_{\theta\delta e}.\alpha \longleftrightarrow K_{a_n\delta e}.a_n \approx -K_{a_n\delta e}.V.z_\alpha$$

$$\longrightarrow K_{\theta\delta e} \longleftrightarrow -K_{a_n\delta e}.V.z_\alpha \qquad (5.3)$$

From the full order root loci of figures 5.1 and 5.2, it can be seen that this reduced model performs reasonably well, although there is a zero in the full order root loci that influences the damping of the short period for very high feedback gains. Points have been marked that more or less correspond to a constant feedback gain for α, by scheduling the gain for a_n with $1/\rho V^2$. As expected, the short period then requires a constant feedback gain for $q\bar{c}/V$ to maintain a relative damping of circa $\zeta = 0.7$.

Comparing figures 3.1 (a) and (5.1 (a), the effects on the frequency of the short period oscillation are quite similar, if using (5.3):

$$K_{\theta\delta e} = -4.0$$

$$K_{a_n\delta e} = -\frac{-4}{50 * -1.3099} \approx -0.06 \qquad (5.4)$$

The elevator effectiveness as a steady state solution to the short period approximation can also be approximated by using (3.5) and (5.3):

$$H_{\alpha\delta ess} \approx \frac{m_{\delta e}z_q}{z_\alpha.(m_q - K_{q\delta e}.(V/\bar{c}).m_{\delta e}) - z_q.(m_\alpha + K_{a_n\delta e}.V.z_\alpha.m_{\delta e})}$$

$$H_{q\delta ess} \approx \frac{-m_{\delta e}z_\alpha}{z_\alpha.(m_q - K_{q\delta e}.(V/\bar{c}).m_{\delta e}) - z_q.(m_\alpha + K_{a_n\delta e}.V.z_\alpha.m_{\delta e})} \qquad (5.5)$$

For strong feedback gains $K_{a_n \delta e}$, this reduces to:

$$H_{\alpha\delta ess} \approx \frac{1}{-K_{a_n \delta e}.V.z_\alpha}$$

$$H_{q\delta ess} \approx \frac{1}{K_{a_n \delta e}.V.z_q} \qquad (5.6)$$

5.3 The phugoid approximation

In the phugoid approximation, $\hat{u}$ is allowed to vary and the elevator effectiveness is assumed to be that for a steady state in the short period approximation. Since a_n contains a component $-V.z_u.\hat{u}$ due to u, as given in equation (5.1), there will be feedback of $\hat{u}$ on elevator in the phugoid approximation. Introducing this feedback in the equations (2.23), we have, neglecting x_q:

$$\begin{pmatrix} \dot{\hat{u}} \\ \dot{\gamma} \end{pmatrix} = \begin{pmatrix} x_u + K_{a_n\delta e}.V.z_u.H_{\alpha\delta ess}.(x_\theta + x_\alpha) & x_\theta \\ -z_u + K_{a_n\delta e}.V.z_u.H_{q\delta ess}.(V/\bar{c}) & 0 \end{pmatrix} \begin{pmatrix} \hat{u} \\ \gamma \end{pmatrix} + \begin{pmatrix} H_{\alpha\delta ess}.(x_\theta + x_\alpha) & x_{\delta t} \\ H_{q\delta ess}.(V/\bar{c}) & 0 \end{pmatrix} \begin{pmatrix} \delta_e \\ \delta_t \end{pmatrix} \tag{5.7}$$

For very large $K_{a_n\delta e}$, we can substitute the elevator effectiveness (5.6) to give, with $z_q = V/\bar{c}$:

$$\begin{pmatrix} \dot{\hat{u}} \\ \dot{\gamma} \end{pmatrix} = \begin{pmatrix} x_u + \frac{z_u}{z_\alpha}.(x_\theta + x_\alpha) & x_\theta \\ 0 & 0 \end{pmatrix} \begin{pmatrix} \hat{u} \\ \gamma \end{pmatrix} + \begin{pmatrix} H_{\alpha\delta ess}.(x_\theta + x_\alpha) & x_{\delta t} \\ H_{q\delta ess}.(V/\bar{c}) & 0 \end{pmatrix} \begin{pmatrix} \delta_e \\ \delta_t \end{pmatrix} \tag{5.8}$$

In other words, the flight path angle tends to become indifferent because any $\dot{\gamma}$ is made impossible by the strong feedback of a_n; and the speed tends toward a first order system of very small eigenvalue. The full order root loci of figure 5.1 show, that the phugoid poles do not quite reach the origin in practice, but the basic tendency is as predicted. This means, that for systems with considerable feedback of the normal acceleration, the extended short period approximation of equation (2.25) can be used, together with the elevator effectiveness according to (5.5), or even (5.6). When using (5.6), adding feedback of the flight path angle will result in the following system:

$$\dot{\gamma} = -K_{\gamma\delta e}.H_{q\delta ess}.V/\bar{c} =$$

$$= \quad - \frac{K_{\gamma\delta e}}{K_{a_n\delta e}} \cdot \frac{1}{c.z_q} \quad \approx \quad - \frac{K_{\gamma\delta e}}{K_{a_n\delta e}} \cdot \frac{1}{V} \qquad (5.9)$$

In figures (5.3) the full order root loci are given for precisely such a system with strong feedback gain $K_{a_n\delta e}$, and the approximation (5.9) is seen to do fairly well. Taking the speed of 50 m/s for example, we have on substituting in (5.9):

$$\dot{\gamma} = \quad - \frac{-4.0}{-0.06} \cdot \frac{1}{50} = -1.33 \qquad (5.10)$$

The other speeds have been set up to give the same eigenvalue. There is a bias in the results, the eigenvalues all being around -1.0; but the results are consistent and much less dependent on centre of gravity variation than for flight path angle control without feedback of normal acceleration, due to the largely artificial static stability. It would seem, that the original aim in this chapter of creating a system that has logical reference values, good behaviour in turbulence and robustness to centre of gravity variations can indeed be brought nearer by combining feedback of normal acceleration with feedback of the flight path angle.

5.4 Adding feedback of altitude

Just as in the case of θ feedback and γ feedback, the combined feedback of a_n and γ can be used as a basis for altitude control. We will consider the extreme case of (5.9) only, and expand this with the altitude as a state variable. Again using (5.6) with $z_q = V/\bar{c}$, the much simplified system is:

$$\begin{pmatrix} \dot{h} \\ \dot{\gamma} \end{pmatrix} = \begin{pmatrix} 0 & V \\ -\frac{K_{h\delta e}}{K_{a_n\delta e}} \cdot \frac{1}{V} & -\frac{K_{\gamma\delta e}}{K_{a_n\delta e}} \cdot \frac{1}{V} \end{pmatrix} \begin{pmatrix} h \\ \gamma \end{pmatrix} \qquad (5.11)$$

with characteristic equation:

$$\lambda^2 + \lambda \cdot \left(\frac{K_{\gamma\delta e}}{K_{a_n\delta e}} \cdot \frac{1}{V} \right) + \frac{K_{h\delta e}}{K_{a_n\delta e}} = 0 \qquad (5.12)$$

For a relative damping of $\zeta = 0.7$, the formula for the root of a quadratic equation requires:

$$\frac{K_{h\delta e}}{K_{a_n\delta e}} = \frac{1}{2} \cdot \left(\frac{K_{\gamma\delta e}}{K_{a_n\delta e}} \cdot \frac{1}{V} \right)^2 \qquad (5.13)$$

The full order root loci of figures 5.3 show that for a strong feedback gain, this relation predicts $K_{h\delta e}$ well, only if for the damping between parentheses the actual eigenvalue of the γ-movement is used as found in the full order root loci of figures 5.2. If the predicted value of -1.33 is used, then the $K_{h\delta e}$ needed is overestimated considerably. For 50 m/s, for instance the point marked in figure 5.3 (a) would be:

$$K_{h\delta e} = \frac{1}{2} \cdot 0.06 \cdot (-1.33)^2 = 0.053 \qquad (5.14)$$

Apart from this difference, the feedbacks used produce a basis for an altitude hold mode, where pole placement by hand is possible, and the system is almost independent of centre of gravity location. The feedback gains used may be much too high for comfort, though, in more than one respect. The feedback of h can be interpreted as an outer loop over the γ control, commanding γ_i; and the feedback of γ as an outer loop over the a_n control, commanding a_{n_i}.

6. THE USE OF AUTOTHROTTLE

6.1 Introduction

It has been mentioned in previous chapters, that in altitude control by elevator, and in flight path angle control by elevator in general, there is a problem with the pole of the so-called "energy mode" near the origin. The pole is marginally stable or unstable, depending on the flight regime. This problem can be solved by the use of autothrottle. Two different philosophies of achieving this will be discussed here.

A few words on the autothrottle itself are called for. There is, of course a transfer function governing the the response of the engine power and propeller thrust to control application. The dynamics involved have been ignored here. This is probably justified for a first look at viable control laws, since the piston engine responds fairly quickly, and the throttle is not used for feedback of variables subject to rapid change; partly to preserve the engine, partly because thrust has little effect on the fast modes of the aircraft anyway *). The input vector for the throttle in our linear system description can be related to a number of control inputs. In the 1982 model contained in CASPAR, inlet manifold pressure and rpm were available as inputs, their associated input vectors differing only by a factor because they both operate on engine power. Quite remarkably, these input vectors show twice as much influence of the throttle on the vertical Z-equation (in a negative, that is upward, sense) than they do on the X-equation; and this is in body axes, the situation is aggravated when converting to stability axes. This unlikely phenomenon is not present in the 1968 model. Unfortunately, the numerical values in the 1968 model and in the 1982 model cannot be directly compared, since in the older model the input signal is defined to be a non-dimensional total head rise in the propeller wake. Despite this, we will consider the direct lift effect of throttle apllication as a side effect in our analysis. It can interfere with the interpretation of the full order root loci, however.

In this report, inlet manifold pressure has been used as the primary feedback channel. The effectiveness of this input depends on rpm, air density and airspeed. Moreover, the inlet manifold pressure cannot be allowed to vary freely at any rpm. For these reasons, developing a combined single input to manage the engine, with a simple, well defined output such as a thrust, is certainly worth considering.

---

*) Somewhat surprisingly, in ref.7 angle of attack is used as a feedback signal to the autothrottle of a carrier-based fighter aircraft.

6.2 Feedback of airspeed on throttle

The classical use of autothrottle is for feedback of the airspeed. The results of this feedback will be considered in this paragraph. Since the short period is not normally influenced much by the throttle, the phugoid approximation of (2.23) will be used, expanded with the altitude as a state variable:

$$\begin{pmatrix} \dot{\hat{u}} \\ \dot{h} \\ \dot{\gamma} \end{pmatrix} = \begin{pmatrix} x_u & 0 & x_\theta \\ 0 & 0 & V \\ -z_u & 0 & 0 \end{pmatrix} \begin{pmatrix} \hat{u} \\ h \\ \gamma \end{pmatrix} + \begin{pmatrix} H_{\alpha\delta ess}.(x_\alpha + x_\theta) + H_{q\delta ess} & x_{\delta t} \\ 0 & 0 \\ H_{q\delta ess}.V/\bar{c} & 0 \end{pmatrix} \begin{pmatrix} \delta e \\ \delta t \end{pmatrix} \qquad (6.1)$$

This implies that we have neglected the effects that $z_{\delta t}$ and $m_{\delta t}$ may have, relative to the natural value of $-z_u$, by way of the steady state solution of the short period oscillation (2.16), if feedback of $\hat{u}$ on throttle is used. This is normally quite justified.

It can be seen, that feedback of speed on autothrottle is an excellent way of adding damping to the system, since the main effect falls on the system matrix diagonal, effectively changing x_u into $x_u - K_{u\delta t}.x_{\delta t}$. Physically (by assuming speed to become a constant) as well as by inspection of the characteristic equation, it can be seen that for very large $K_{u\delta e}$ the system reduces to:

$$\begin{pmatrix} \dot{h} \\ \dot{\gamma} \end{pmatrix} = \begin{pmatrix} 0 & V & h \\ 0 & 0 & \gamma \end{pmatrix} + \begin{pmatrix} 0 \\ H_{q\delta ess}.V/\bar{c} \end{pmatrix} .\delta e \qquad (6.2)$$

This has been called in paragraph 2.4 (c): the extended short period approximation. The classical method of designing an altitude hold mode is by assuming that (6.2) holds exactly, whenever autothrottle is used to control the speed. Therefore feedback of $\hat{u}$ on autothrottle is sometimes referred to as phugoid damping; it would be more accurate to say that it makes the phugoid, or the flight path angle, indifferent. In a preliminary study of the 1968 model, not reproduced here, this approximation fitted the full order root loci quite well. For the present 1982 model, we find the root locus of figure 6.1. It shows the feedback to actually cause instability if made too strong, and to have a visible effect on the short period oscillation. This peculiar behaviour, which will also be found in the altitude hold mode yet to be discussed, is probably due to the excessive value of $z_{\delta t}$ in the 1982 model.

6.3 Feedback of specific energy on throttle

An alternative method of using autothrottle can be derived from physical reasoning. The name of "energy mode" for the pole that remains near the origin when flight path angle control is exerted, points in this direction. In the phugoid mode, energy is almost constant although it is periodically exchanged between speed and altitude. The elevator as an input also does not have much influence on the total energy, but primarily only on its distribution between speed and altitude. Energy, being almost invariant if only elevator feedback is used, is therefore an interesting physical variable. It can be expressed as the sum of kinetic and potential energy, to give (including perturbations):

$$E = \frac{1}{2}.m.(V+u)^2 + m.g.(h_o+h)$$
$$= \frac{1}{2}.m.V^2 + m.V.u + \frac{1}{2}.m.u^2 + m.g.h_o + m.g.h$$

Using the steady-state condition in horizontal flight as an energy reference, neglecting the higher order term in u^2, and dividing by the mass, we obtain the perturbation in specific energy e:

$$e = V.u + g.h = V^2.\hat{u} + g.h \qquad (6.3)$$

For convenience in analysing the proposed feedback, we will replace $\hat{u}$ in the system description (6.1) by e, using a simple linear transformation $\underline{P}$ of the kind used before in chapter 2:

$$(\hat{u}+h.g/V^2 \quad h \quad \gamma)^T = \underline{P}.(\hat{u} \quad h \quad \gamma)$$

$$\underline{P} = \begin{pmatrix} V^2 & g & 0 \\ 0 & 1 & 0 \\ 0 & 0 & 1 \end{pmatrix} \qquad \underline{P}^{-1} = \begin{pmatrix} 1/V^2 & -g/V^2 & 0 \\ 0 & 1 & 0 \\ 0 & 0 & 1 \end{pmatrix} \qquad (6.4)$$

Using $x_\theta = g/V$, this produces the system:

$$\begin{pmatrix} \dot{e} \\ \dot{h} \\ \dot{\gamma} \end{pmatrix} = \begin{pmatrix} x_u & -g.x_u & 0 \\ 0 & 0 & V \\ -z_u/V^2 & z_u.g/V^2 & 0 \end{pmatrix} \begin{pmatrix} e \\ h \\ \gamma \end{pmatrix} +$$
$$+ \begin{pmatrix} V^2.H_{\alpha\delta ess}.(x_\alpha+x_\theta) + H_{q\delta ess}.V^2.x_q & V^2.x_{\delta t} \\ 0 & 0 \\ H_{q\delta ess}.V/\bar{c} & 0 \end{pmatrix} \begin{pmatrix} \delta e \\ \delta t \end{pmatrix} \qquad (6.5)$$

This system is identical to (6.1), but it invites feedback of the specific energy on throttle, rather than of speed alone. In other words, to the feedback of speed in the previous paragraph we now add a proportionate amount of altitude feedback on throttle. The feedback gain will be called $K_{e\delta t}$:

$$\delta_t = -K_{e\delta t}.e \qquad (6.6)$$

This feedback effectively changes the value of x_u in the top left corner of (6.5) into $x_u - K_{e\delta t}.V^2.x_{\delta t}$. For large values of $K_{e\delta t}$, the system reduces to:

$$\begin{pmatrix} \dot{h} \\ \dot{\gamma} \end{pmatrix} = \begin{pmatrix} 0 & V & h \\ z_u.g/V^2 & 0 & \gamma \end{pmatrix} + \begin{pmatrix} 0 \\ H_{q\delta ess}.V/\bar{c} \end{pmatrix} .\delta e \qquad (6.7)$$

Comparing this to (2.23) and setting $V.u = -g.h$, we can see that this is almost identical to the phugoid mode, barring the fact that what small natural damping there was in the phugoid, has disappeared. This result is really quite obvious, because the perturbation in energy represented by the phugoid mode normally decays very slowly due to the presence of x_u; this decay is halted by a feedback that keeps the energy constant at any value once established. The energy mode, which had been almost decoupled from the system by nature, only becomes more so when feedback of the energy on throttle is added.The resulting reduced system (6.7) can be damped by elevator and turned into an altitude hold mode or similar, without involving the throttle in any way.Since the engine is a power source, it is perfectly natural to use the throttle only for maintaining the energy balance, and to shield it from activation by all modes which do not affect the power balance.

Full order root loci for this feedback are given in figures 6.2. They behave entirely as expected, and in fact the simple equation that results by using the feedback (6.6) in the top row of (6.5):

$$\dot{e} = x_u - K_{e\delta t}.V^2.x_{\delta t} \qquad (6.8)$$

describes the movement of the energy pole quite well; the only disturbance is a visible movement of the short period poles, probably caused by the excessive value of $z_{\delta t}$. It appears, that feedback of the specific energy is more robust to this effect than feedback of speed.

Additional root loci (figures 3.3) were made for proportional-integral feedback of the specific energy with a time constant of 5 seconds; these

root loci also behave as a completely decoupled second order system of the form:

$$s.e = x_u - K_{e\delta t}.V^2.x_{\delta t}.(1 + 1/5s) \qquad (6.9)$$

with characteristic equation:

$$\lambda^2 + \lambda.(-x_u + K_{e\delta t}.V^2.x_{\delta t}) + \frac{K_{e\delta t}.V^2.x_{\delta t}}{5}$$

The results obtained in this chapter strongly indicate, that whenever a reference for h is available, feedback of the speed via the throttle should be replaced by feedback of the perturbation in specific energy, since the latter is physically more logical and in addition simplifies the control synthesis procedure. Additional advantages for feedback of energy on throttle instead of speed are claimed in reference (6) with regards to simplified overall system structure and effective response to energy loss in wind shear.

7. ALTITUDE HOLD MODE AND GLIDE SLOPE

7.1 Classical altitude hold mode

The classical altitude hold mode is based on phugoid damping by pitch attitude feedback, combined with feedback of altitude on elevator. The feedback of altitude can also be defined in series with the θ-feedback:

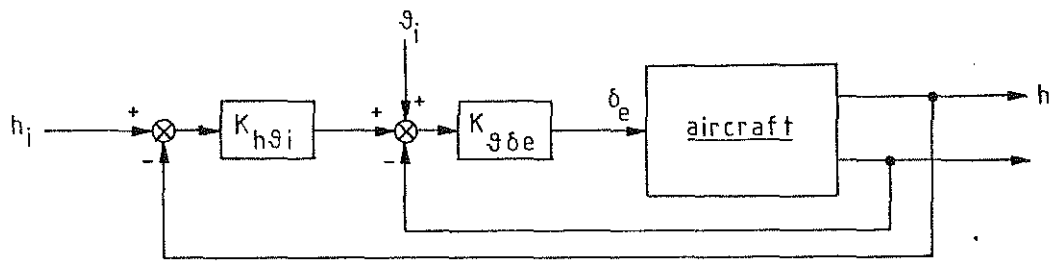

This is equivalent to parallel feedback, such as in the schemes of figures 3.3, if $K_{h\delta e} = K_{h\theta_i}.K_{\theta\delta e}$. In this form, the altitude hold mode is seen as functioning much in the same way that a human pilot controls the flight path, primarily by pitch attitude inner loop control. It has already been pointed out that this feedback leads to a marginally stable energy mode. The energy mode is actually unstable at the slowest speed examined, of 35 m/s. This speed is apparently below the speed for minimum power required. We will therefore use this speed for checking the reduced order models found in the previous paragraph against full order root loci.

(a) feedback of specific energy on throttle

When feedback of specific energy on the throttle is used to stabilize the energy mode, the reduced order phugoid model with damping removed, as in equation (6.7), should be used. Adding feedback of h and θ on elevator, and separating the θ feedback into γ feedback and α feedback as per chapter 3, this produces the model:

$$\begin{pmatrix} \dot{h} \\ \dot{\gamma} \end{pmatrix} = \begin{pmatrix} 0 & V \\ z_u.g/V^2 & -K_{h\delta e}.H_{q\delta ess}.V/\bar{c} \end{pmatrix} \begin{pmatrix} h \\ \gamma \end{pmatrix} \qquad \begin{matrix} -K_{\theta\delta e}.H_{q\delta ess}.V/\bar{c} \end{matrix} \qquad (7.1)$$

with characteristic equation:

$$\lambda^2 + \lambda.(K_{\theta\delta e}.H_{q\delta ess}.V/\bar{c}) + (-z_u.g/V + K_{h\delta e}.H_{q\delta ess}.V^2/\bar{c})$$

where $H_{q\delta ess}$ is the steady state elevator effectiveness in the short period approximation in the presence of θ feedback, according to equation (3.5). We shall use the feedback gains marked earlier in figure 3.3 (c):

$$K_{\theta\delta e} = -2.0$$
$$K_{h\delta e} = -0.014$$

Substituting $K_{\theta\delta e}$ and the relevant stability derivatives from table 2.5 (c) into (3.5), we have:

$$H_{q\delta ess} = -0.0107 \qquad (7.2)$$

Using this, the characteristic equation of (7.2) becomes:

$$\lambda^2 + 0.472\,\lambda + 0.227 = 0 \qquad (7.3)$$

the roots are: $\lambda_{1,2} = -0.236 \pm 0.414\,j$,

which is almost exactly equal to the poles found in the full order root locus of figure 3.3 (c). When adding feedback of specific energy on the throttle, these poles should not be influenced. The full order root loci of figure 7.1 confirm this. The only result of adding the feedback of specific energy e on the throttle should be to stabilise the energy pole according to equation (6.9). This is reasonably borne out by the point marked in figure 7.1:

$$\dot{e} = (x_u - K_{e\delta t}.V^2.x_{\delta t}).e$$
$$= 0.009773 - 0.1\,.(35)^2.\,0.00125 = -0.143\,e \qquad (7.4)$$

The reason that this result is not very accurate is that the short period poles, and to a lesser degree also the h/θ poles do move under the feedback. This is probably due to the excessive value of $z_{\delta t}$ in the 1982 "Beaver" model used.

(b) <u>feedback of speed on throttle</u>

When using feedback of speed on throttle, the system tends to reduce to the extended short period approximation, as in (6.2). The result is is really identical to the system just described in (7.2), except for the absence of the term $z_u.g/V^2$. We can therefore simply eliminate this from the characteristic equation (7.3), to find:

the roots are: $\lambda_{1,2} = -0.236 \pm 0.244\ j$

Since without any feedback on the throttle, the roots of the phugoid approximation (7.3) are found, the roots near the origin can be expected to form a root locus as sketched below:

<u>the expected behaviour of the roots near the origin for adding feedback of speed on throttle to an altitude hold mode</u>

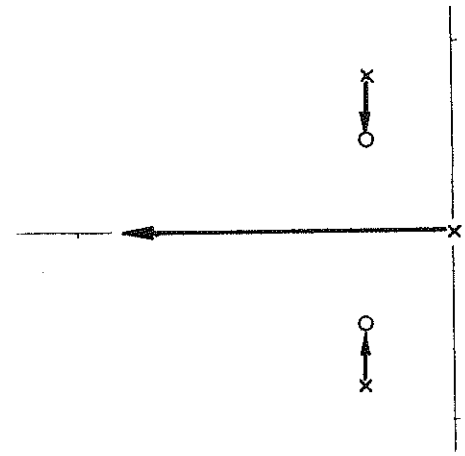

The full order root loci are given in figure 7.2. The points marked have the same effective feedback gain for u as those marked for the specific energy feedback in figure 7.1. It can be seen, that the root locus initially behaves as predicted, but the poles go unstable for higher feedback gains. Since it was suspected that this abnormal behaviour was due to the excessive numerical value of $z_{\delta t}$ in the model, the root locus of figure 7.2 was replotted as figure 7.3, after eliminating $z_{\delta t}$ from the model (in body axes). The system now seems to behave as sketched above only for very large feedback gains; but for moderate feedback gains the roots actually make a detour along the real axis. All this makes full order pole placement by reduced order methods next to impossible for the feedback of speed on throttle, and this impression is corroborated by earlier efforts, not reproduced here, at adding this feedback to various altitude hold modes in the 1968 model. The feedback of speed on throttle will always move all the poles in the vicinity of the origin about in a rather unpredictable way.

It should be stressed that this does not imply, that the extended short period approximation produces meaningless results. The response of third order systems can be very similar to that of second order systems, and it is quite feasible that the extended short period approximation could produce time histories very similar to those of the full order system. But in the present synthesis procedure, where reduced order models are continually accompanied by full order root loci to check on their validity, the systematic verification is lost for this feedback. This problem has not been investigated further, since it is felt that feedback of the specific energy is probably a physically more promising line of development anyway.

7.2 Integration in the altitude hold mode

In the case of a classical altitude hold mode, using θ feedback, the reference value for θ has to be set when engaging the mode, and updated if flight conditions vary. Probably the only practical way to achieve this, is by using integrating action in the feedback of the altitude. This integration introduces a new pole, which is usually chosen to be very slow in order not to reduce the damping of the other poles too much. This does mean, that if this pole is excited, e.g. by engaging the altitude hold mode in a pitch attitude that does not correspond to level flight, a bias in altitude results that will decay only very slowly.

This is one respect in which feedback of γ is preferable to feedback of θ for altitude hold mode damping, since the reference value for γ is always known in advance upon engaging either altitude hold mode or glide slope mode. Still, integrating action in the feedback will always be necessary, if only because the steady state elevator angle to fly the aircraft straight and level will vary with centre of gravity variations, making the reference elevator position $\delta_e = 0$ arbitrary. Figure 7.4 gives a full order root locus plot for adding integrating action to a very stiff altitude hold mode, based on feedback of normal acceleration and flight path angle on elevator, and of specific energy on throttle. If integrating action is used in the feedback of altitude on elevator, then PI-action can be used in the throttle channel as well, to eliminate any steady state error in speed as well as in altitude. Figure 7.4 serves to illustrate two points: adding modest integrating action need not be detrimental to the relative damping of the altitude hold mode poles, and the energy mode and altitude/flight path angle modes are indeed completely decoupled in the present system setup.

The system given here does not pretend to be more than a basic structure that might be used for an altitude hold mode. It is probably far too stiff in practice, and the gains will have to be adjusted in simulation. The simplified methods of analysis given here, however can serve as a guide to the way in which the different gains relate to each other, and the types of gain scheduling with speed to be expected.

7.3 Glide slope mode

The glide slope mode is basically no different from an altitude hold mode, since in both cases feedback is used of an altitude error relative to a reference plane, the only difference being that on the glide slope the plane is not horizontal and the steady state is a descending flight path.

The glide slope signal is not really proportional to the altitude difference between aircraft and glide path, but rather to an angular difference as seen from the transmitter. Since this would make the equivalent feedback of altitude difference inversely proportional to the range to station, it is preferable to use some form of gain scheduling with range, to keep the feedback near the design point. Range information can be extracted from marker beacons, the altitude while on the glide path, and DME.

7.4 Speed control by elevator

If the throttle is not used for feedback of speed, but either for that of specific energy or not at all, then according to chapter 6 there is almost no short-term variation in V.u+g.h. If elevator can be used to control the short-term variation of altitude, provided phugoid damping is present, then a very similar short term control of airspeed by elevator should also be possible; in fact, feedback of -(V/g).u should be almost equivalent to feedback of h. An important difference is, of course, that for feedback of u the h pole remains indifferent in the origin, while in the case of feedback of h the energy mode may go unstable.
Figure 7.5 gives a full order root locus plot for this feedback. Comparing this to figure 5.4 (a), the similarity is obvious; in fact, the analysis of equations (5.11) to (5.13) gives more accurate results for feedback of (-V/g).u than it did for h.

This result means, that if feedback of specific energy on the throttle is used, one has a choice as to what is considered to be most important in short term control: speed or altitude, or any combination of the two. In reference (6), this concept of using the throttle to control total energy, and the elevator to control the ditribution of this energy between speed and altitude, is elaborated upon. It is claimed that by making it into the basis of the control concept many advantages are gained. One of these is the effortless transition from control of altitude or flight path angle to speed control if the throttles reach their limits.

8. FEEDFORWARD COMPENSATION OF DISTURBANCES

8.1 Turn compensation

In a coordinated turn, a "g" force is experienced In horizontal flight, the normal load factor becomes:

$$n = 1/\cos\varphi \qquad (8.1)$$

An extra angle of attack and a q-motion are present, very similar to those in a symmetric pull-up manoeuvre with the same amount of "g" force. A (negative) elevator deflection is therefore needed in a horizontal turn, to prevent loss of altitude. This elevator bias can be computed (ref.3) and fed forward to the elevator channel. It does, however vary with c.g. position and lift coefficient, making the compensation approximate at best. More importantly, it has to be realised that in a steady turn the reference values for any feedback of a_n, $q\bar{c}/V$ or θ have to be temporarily adjusted. In a horizontal turn, we have (ref.3):

$$a_n = (n-1).g = g.\left(\frac{1}{\cos\varphi} - 1\right)$$

$$q = \frac{g}{V}.\left(n - \frac{1}{n}\right) = \frac{g}{V}.\sin\varphi.\tan\varphi \qquad (8.2)$$

The reference values for the feedbacks have to be adjusted acoordingly.

8.2 Flap deflection

When flaps are selected, there is a marked effect on the flight path, and also on speed. In an automatic control system, information on flap position is obviously available and should be used to compensate, instead of waiting for the flight path deviation to occur. A simple preliminary model for flap action has been added to the system equations (ref.10). It consists of only a linear input vector:

$$\Delta \begin{pmatrix} \hat{u} \\ \dot{\gamma} \\ \dot{\alpha} \\ \dot{q}\bar{c}/V \end{pmatrix} = \begin{pmatrix} -0.0652 \\ -0.369 \\ 0 \\ 0.0934 \end{pmatrix} \delta_f \text{ (rad)} \qquad (8.3)$$

A time history for the 1968 model of the "Beaver" aircraft, with modest θ feedback for phugoid damping, for a step input on this input vector is given in figure 8.1. The response shows a typical "ballooning" effect, the aircraft trading speed for altitude. This is followed by a steady climb at the new speed, due to trim change.

The bias needed in throttle and elevator settings to cancel the effect of flap deflection in stationary flight can be found by setting $\underline{\dot{x}} = 0$, and the requirements $\hat{u} = 0$ and $q\bar{c}/V = 0$, leaving four unknowns in the system equations:

$$\underline{0} = \underline{\dot{x}} = \underline{A}.\underline{x} + \underline{B}.\underline{u} \qquad (8.3)$$

Separating the matrices into columns, we have:

$$(\underline{a}_1\ \underline{a}_2\ \underline{a}_3\ \underline{a}_4).(\hat{u}\ \alpha\ \theta\ q\bar{c}/V)^T + (\underline{b}_1\ \underline{b}_2\ \underline{b}_3).(\delta e\ \delta t\ \delta f)^T = 0$$

Bringing all known factors to the right hand side of the equation:

$$(\underline{a}_2\ \underline{a}_3\ \underline{b}_1\ \underline{b}_2).(\alpha\ \theta\ \delta e\ \delta t)^T = -\underline{b}_3.\delta f \qquad (8.5)$$

Solving this in the usual way, an elevator and throttle setting are found. These can be used as a feed forward compensation to accompany flap deflection. The step response to a 15° flap deflection of this statically compensated system is given in figure 8.2; it is obvious that there is no need for any further dynamic feedforward schemes. The throttle feedforward is very large, and probably not always desirable in practice. Without the use of throttle feedforward, there is a choice of static elevator compensation to make $\hat{u} = 0$, leading to a flight path gently going into a descent, or for $\gamma = 0$, leading to the "ballooning" effect followed by

horizontal flight at a slower speed. For short term invariance of flight path angle, for instance on flap retraction during climbout under manual control, the compensation for $\hat{u} = 0$ is clearly the better choice.

The effect of flap deflection on the wing lift is similar to a change in angle of attack. There is also an influence on the balance of moments. The elevator is called upon to reduce the angle of attack to counteract the change in lift. A serious problem with this elevator feedforward is its dependence on the position of the centre of gravity of the aircraft. This will in practice necessitate an average setting. The uncompensated part of the flap effect then becomes an "unknown" input signal, the effects of which can only be reduced by feedback.

9. CONCLUSIONS

The method of root locus analysis in reduced order models has been used to compare some of the basic possible feedback structures for controlling the symmetric motions of the aircraft.

For the use of throttle, feedback of speed has been compared to feedback of the perturbation in total energy (kinetic and potential). In the latter case, the phugoid approximation is seen to be a better choice of reduced order model for analysis and synthesis than the more usual extended short period approximation, providing the proper elevator effectiveness is used. It would seem, that feedback of the energy is to be preferred in all cases where a reference value for both speed and altitude is available.

For the use of elevator, direct feedback of the flight path angle has been compared to the more usual pitch attitude based system. No definite conclusions can be drawn here, since both systems have their virtues. The extent to which feedback of θ and of γ differ in practice, depends among other things on the stiffness of the feedbacks used, and these cannot be chosen on the basis of a few root loci.

It has become increasingly obvious, that for successful aircraft control design, the whole spectrum of analysis and synthesis methods is indispensable, including simulation. The feedback of γ, for one thing, is not possible without the use of modern instrumentation and state reconstruction techniques, and the difference between the various feedback structures cannot be fairly judged without some stochastic analysis, and gain optimization. As a first impression, it would seem that for very "stiff" systems a combination of feedback of flight path angle an normal acceleration could be superior to the classical pitch attitude based system.

A lot of further study is required before a practical control system can be implemented with confidence. Some of the major concerns are:

- best choice of feedback gains

- implementation of a throttle management system with a single input, and a simple well-defined output such as thrust or power

- an analysis of the robustness of the control system against sensor failure, thrust limiting and other effects suddenly cancelling one or more feedbacks completely, cf. reference 6

- an analysis of mode switching; fading in completely new modes should be avoided as much as possible, since this leaves the aircraft unattended to during part of the transition. This may be acceptable for the "Beaver", but for inherently unstable aircraft this is not a viable method. Therefore, inner loop control should be left untouched, and mode switching could be accomplished by fading only outer loop control, or better still, by initializing the references of the new mode to give the same elevator angle as the one presently flown.

- an analysis of control wheel steering: the aircraft can be flown by hand through the automatic control system. This puts requirements on the transfer function between control input and aircraft response. Here, too

there is a basic choice between classical pitch attitude control and direct flight path angle control. The latter system, with decoupled speed control, is under development by Boeing at the moment (refs.5, 6).

It would certainly be worthwile to do some research on literature about the present developments at Boeing, Airbus and other industries, to check on the progress made there in the use of the newer design concepts.

REFERENCES

1. Lammertse, P.: Structuren en versterkingsfactoren voor een asymmetrische regeling voor de DHC-2 "Beaver", afstudeerverslag, Delft 1984

2. Anon.: Dictaat Vliegeigenschappen II, Delft 1972

3. O.H.Gerlach: Vliegeigenschappen I, Dictaat VTH D-10, Delft 1967, plus aanvulling volgnummer 321

4. O.H.Gerlach Calculation of the response of an aircraft to random atmospheric turbulence Part I. Symmetric motions Delft Report VTH-138, 1966

5. Lambregts, A.A., D.G.Cannon: Development of a control wheel steering mode and suitable displays that reduce pilot workload and improve efficiency and safety of operation in the terminal area and in windshear. AIAA 79-1887.

6. Lambregts, A.A.: Functional integration of vertical flight path and speed control using energy principles. NASA CP-2296.

7. Urnes, J.M. e.a.: Development of the Navy h-dot automatic carrier landing system designed to give improved approach control in air turbulence. AIAA 79-1772.

8. Condon, P.: Fly-by-wire for airliners Interavia magazine, 12-1982

9. Hoogstraten, J.A.: A survey of CASPAR, the Control System Analysis and Synthesis Program package for Aerospace Research. Report LR-336, February 1983.

10. Blok, A.J.: personal communication

11. Blakelock, J.H.: Automatic control of aircraft and missiles. John Wiley & Sons, New York, 1965.

12. Mitchell, A.R.: Direct force mode flight control for vectored lift fighter. AIAA 79-1744.

13. Etkin, B.: Dynamics of atmospheric flight. John Wiley & Sons, New York, 1972.(ISBN 0-471-24620-4)

14. Van Nauta Lemke, H.R.(ed.): Ontwerpen en berekenen met polen en nulpunten. Regeltechnische Monografieën, deel 3, 1965.

table 2.1: WEIGHT AND BALANCE IN MODELS USED

BEAVER MODEL 1968:

relevant values:

$m = 2215$ kg

$I_{yy} = 6549.9$ kgm^2

further values required by CASPAR LINMAIN as input data:

$I_{xx} = 4167.8$ kgm^2

$I_{zz} = 9806.6$ kgm^2

$J_{xz} = -359.9$ kgm^2

BEAVER MODEL 1982:

relevant values:

$m = 2342.5$ kg

$I_{yy} = 6948.8$ kgm^2

further values required by CASPAR LINMAIN as input data:

$I_{xx} = 5345.5$ kgm^2

$I_{zz} = 11198.5$ kgm^2

$J_{xz} = 171.6$ kgm^2

forward c.g. position:	x_{cg} = 0.276 m	(17.4 % m.a.c.)
	z_{cg} = -0.892 m	
standard c.g. position:	x_{cg} = 0.494 m	(31.1 % m.a.c.)
	z_{cg} = -0.892 m	
rear c.g. position:	x_{cg} = 0.639 m	(40.2 % m.a.c.)
	z_{cg} = -0.892 m	

table 2.2: LINEARIZED MODEL OF DHC-2 "BEAVER" (MODEL 1968)
FULLY DIMENSIONAL STATE VECTOR (u w θ q h)
IN BODY AXES
50 M/S (OBSOLETE MODEL)

$$\underline{A} = \begin{pmatrix} -0.034911 & 0.25407 & -9.745 & -5.3417 & 0 \\ -0.21109 & -1.57 & -1.0463 & 48.105 & 0 \\ 0 & 0 & 0 & 1 & 0 \\ 0.027258 & -0.20729 & 0 & -4.1307 & 0 \\ (0) & (-1) & 50 & 0 & 0 \end{pmatrix}$$

$$\underline{B} = \begin{pmatrix} 0 & 1.9414 \\ -7.7656 & -.47186 \\ 0 & 0 \\ -15.845 & 0 \\ 0 & 0 \end{pmatrix}$$

$V = 50$ m/s
$h = 1800$ mSA
$\gamma = 0$ rad
$p_z = 22,2$ "Hg
$n = 2000$ rpm

table 2.3 (a): LINEARIZED MODEL OF THE DHC-2 "BEAVER" (MODEL 1982)
FULLY DIMENSIONAL STATE VECTOR (u w θ q h)
IN BODY AXES
50 M/S STANDARD C.G.

$$\underline{A} = \begin{pmatrix} -0.035711 & 0.26871 & -9.7375 & -5.9269 & 0 \\ -0.14789 & -1.3128 & -1.1144 & 46.879 & 0 \\ 0 & 0 & 0 & 1 & 0 \\ 0.04120 & -0.19451 & 0 & -3.5434 & 0 \\ 0.1137 & -0.99351 & 50.0 & 0 & 0 \end{pmatrix}$$

$$\underline{B} = \begin{pmatrix} 0 & 0.074575 \\ -7.4618 & -0.14023 \\ 0 & 0 \\ -13.525 & -0.028336 \\ 0 & 0 \end{pmatrix}$$

$$\underline{C} = \begin{pmatrix} -0.035711 & 0.26871 & 0 & -0.22713 & 0 \\ -0.14789 & -1.3128 & 0 & -2.795 & 0 \end{pmatrix}$$

$$\underline{D} = \begin{pmatrix} 0 & 0.074575 \\ -7.4618 & -0.14023 \end{pmatrix}$$

V = 50 m/s
h = 1800 mSA
α = 0.11424 rad
(6°33')
γ = 0.000 rad
p_z = 21.3 "Hg
n = 2000 rpm

table 2.3 (b): LINEARIZED MODEL OF THE DHC-2 "BEAVER" (MODEL 1982)
FULLY DIMENSIONAL STATE VECTOR (u w θ q h)
IN BODY AXES
80 M/S STANDARD C.G.

$$\underline{A} = \begin{pmatrix} -0.062973 & 0.22551 & -9.8004 & -2.7413 & 0 \\ -0.073865 & -2.3783 & 0.11133 & 75.492 & 0 \\ 0 & 0 & 0 & 1 & 0 \\ 0.028146 & -0.26414 & 0 & -5.6695 & 0 \\ -0.011359 & -0.99993 & 79.932 & 0 & 0 \end{pmatrix}$$

$$\underline{B} = \begin{pmatrix} 0 & 0.051429 \\ -19.102 & -0.096709 \\ 0 & 0 \\ -34.624 & -0.019541 \\ 0 & 0 \end{pmatrix}$$

$$\underline{C} = \begin{pmatrix} -0.062973 & 0.2251 & 0 & -0.36342 & 0 \\ -0.073865 & -2.3783 & 0 & -4.4721 & 0 \end{pmatrix}$$

$$\underline{D} = \begin{pmatrix} 0 & 0.051429 \\ -19.102 & -0.096709 \end{pmatrix}$$

V = 80 m/s
h = 1800 mSA
α = 0.029728 rad (+1°42')
γ = -0.041088 rad (-2°21') (N.B. flight not horizontal)
p_z = 37.0 "Hg
n = 2300 rpm

table 2.3 (c): LINEARIZED MODEL OF THE DHC-2 "BEAVER" (MODEL 1982)
FULLY DIMENSIONAL STATE VECTOR (u w θ q h)
IN BODY AXES
35 M/S STANDARD C.G.

$$\underline{A} = \begin{pmatrix} -0.025526 & 0.35902 & -9.4515 & -9.3972 & 0 \\ -0.20371 & -0.73242 & -2.5941 & 31.802 & 0 \\ 0 & 0 & 0 & 1 & 0 \\ 0.075989 & -0.16540 & 0 & -2.4804 & 0 \\ 0.26468 & -0.96433 & 35.0 & 0 & 0 \end{pmatrix}$$

$$\underline{B} = \begin{pmatrix} 0 & 0.093489 \\ -3.6563 & -0.1758 \\ 0 & 0 \\ -6.6272 & -0.035523 \\ 0 & 0 \end{pmatrix}$$

$$\underline{C} = \begin{pmatrix} -0.025526 & 0.35902 & 0 & -0.15899 & 0 \\ -0.20731 & -0.73242 & 0 & -1.95659 & 0 \end{pmatrix}$$

$$\underline{D} = \begin{pmatrix} 0 & 0.093489 \\ -3.6563 & -0.1758 \end{pmatrix}$$

V = 35 m/s
h = 1800 mSA
α = .26711 rad
(15°18')
γ = 0.00 rad
p_z = 20.0 "Hg
n = 2000 rpm

table 2.3 (d): LINEARIZED MODEL OF THE DHC-2 "BEAVER" (MODEL 1982)
FULLY DIMENSIONAL STATE VECTOR (u w θ q h)
IN BODY AXES
50 M/S FORWARD C.G.

$$\underline{A} = \begin{pmatrix} -0.03468 & 0.27991 & -9.7283 & -6.2855 & 0 \\ -0.1424 & -1.2973 & -1.1919 & 46.836 & 0 \\ 0 & 0 & 0 & 1 & 0 \\ 0.060369 & -0.28877 & 0 & -3.7485 & 0 \\ 0.1216 & -0.99257 & 50 & 0 & 0 \end{pmatrix}$$

$$\underline{B} = \begin{pmatrix} 0 & 0.074733 \\ -7.4618 & -0.014052 \\ 0 & 0 \\ -14.072 & -0.038709 \\ 0 & 0 \end{pmatrix}$$

$$\underline{C} = \begin{pmatrix} -0.03468 & 0.27791 & 0 & -0.22713 & 0 \\ -0.1424 & -1.2973 & 0 & -2.795 & 0 \end{pmatrix}$$

$$\underline{D} = \begin{pmatrix} 0 & 0.074733 \\ -7.4618 & -0.14015 \end{pmatrix}$$

V = 50 m/s
h = 1800 mSA
α = .12146 rad
(6°58')
γ = 0.000 rad
p_z = 21.0 "Hg
n = 2000 rpm

table 2.3 (e): LINEARIZED MODEL OF THE DHC-2 "BEAVER" (MODEL 1982)
FULLY DIMENSIONAL STATE VECTOR (u w θ q h)
IN BODY AXES
50 M/S AFT C.G.

$$\underline{A} = \begin{pmatrix} -0.036395 & 0.26135 & -9.7429 & -5.690 & 0 \\ -0.15163 & -1.323 & -1.0656 & 46.905 & 0 \\ 0 & 0 & 0 & 1 & 0 \\ 0.028835 & -0.13014 & 0 & -3.4065 & 0 \\ 0.10872 & -0.99407 & 50.0 & 0 & 0 \end{pmatrix}$$

$$\underline{B} = \begin{pmatrix} 0 & 0.07447 \\ -7.4618 & -0.14003 \\ 0 & 0 \\ -13.159 & -0.021437 \\ 0 & 0 \end{pmatrix}$$

$$\underline{C} = \begin{pmatrix} -0.036395 & 0.26134 & 0 & -0.22713 & 0 \\ -0.15163 & -1.323 & 0 & -2.795 & 0 \end{pmatrix}$$

$$\underline{D} = \begin{pmatrix} 0 & 0.07447 \\ -7.4618 & -0.14003 \end{pmatrix}$$

V = 50 m/s
h = 1800 mSA
α = 0.10947 rad
(6°01')
γ = 0.00 rad
p_z = 21.5 "Hg
n = 2000 rpm

table 2.4: TRANSFORMATION OF THE SYSTEM MATRIX ELEMENTS FROM FULLY DIMENSIONAL SYSTEM IN BODY AXES (WITH ASTERISK) TO NON DIMENSIONAL STATE VECTOR IN STABILITY AXES

$$x_u = x_u^* \cos^2\alpha_o + (x_w^* + z_u^*).\sin\alpha_o.\cos\alpha_o + z_w^* \sin^2\alpha_o$$

$$x_w = x_w^* \cos^2\alpha_o + (-x_u^* + z_w^*).\sin\alpha_o.\cos\alpha_o - z_u^* \sin^2\alpha_o$$

$$z_u = z_u^* \cos^2\alpha_o + (-x_u^* + z_w^*).\sin\alpha_o.\cos\alpha_o - x_w^* \sin^2\alpha_o$$

$$z_w = z_w^* \cos^2\alpha_o - (x_w^* + z_u^*).\sin\alpha_o.\cos\alpha_o + x_u^* \sin^2\alpha_o$$

$$x_\theta = (x_\theta^* \cos\alpha_o + z_\theta^* \sin\alpha_o)/V$$

$$x_q = (x_q^* \cos\alpha_o + z_q^* \sin\alpha_o)/\bar{c}$$

$$z_\theta = (z_\theta^* \cos\alpha_o - x_\theta^* \sin\alpha_o)/V$$

$$z_q = (z_q^* \cos\alpha_o - x_q^* \sin\alpha_o)/\bar{c}$$

$$m_u = (m_u^* \cos\alpha_o + m_w^* \sin\alpha_o).\bar{c}$$

$$m_w = (m_w^* \cos\alpha_o - m_u^* \sin\alpha_o).\bar{c}$$

$$m_\theta = m_\theta^*.\bar{c}/V$$

$$m_q = m_q^*$$

$$x_{\delta e} = (x_{\delta e}^* \cos\alpha_o + z_{\delta e}^* \sin\alpha_o)/V$$

$$z_{\delta e} = (z_{\delta e}^* \cos\alpha_o - x_{\delta e}^* \sin\alpha_o)/V$$

$$m_{\delta e} = m_{\delta e}^*.\bar{c}/V$$

$$x_{\delta t} = (x_{\delta t}^* \cos\alpha_o + z_{\delta t}^* \sin\alpha_o)/V$$

$$z_{\delta t} = (z_{\delta t}^* \cos\alpha_o - x_{\delta t}^* \sin\alpha_o)/V$$

$$m_{\delta t}^* = m_{\delta t}.\bar{c}/V$$

table 2.5 (a): LINEARIZED MODEL OF THE "BEAVER" (MODEL 1982)

NON-DIMENSIONAL STATE VECTOR ($\hat{u}$ α θ $q\bar{c}/V$ h)
AND OUTPUTS A_x/g AND A_y/g
IN STABILITY AXES
50 M/S NORMAL C.G.

$$\underline{A} = \begin{pmatrix} -0.039087 & 0.12251 & -0.1960 & -0.3430 & 0 \\ -0.29409 & -1.3099 & 0 & 29.763 & 0 \\ 0 & 0 & 0 & 31.496 & 0 \\ 0.02978 & -0.3142 & 0 & -3.5434 & 0 \\ 0 & -50 & 50 & 0 & 0 \end{pmatrix}$$

$$\underline{B} = \begin{pmatrix} -0.01701 & 0.00116 \\ -0.1483 & -0.00296 \\ 0 & 0 \\ -0.4294 & -0.00090 \\ 0 & 0 \end{pmatrix}$$

$$\underline{C} = V/g \cdot \begin{pmatrix} -0.039087 & 0.12251 & 0 & -0.3430 & 0 \\ -0.29409 & -1.3099 & 0 & -1.733 & 0 \end{pmatrix}$$

$$\underline{D} = V/g \cdot \begin{pmatrix} -0.01701 & 0.00116 \\ -0.1483 & -0.00296 \end{pmatrix}$$

table 2.5 (b): LINEARIZED MODEL OF THE "BEAVER" (MODEL 1982)

NON-DIMENSIONAL STATE VECTOR ($\hat{u}$ α θ $q\bar{c}/V$ h)
AND OUTPUTS A_x/g AND A_y/g
IN STABILITY AXES
80 M/S NORMAL C.G.

$$\underline{A} = \begin{pmatrix} -0.06051 & 0.15659 & -0.1225 & -0.3126 & 0 \\ -0.14729 & -2.3808 & 0.00503 & 47.584 & 0 \\ 0 & 0 & 0 & 50.394 & 0 \\ 0.03219 & -0.42047 & 0 & -5.6695 & 0 \\ 0 & -80 & 80 & 0 & 0 \end{pmatrix}$$

$$\underline{B} = \begin{pmatrix} -0.00710 & 0.000607 \\ -0.2387 & -0.001227 \\ 0 & 0 \\ -0.6871 & -0.000388 \\ 0 & 0 \end{pmatrix}$$

$$\underline{C} = V/g \cdot \begin{pmatrix} -0.06051 & 0.1565 & 0 & -0.3126 & 0 \\ -0.14279 & -2.3808 & 0 & -2.815 & 0 \end{pmatrix}$$

$$\underline{D} = V/g \cdot \begin{pmatrix} -0.007098 & 0.000607 \\ -0.2387 & -0.001227 \end{pmatrix}$$

N.B. γ = -.41088 rad; $z_\theta^* \approx (g/V).\sin\gamma$

table 2.5 (c): LINEARIZED MODEL OF THE "BEAVER" (MODEL 1982)

NON-DIMENSIONAL STATE VECTOR ($\hat{u}$ α θ $q\bar{c}/V$ h)
AND OUTPUTS A_x/g AND A_y/g
IN STABILITY AXES
35 M/S NORMAL C.G.

$$\underline{A} = \begin{pmatrix} 0.009773 & 0.16489 & -0.2800 & -0.4220 & 0 \\ -0.39784 & -0.721796 & 0 & 20.885 & 0 \\ 0 & 0 & 0 & 22.047 & 0 \\ 0.04705 & -0.2837 & 0 & -2.4804 & 0 \\ 0 & -35 & 35 & 0 & 0 \end{pmatrix}$$

$$\underline{B} = \begin{pmatrix} -0.02757 & 0.00125 \\ -0.10076 & -0.00555 \\ 0 & 0 \\ -0.3006 & -0.00161 \\ 0 & 0 \end{pmatrix}$$

$$\underline{C} = V/g \cdot \begin{pmatrix} 0.009773 & 0.16489 & 0 & -0.4220 & 0 \\ -0.39784 & -0.721796 & 0 & -1.108 & 0 \end{pmatrix}$$

$$\underline{D} = V/g \cdot \begin{pmatrix} -0.02757 & 0.00125 \\ -0.10076 & -0.0555 \end{pmatrix}$$

table 2.5 (d): LINEARIZED MODEL OF THE "BEAVER" (MODEL 1982)

NON-DIMENSIONAL STATE VECTOR ($\hat{u}$ α θ $q\bar{c}/V$ h)
AND OUTPUTS A_x/g AND A_y/g

IN STABILITY AXES
50 M/S FORWARD C.G.

$$\underline{A} = \begin{pmatrix} -0.03651 & 0.1252 & -0.1960 & -0.3556 & 0 \\ -0.2963 & -1.2953 & 0 & 29.765 & 0 \\ 0 & 0 & 0 & 31.496 & 0 \\ 0.0400 & -0.4667 & 0 & -3.7485 & 0 \\ 0 & -50 & 50 & 0 & 0 \end{pmatrix}$$

$$\underline{B} = \begin{pmatrix} -0.0181 & 0.00113 \\ -0.1481 & -0.00216 \\ 0 & 0 \\ -0.4468 & -0.00123 \\ 0 & 0 \end{pmatrix}$$

$$\underline{C} = V/g \cdot \begin{pmatrix} -0.03651 & 0.1252 & 0 & -0.3556 & 0 \\ -0.4468 & -1.2953 & 0 & -1.731 & 0 \end{pmatrix}$$

$$\underline{D} = V/g \cdot \begin{pmatrix} -0.0181 & 0.00113 \\ -0.1481 & -0.00216 \end{pmatrix}$$

table 2.5 (e): LINEARIZED MODEL OF THE "BEAVER" (MODEL 1982)

NON-DIMENSIONAL STATE VECTOR ($\tilde{u}$ α θ $q\bar{c}/V$ h)
AND OUTPUTS A_x/g AND A_y/g
IN STABILITY AXES
50 M/S AFT C.G.

$$\underline{A} = \begin{pmatrix} -0.03984 & 0.1203 & -0.1960 & -0.3348 & 0 \\ -0.2927 & -1.320 & 0 & 29.761 & 0 \\ 0 & 0 & 0 & 31.496 & 0 \\ 0.0229 & -0.2104 & 0 & -3.4065 & 0 \\ 0 & -50 & 50 & 0 & 0 \end{pmatrix}$$

$$\underline{B} = \begin{pmatrix} -0.0163 & 0.00117 \\ -0.1483 & -0.00295 \\ 0 & 0 \\ -0.4178 & -0.00068 \\ 0 & 0 \end{pmatrix}$$

$$\underline{C} = V/g \begin{pmatrix} -0.03984 & 0.1203 & 0 & -0.3348 & 0 \\ -0.2927 & -1.320 & 0 & -1.735 & 0 \end{pmatrix}$$

$$\underline{D} = V/g \begin{pmatrix} -0.0163 & 0.00117 \\ -0.1483 & -0.00295 \end{pmatrix}$$

table 2.6: STEADY-STATE SOLUTIONS TO THE SHORT PERIOD APPROXIMATION TRANSFER FUNCTION FOR δ_e

	$H_{\alpha\delta ess}$		$H_{q\delta ess}$	
	equation (2.17)	equation (2.17) with $z_{\delta e} = 0$	equation (2.17)	equation (2.17) with $z_{\delta e} = 0$
35 m/s	-0.846	-0.814	-0.0244	-0.0281
50 m/s				
forward c.g.	-0.709	-0.741	-0.0272	-0.0309
normal c.g.	-0.951	-0.913	-0.0369	-0.0402
aft c.g.	-1.203	-1.156	-0.0484	-0.0513
80 m/s	-1.016	-0.976	-0.0458	-0.0488

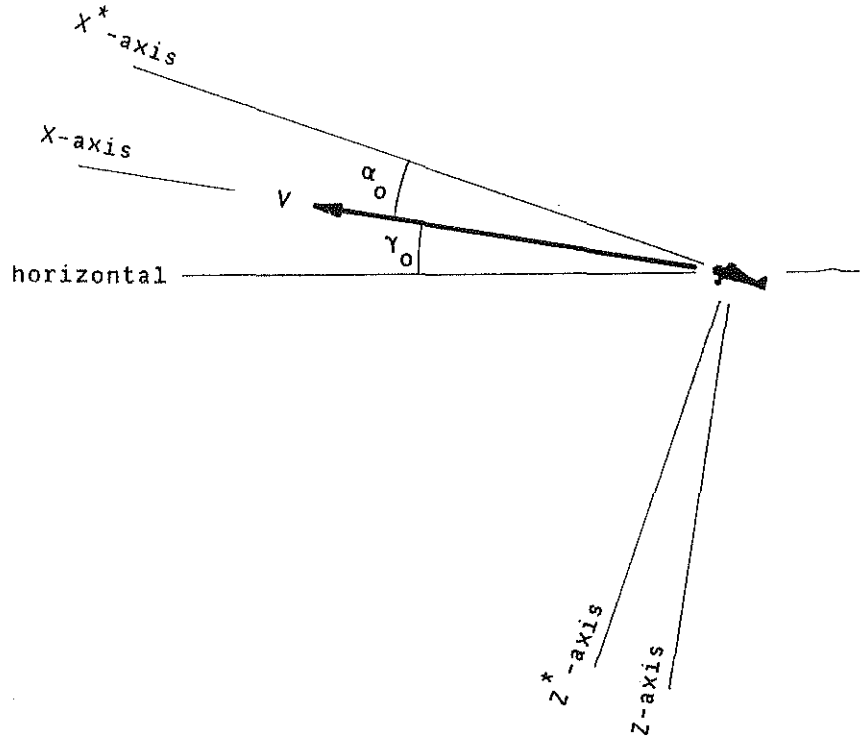

X^*, Z^*	body axes
X, Z	stability axes
V	steady state airspeed
α_o	steady state angle of attack in body axes
γ_o	steady state flight path angle

figure 0.1: The relationship between body axes and stability axes

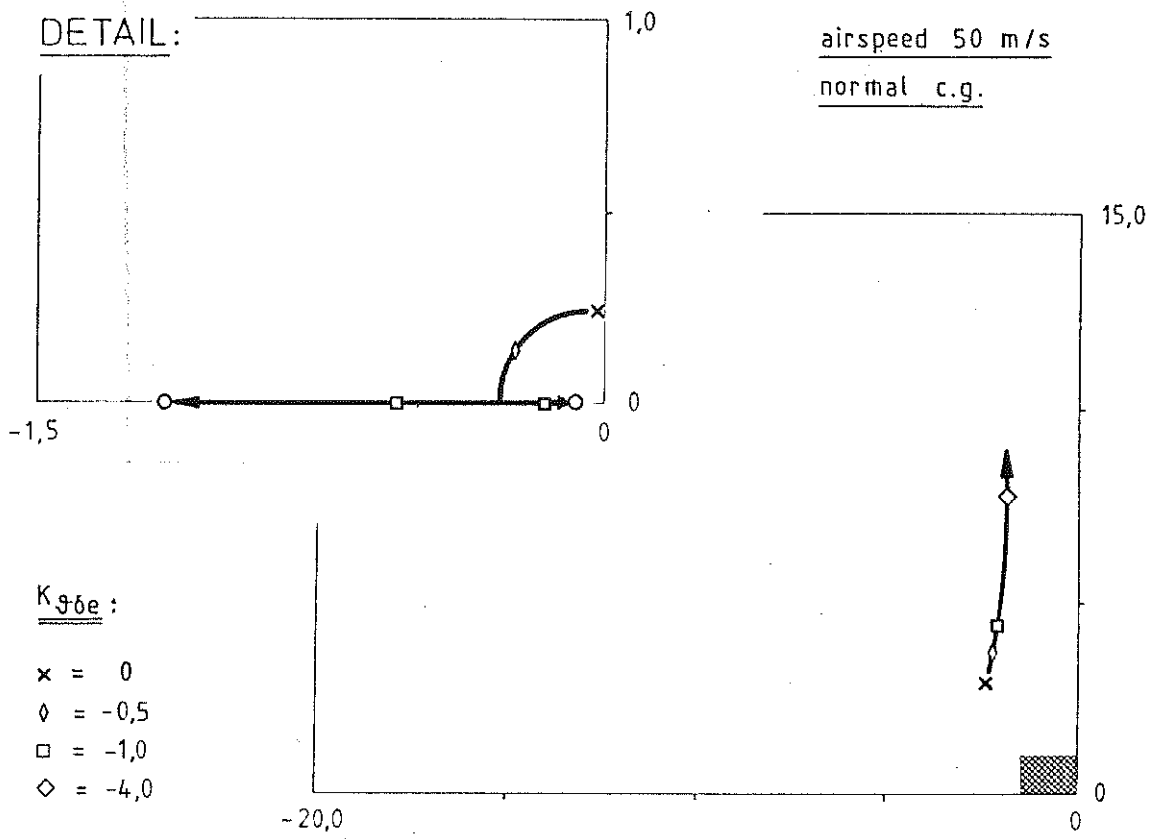

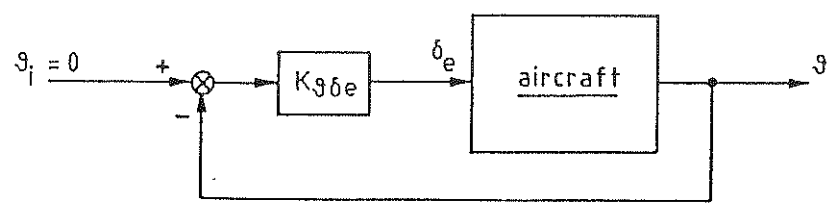

figure 3.1 (a): Root locus for feedback of pitch attitude on elevator

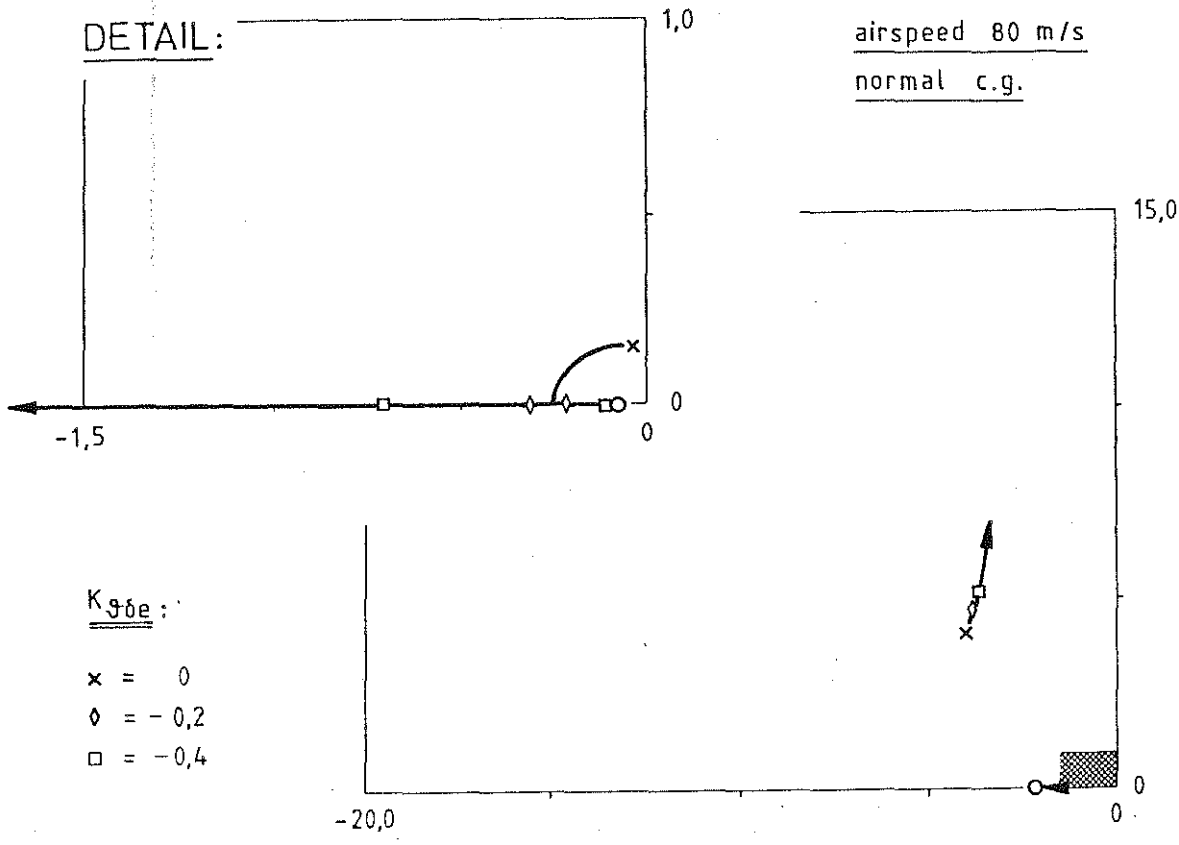

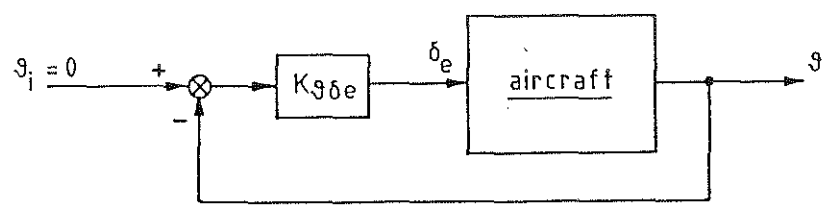

figure 3.1 (b): Root locus for feedback of pitch attitude on elevator

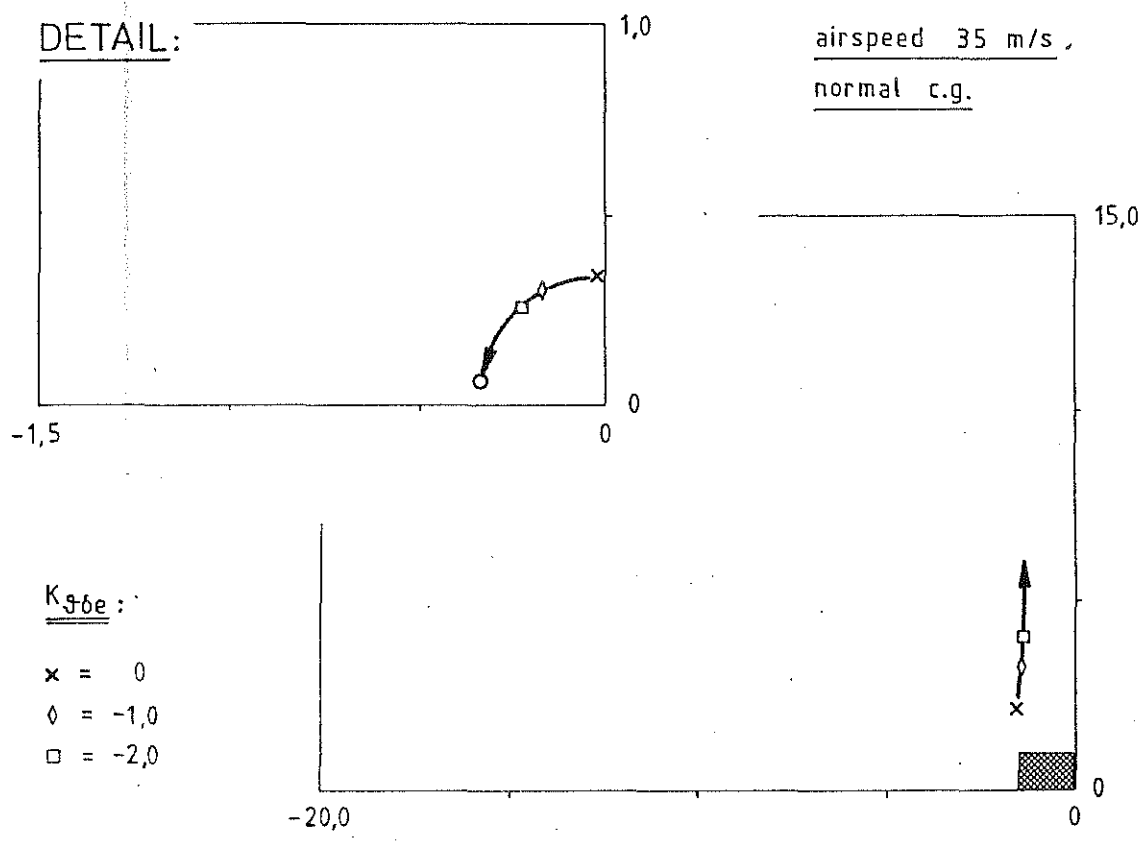

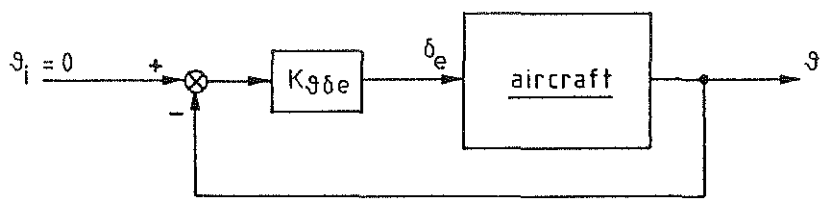

figure 3.1 (c): Root locus for feedback of pitch attitude on elevator

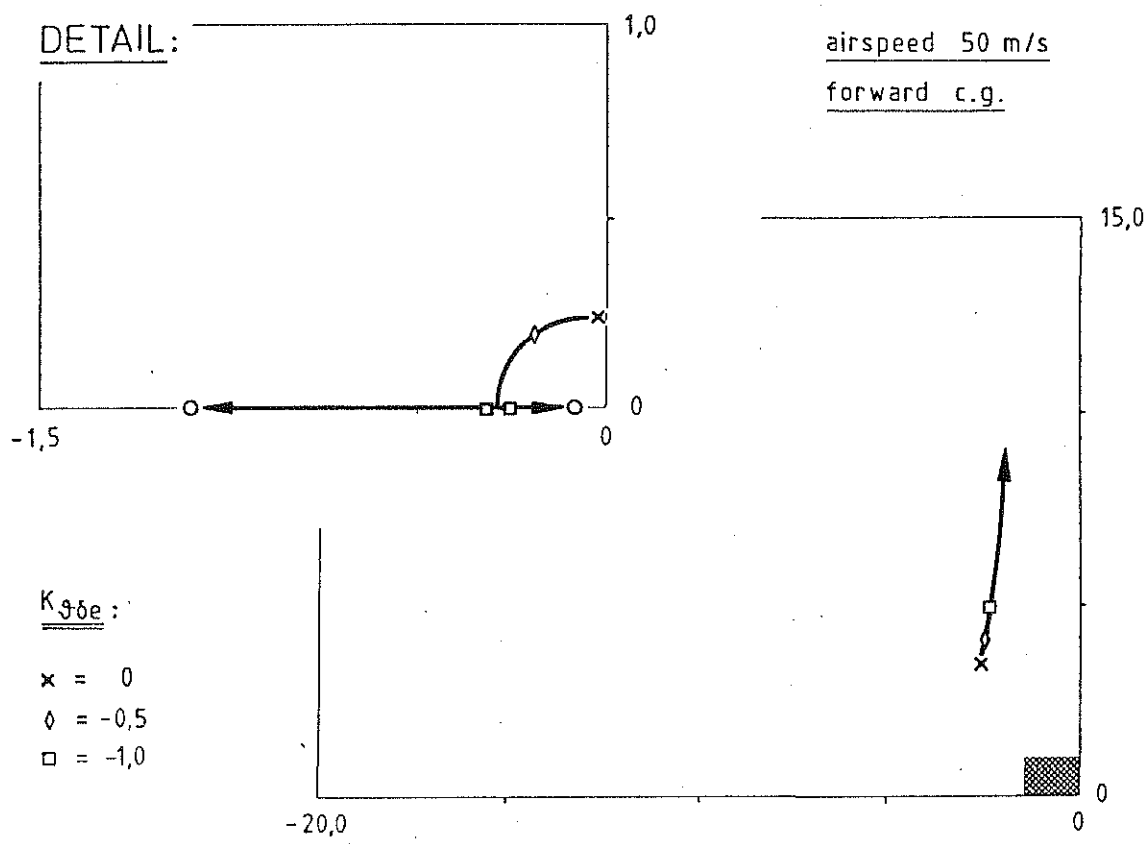

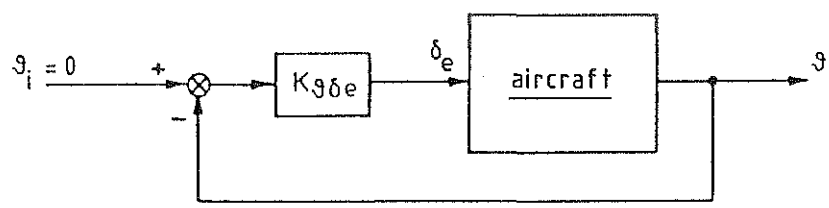

figure 3.1 (d): Root locus for feedback of pitch attitude on elevator

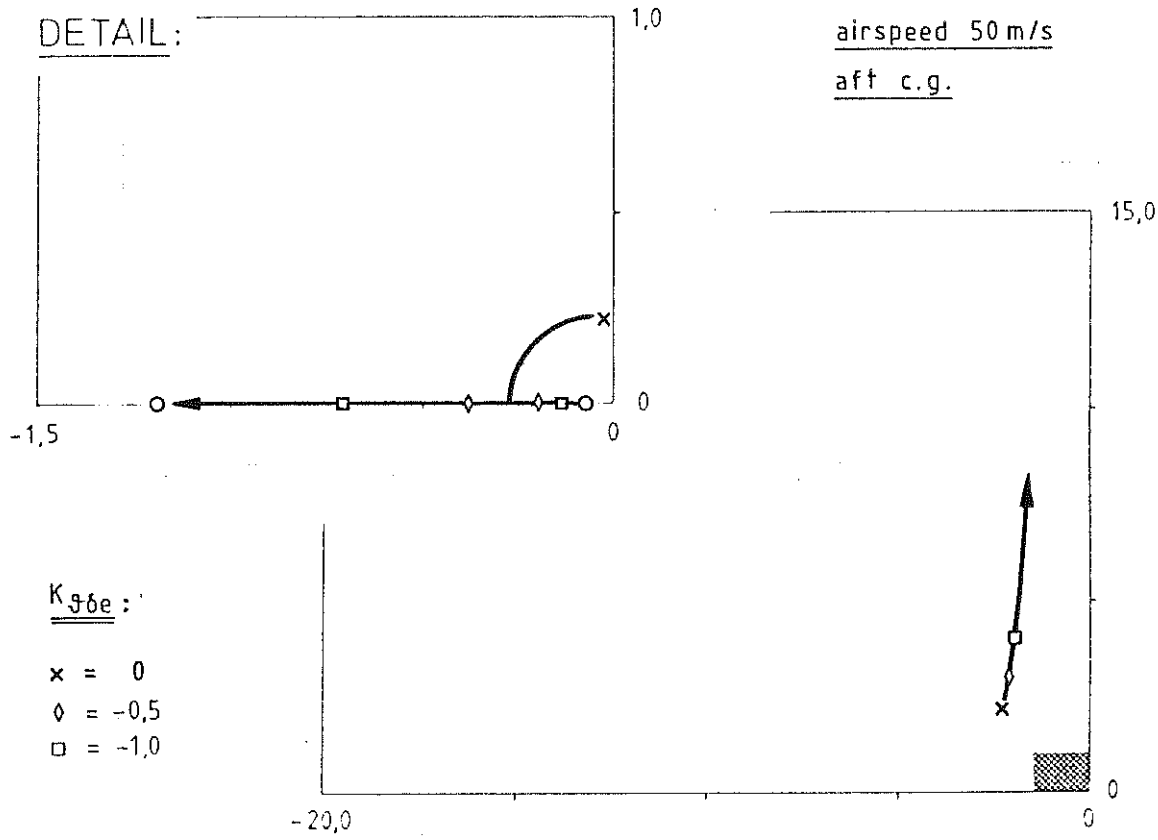

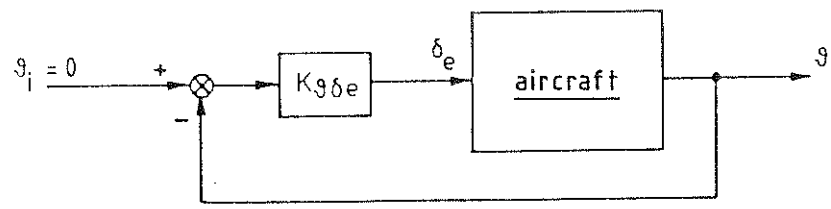

figure 3.1 (e): Root locus for feedback of pitch attitude on elevator

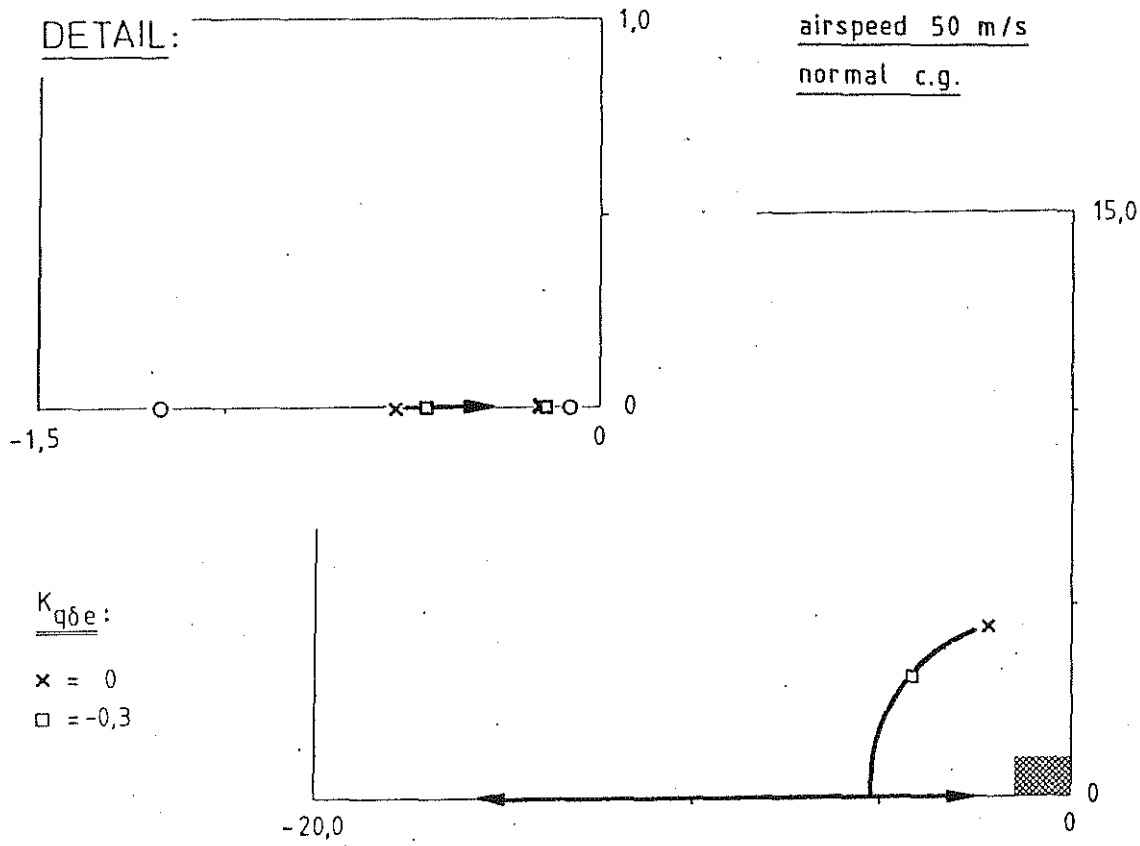

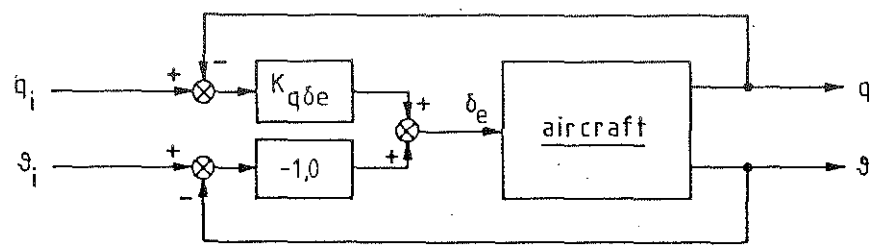

figure 3.2 (a): Root locus for feedback of pitch rate on elevator

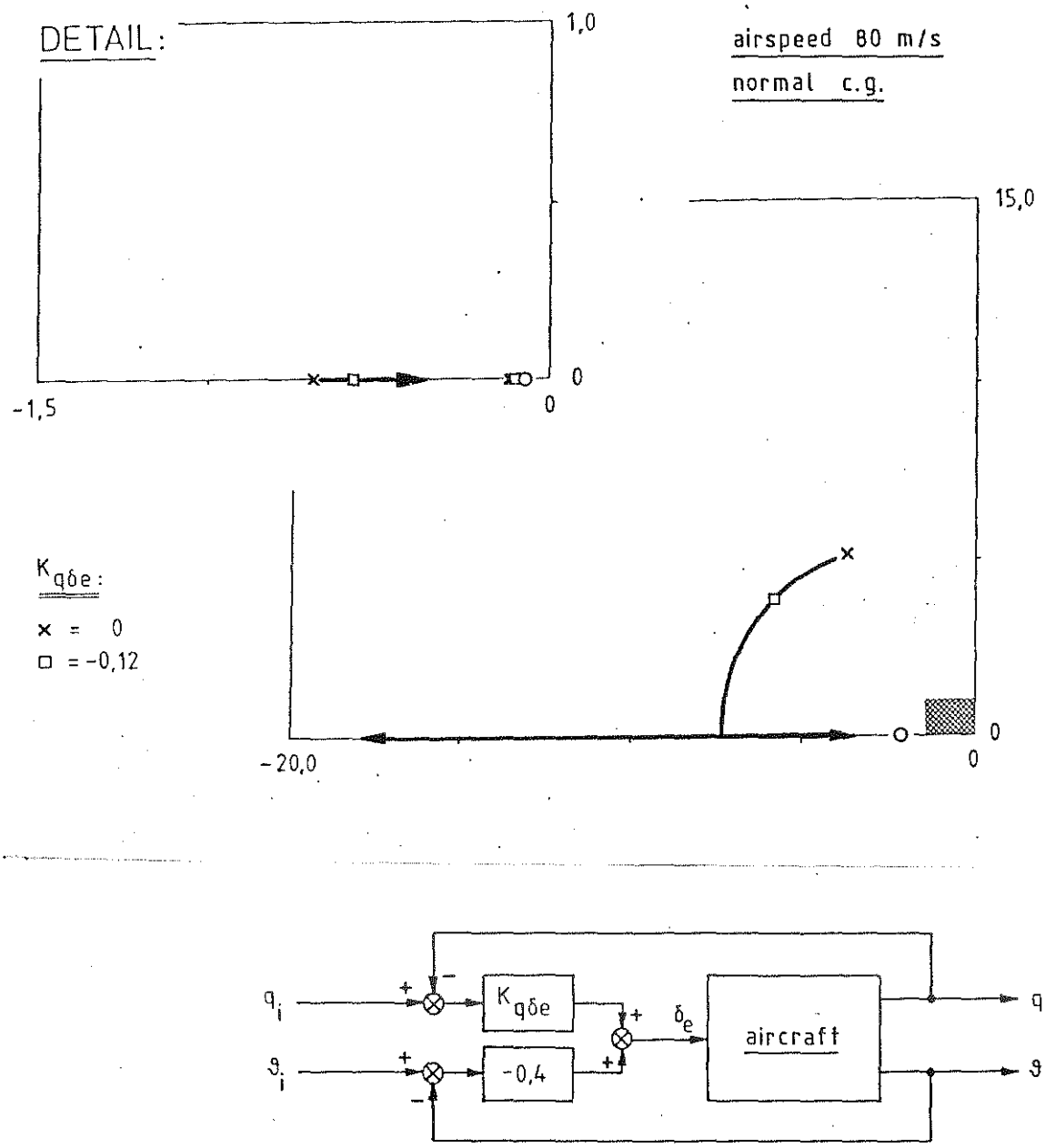

figure 3.2 (b): Root locus for feedback of pitch rate on elevator

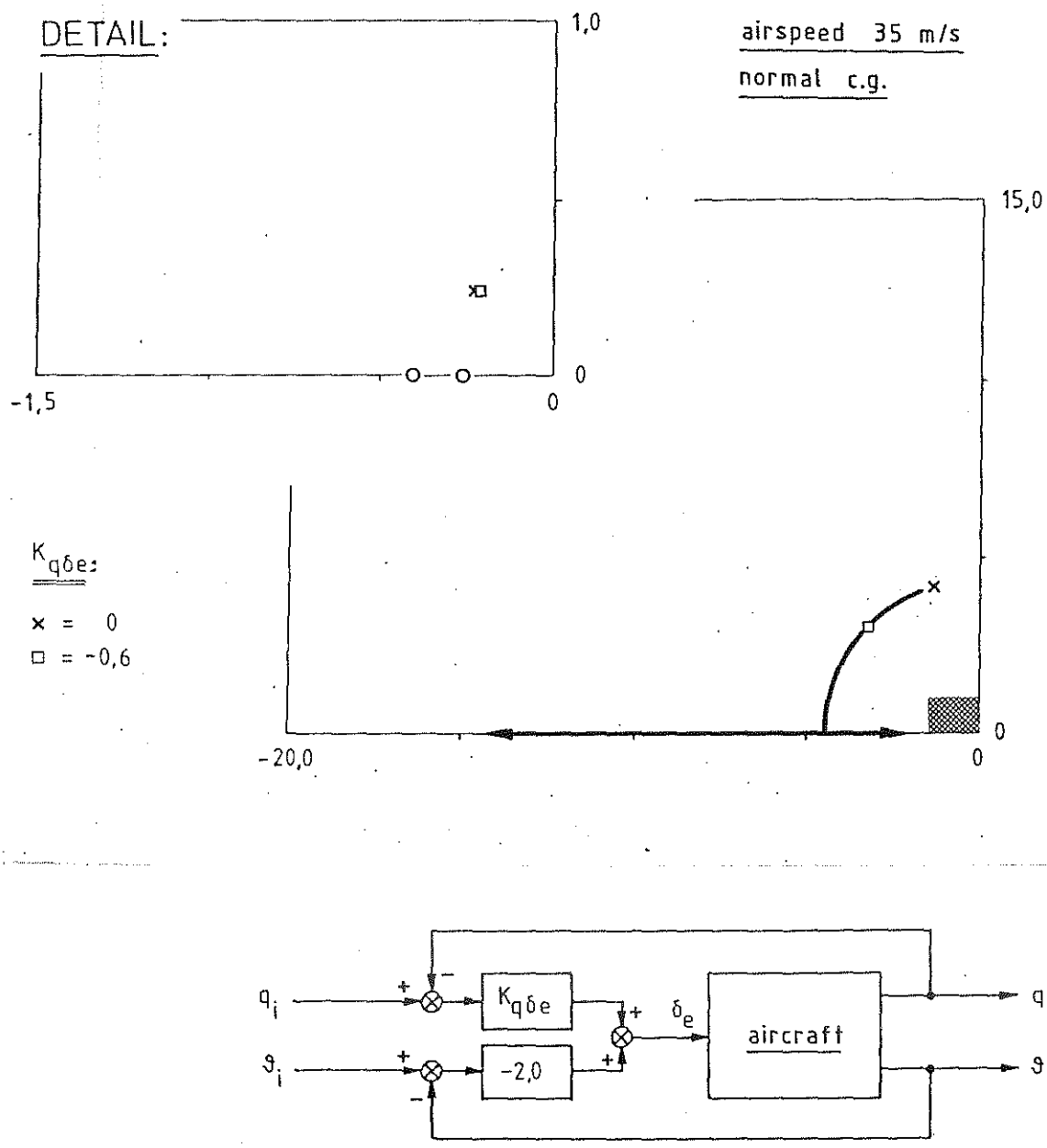

figure 3.2 (c): Root locus for feedback of pitch rate on elevator

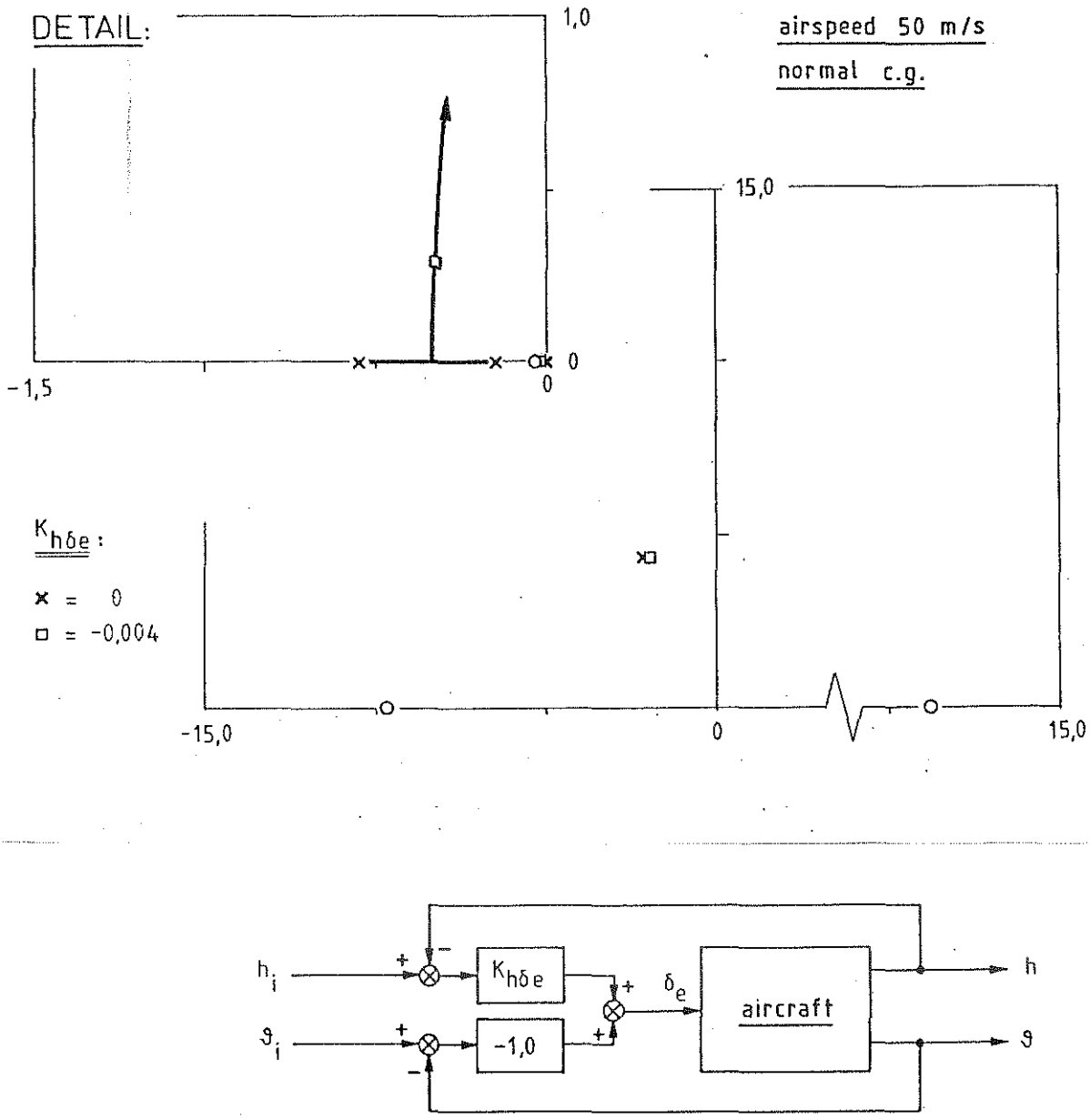

figure 3.3 (a): Root locus for feedback of altitude on elevator

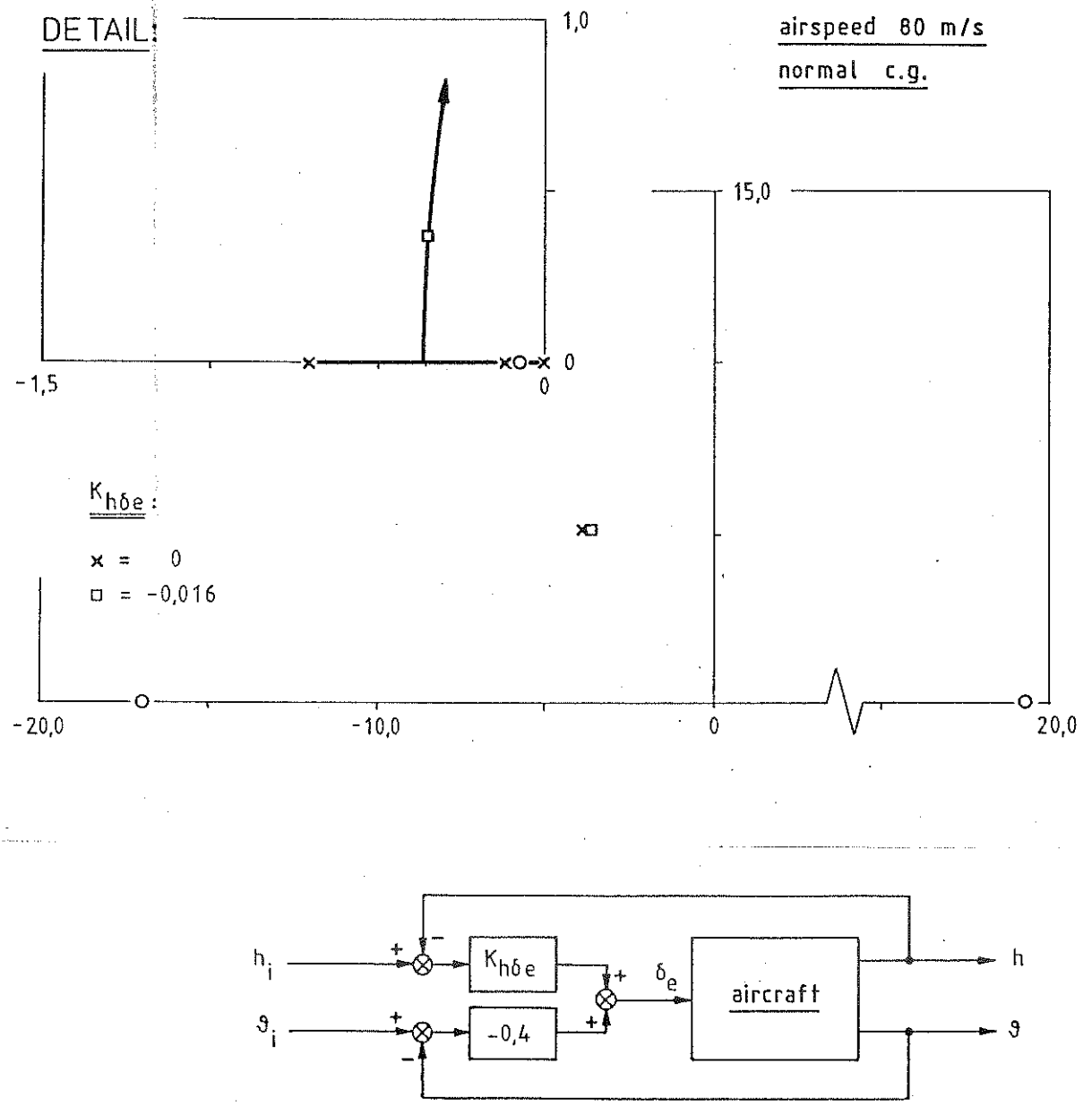

figure 3.3 (b): Root locus for feedback of altitude on elevator

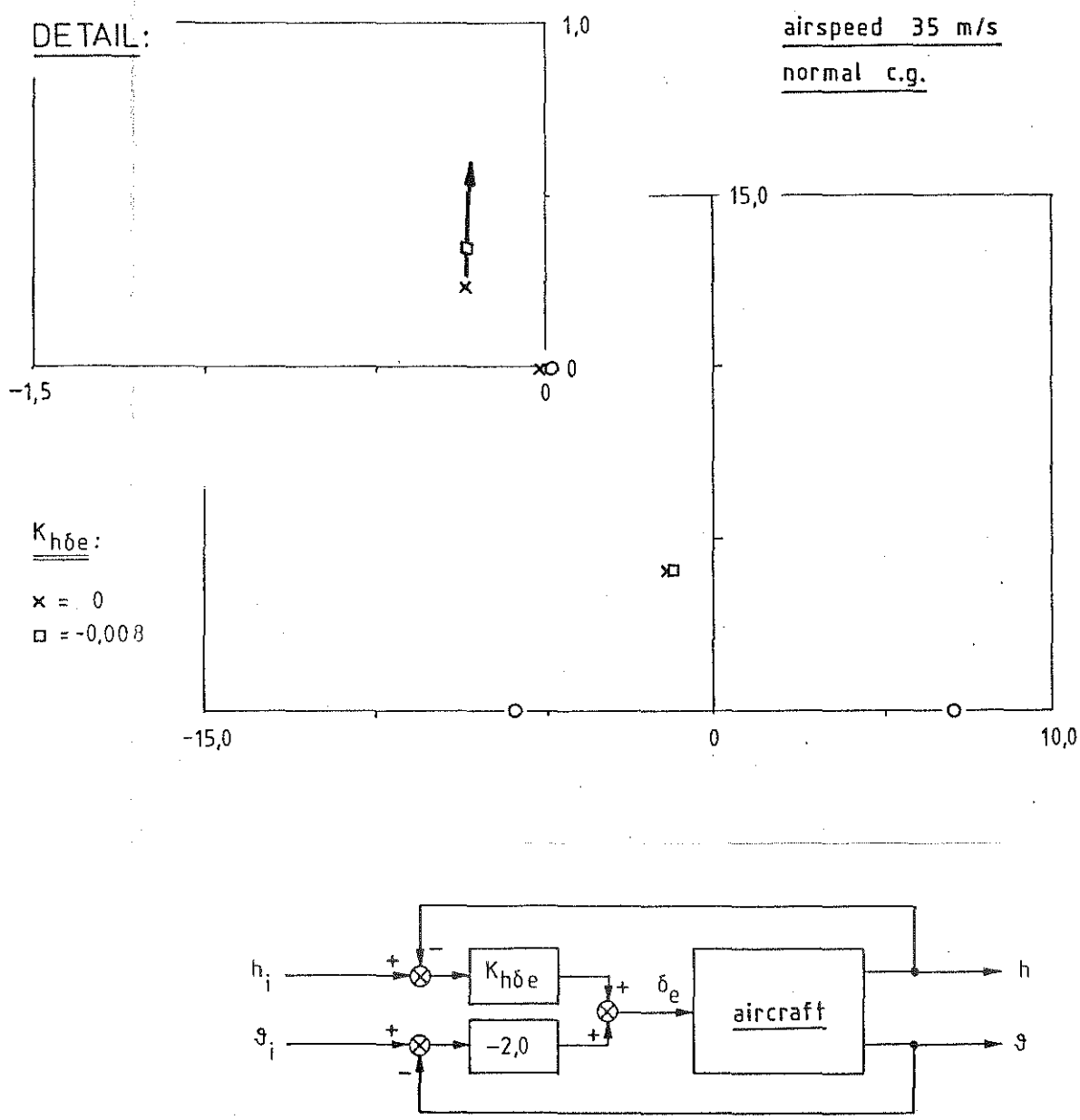

figure 3.3 (c): Root locus for feedback of altitude on elevator

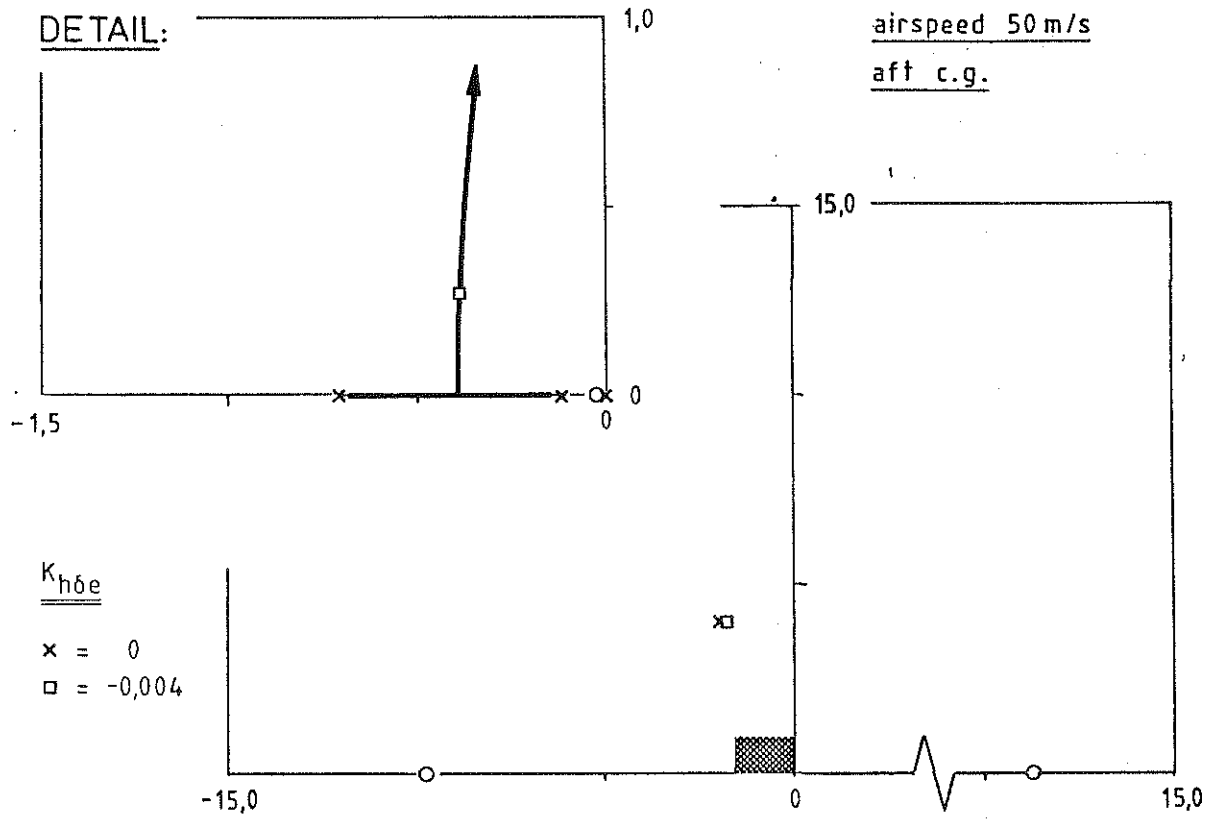

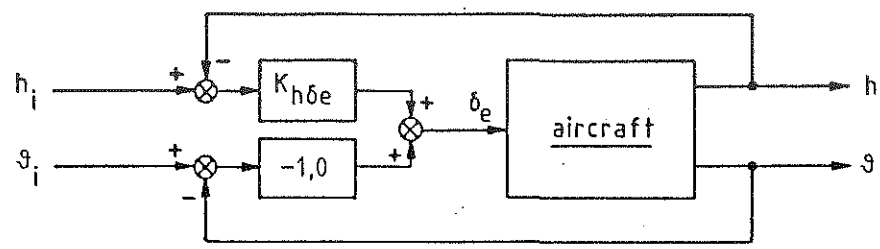

figure 3.3 (e): Root locus for feedback of altitude on elevator

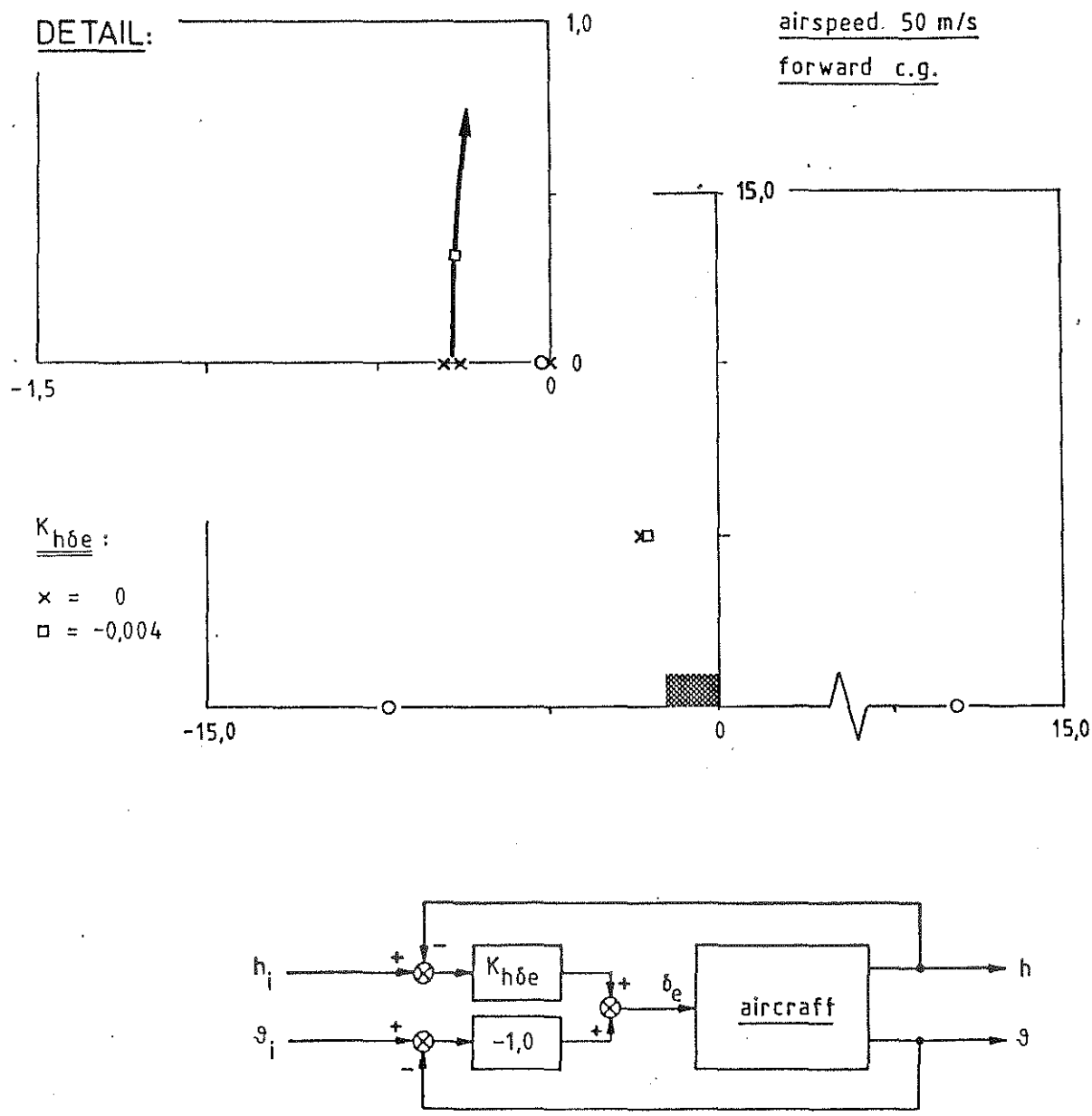

figure 3.3 (d): Root locus for feedback of altitude on elevator

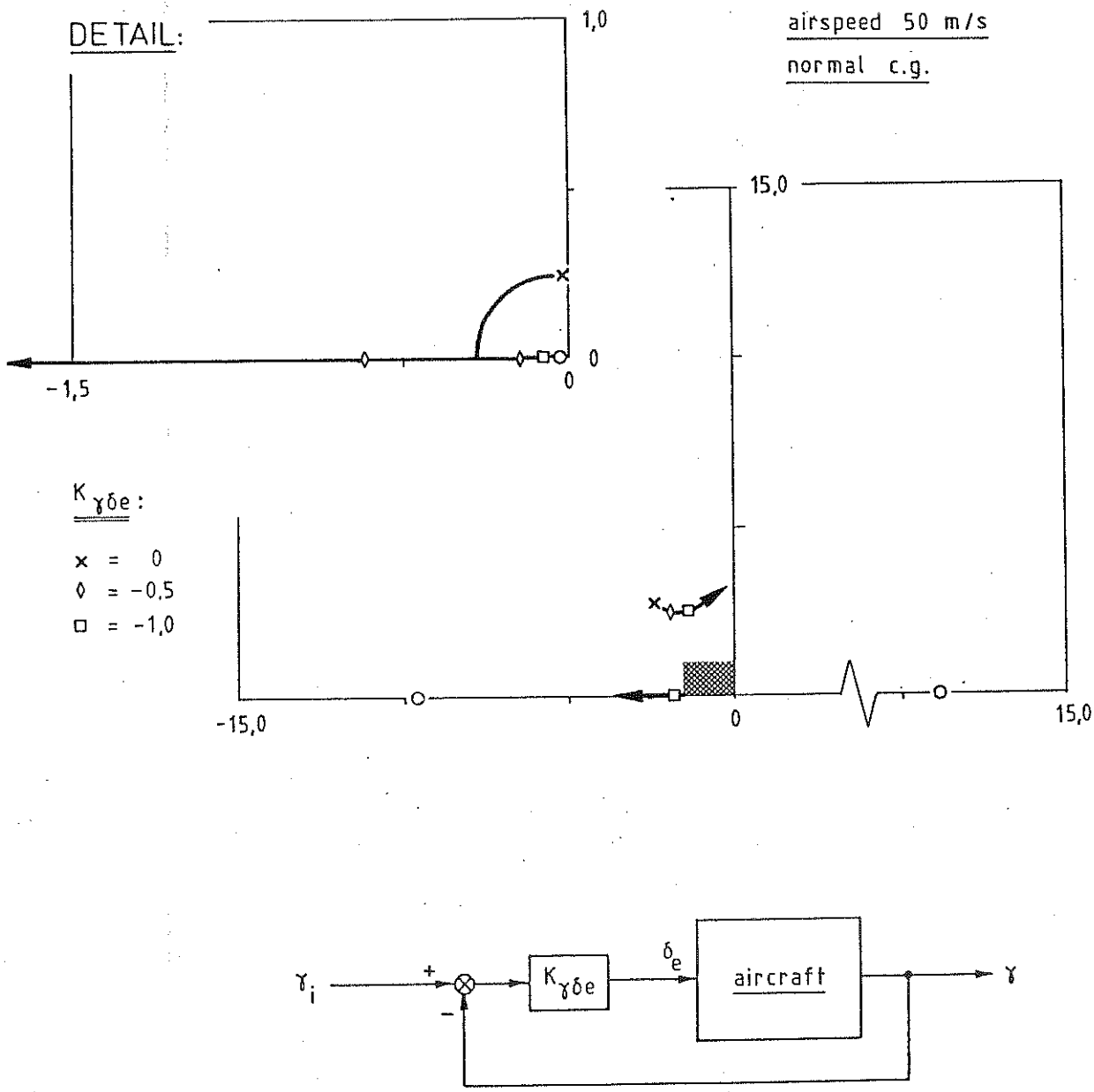

figure 4.1 (a): Root locus for feedback of flight path angle on elevator

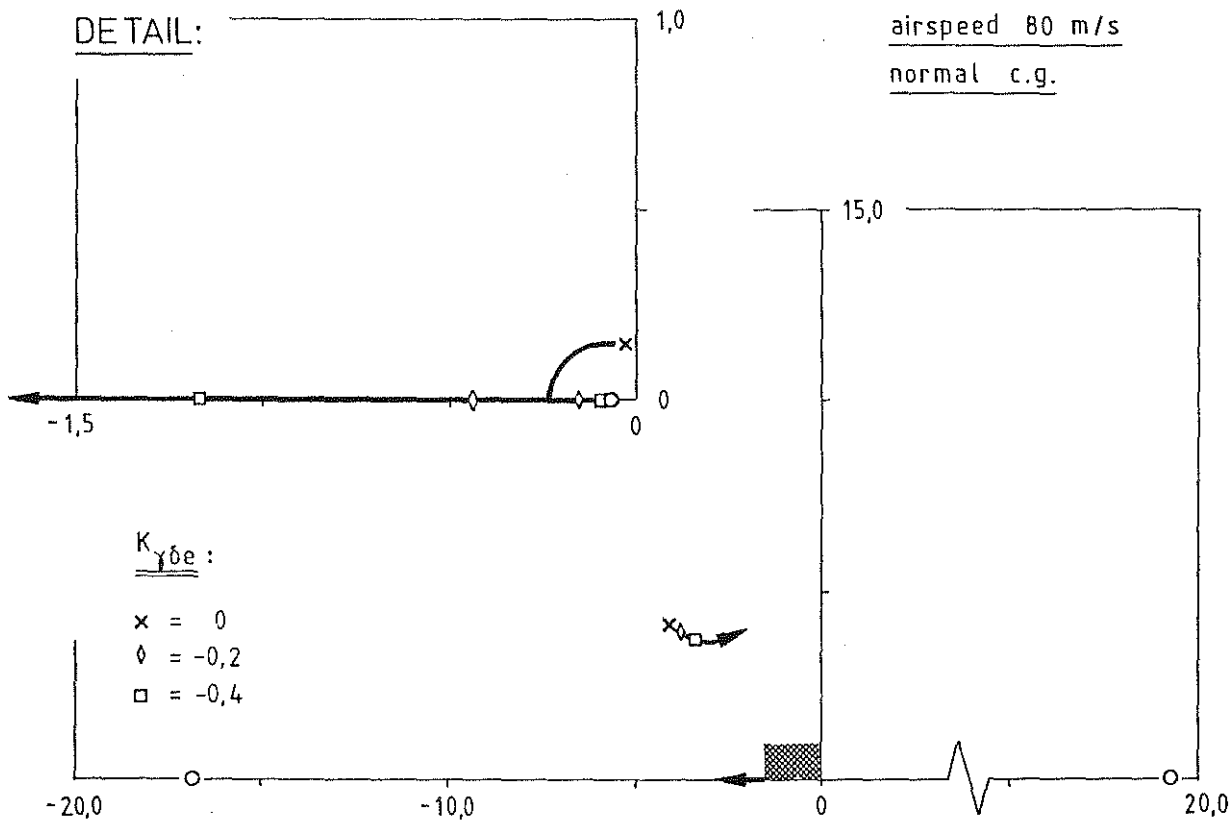

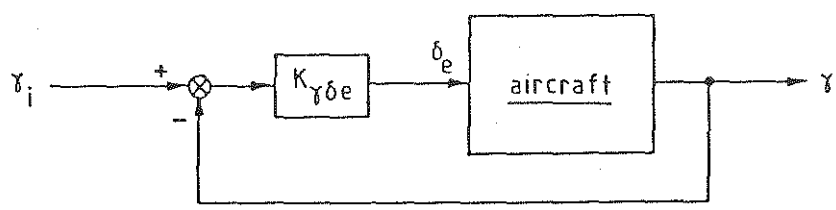

figure 4.1 (b): Root locus for feedback of flight path angle on elevator

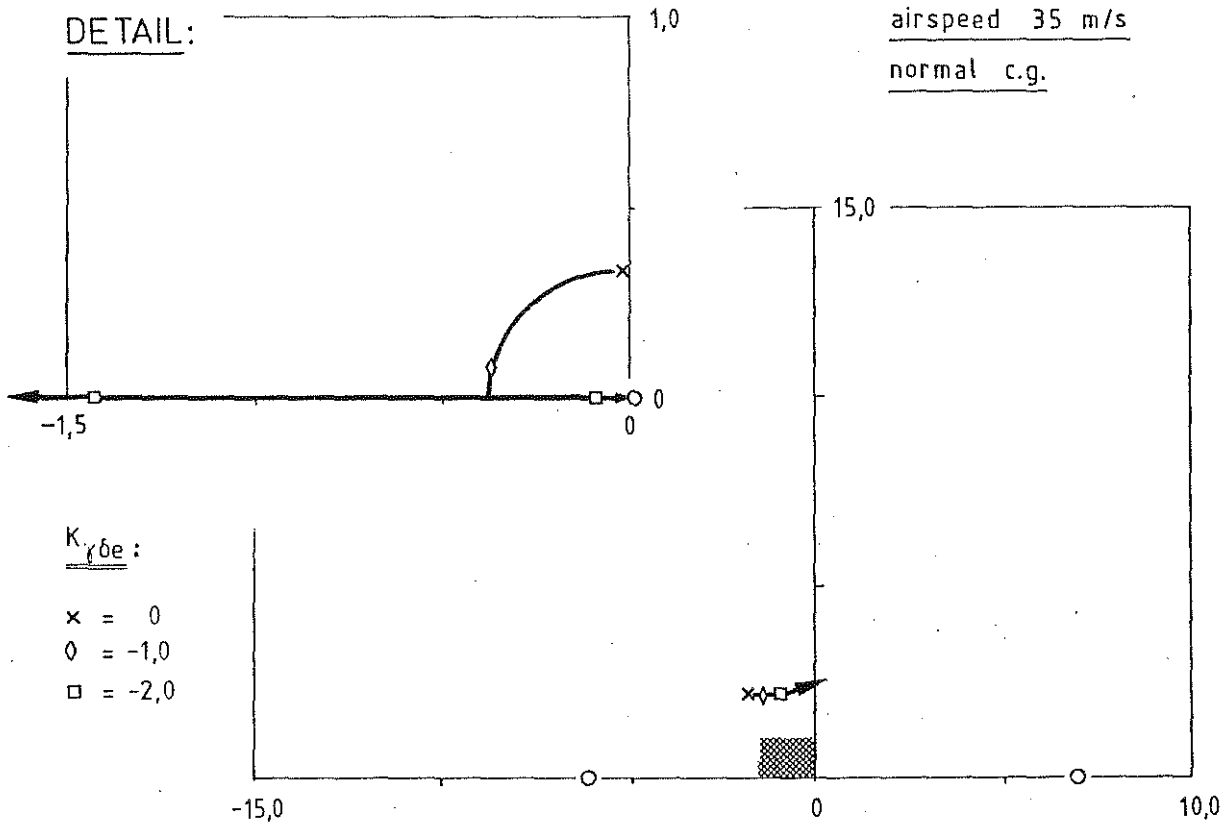

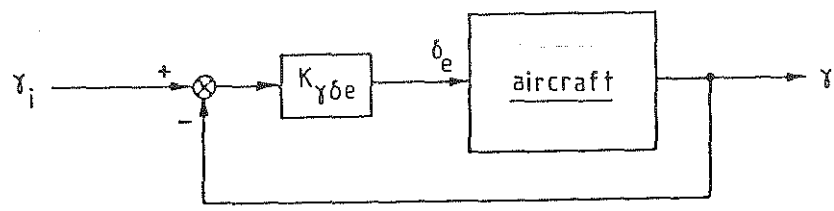

figure 4.1 (c): Root locus for feedback of flight path angle on elevator

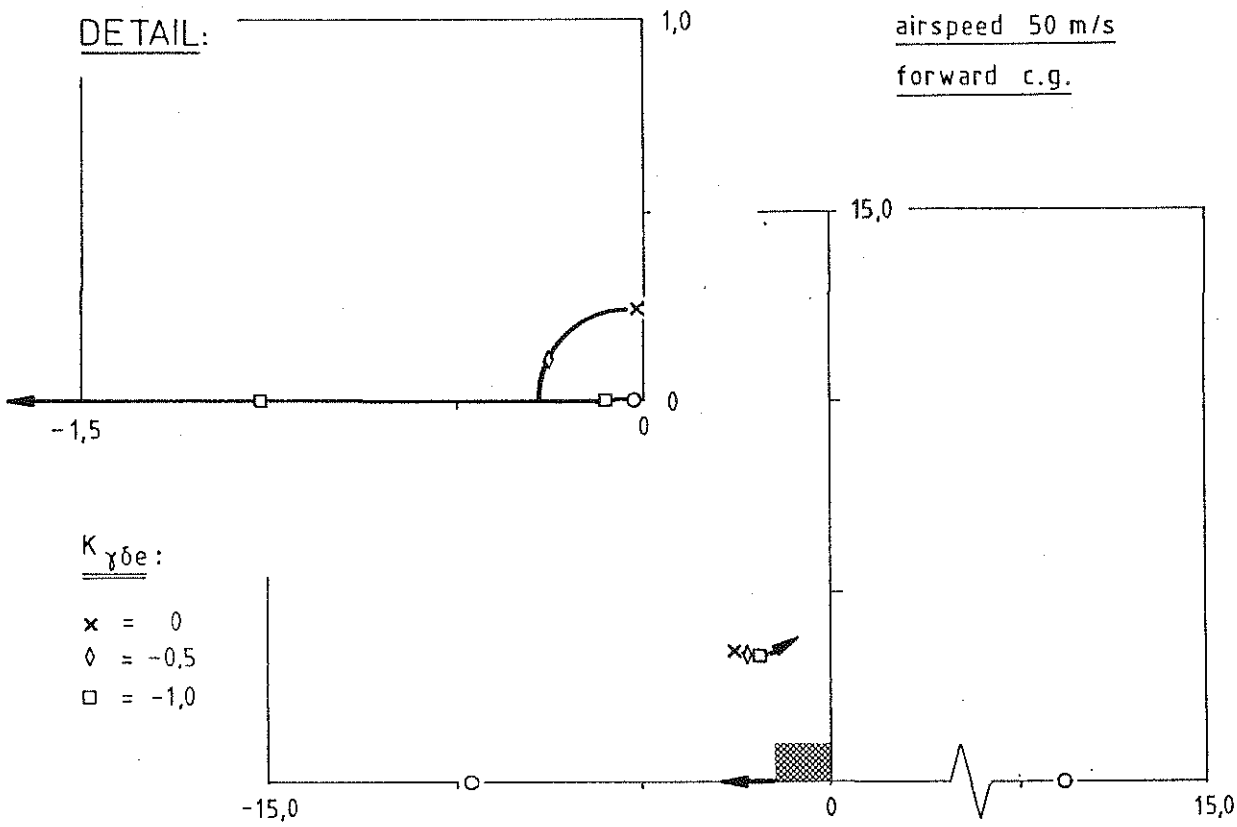

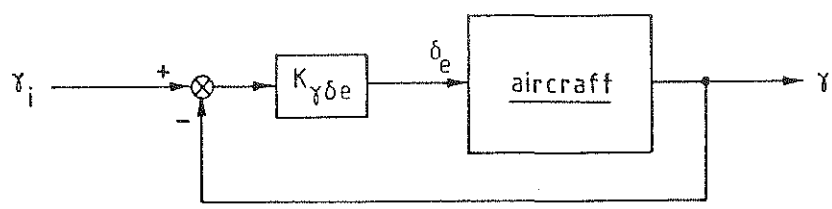

figure 4.1 (d): Root locus for feedback of flight path angle on elevator

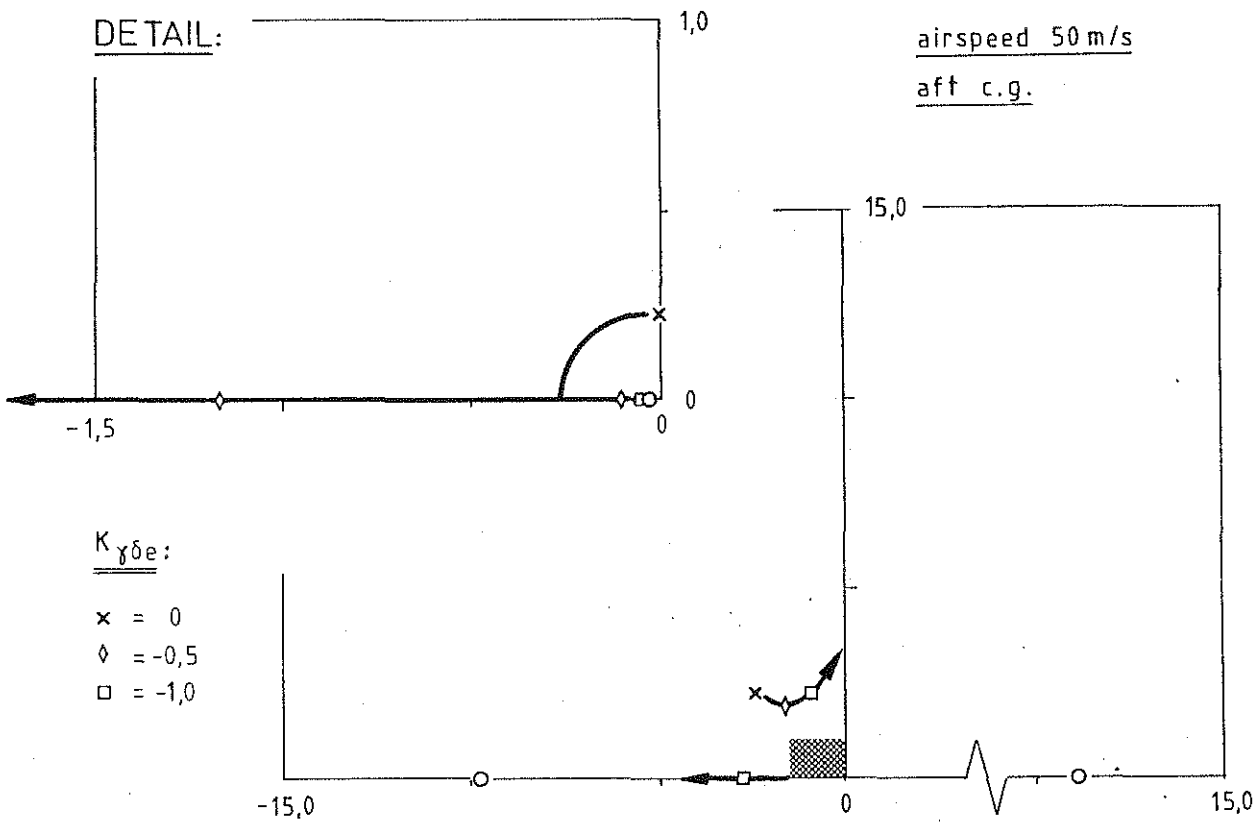

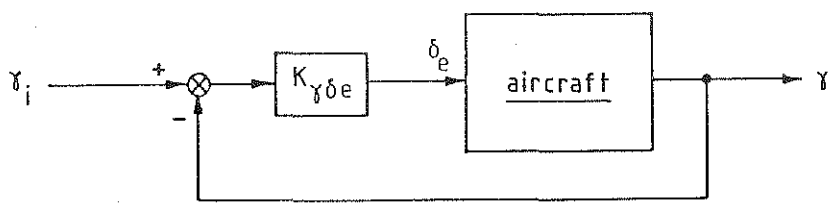

figure 4.1 (e): Root locus for feedback of flight path angle on elevator

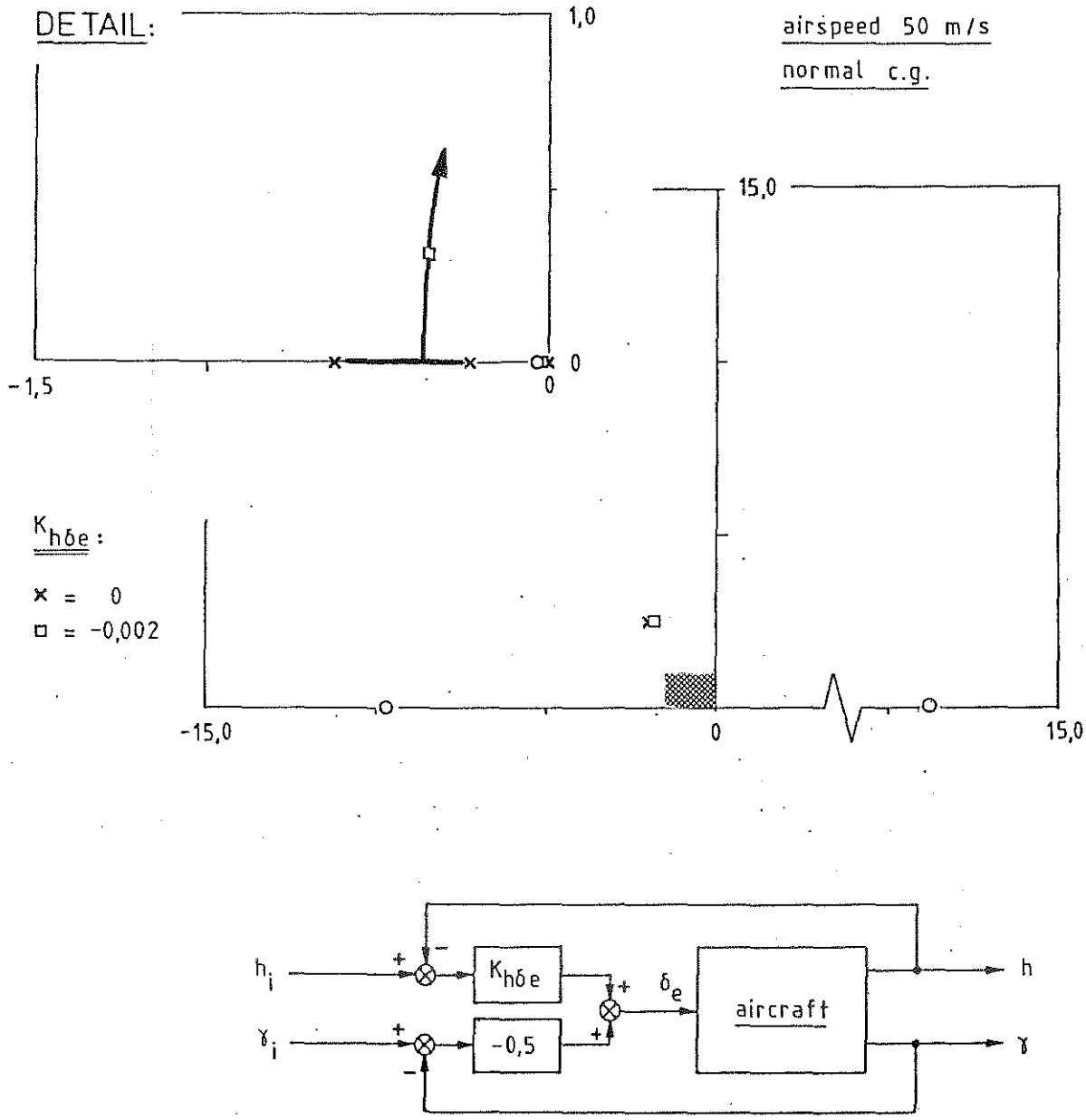

figure 4.2 (a): Root locus for feedback of altitude on elevator

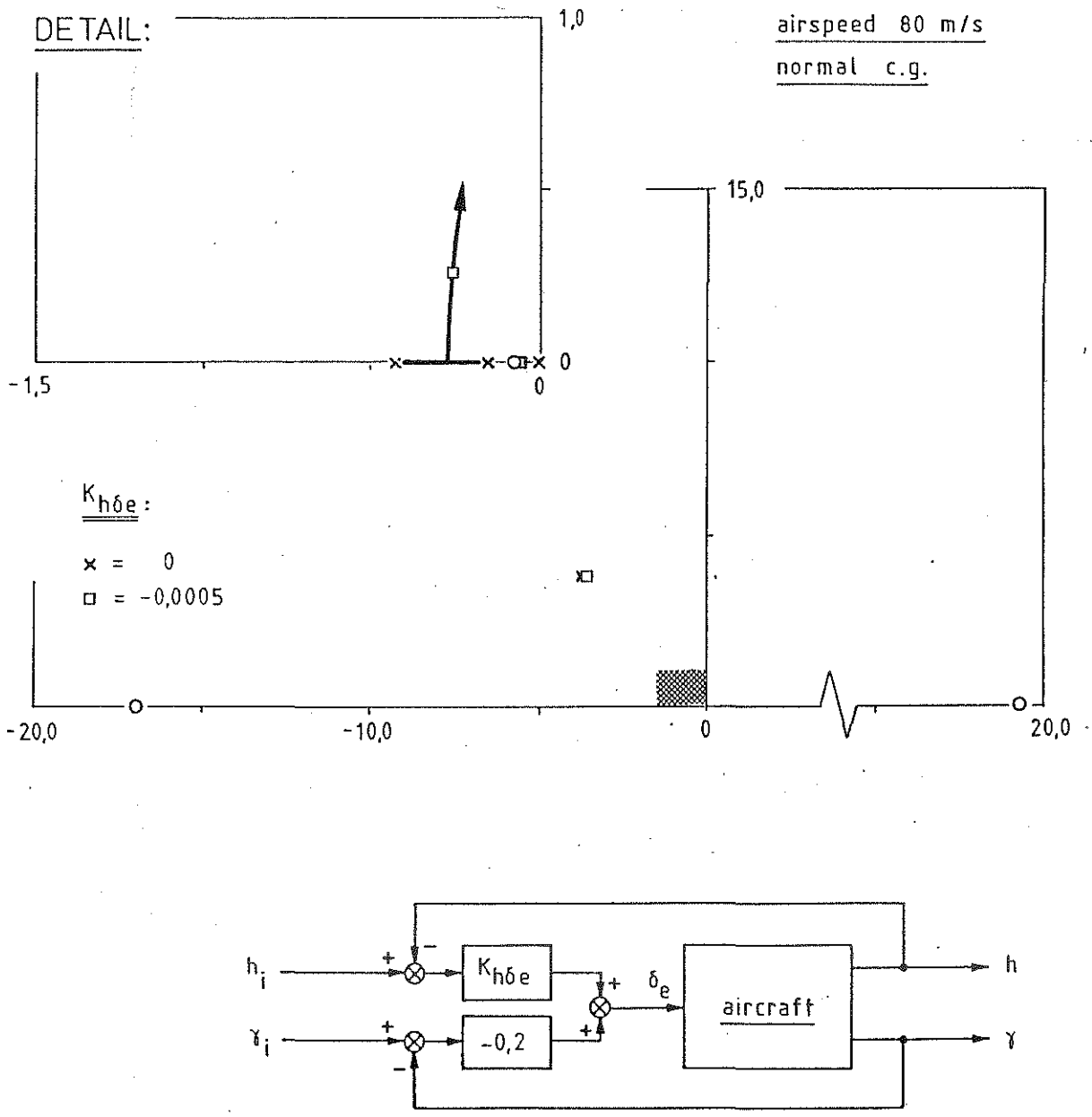

figure 4.2 (b): Root locus for feedback of altitude on elevator

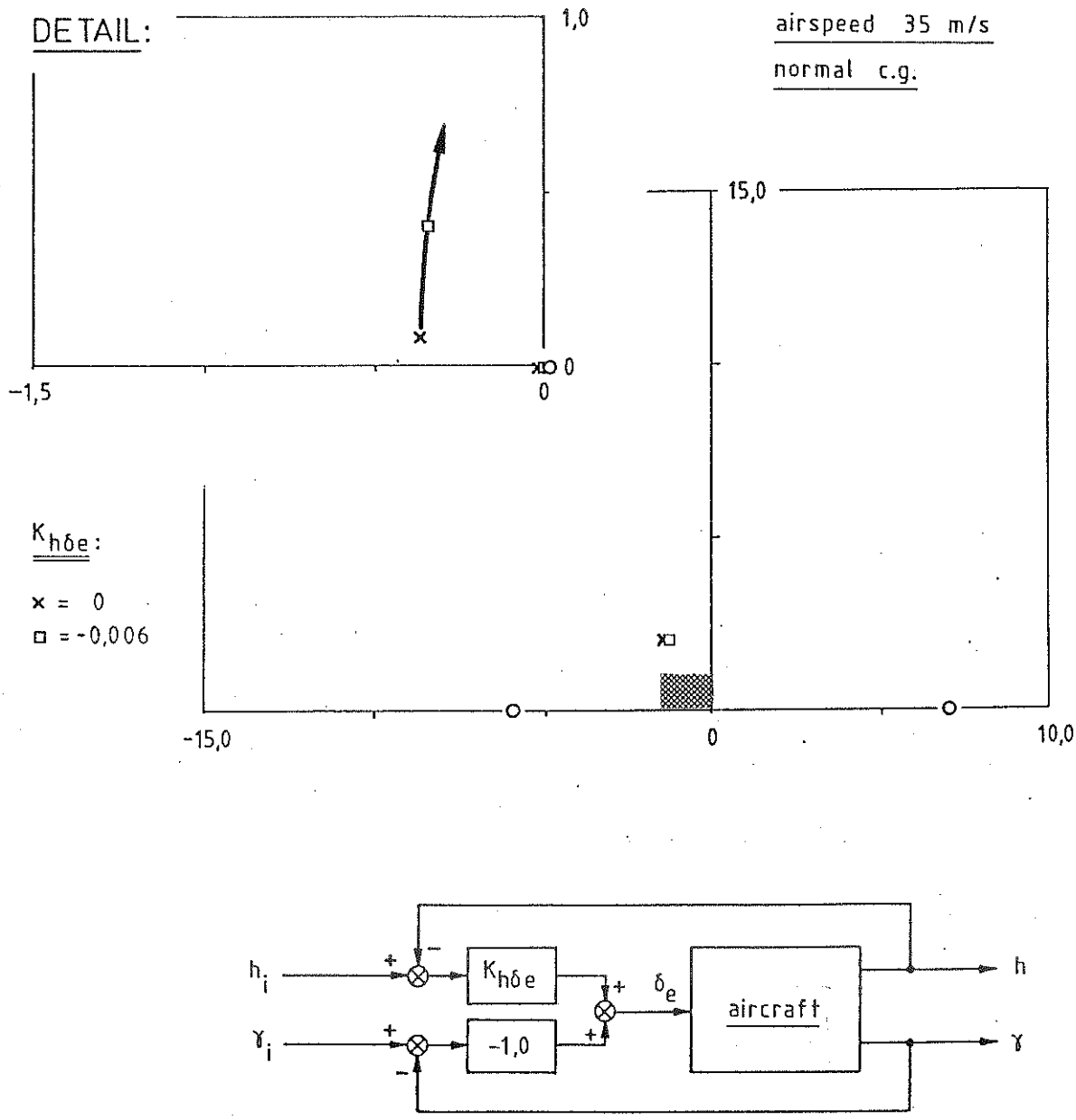

figure 4.2 (c): Root locus for feedback of altitude on elevator

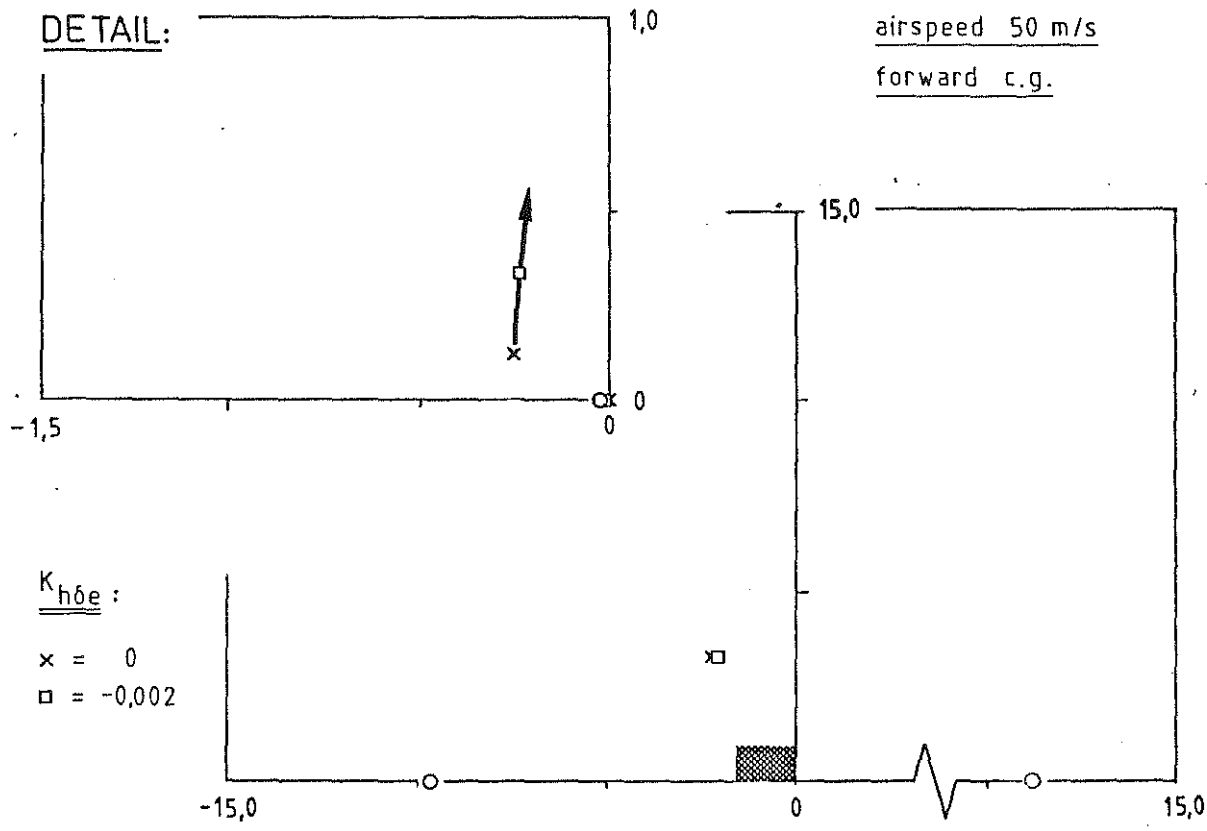

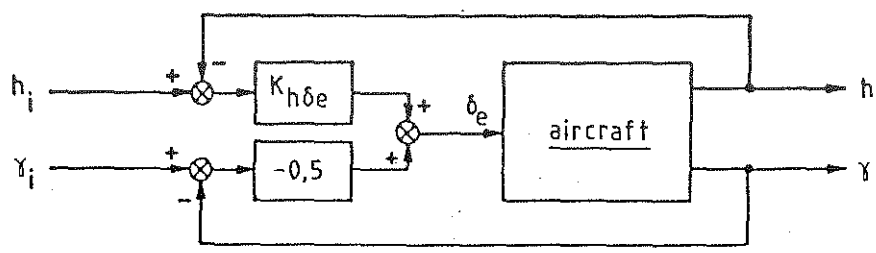

figure 4.2 (d): Root locus for feedback of altitude on elevator

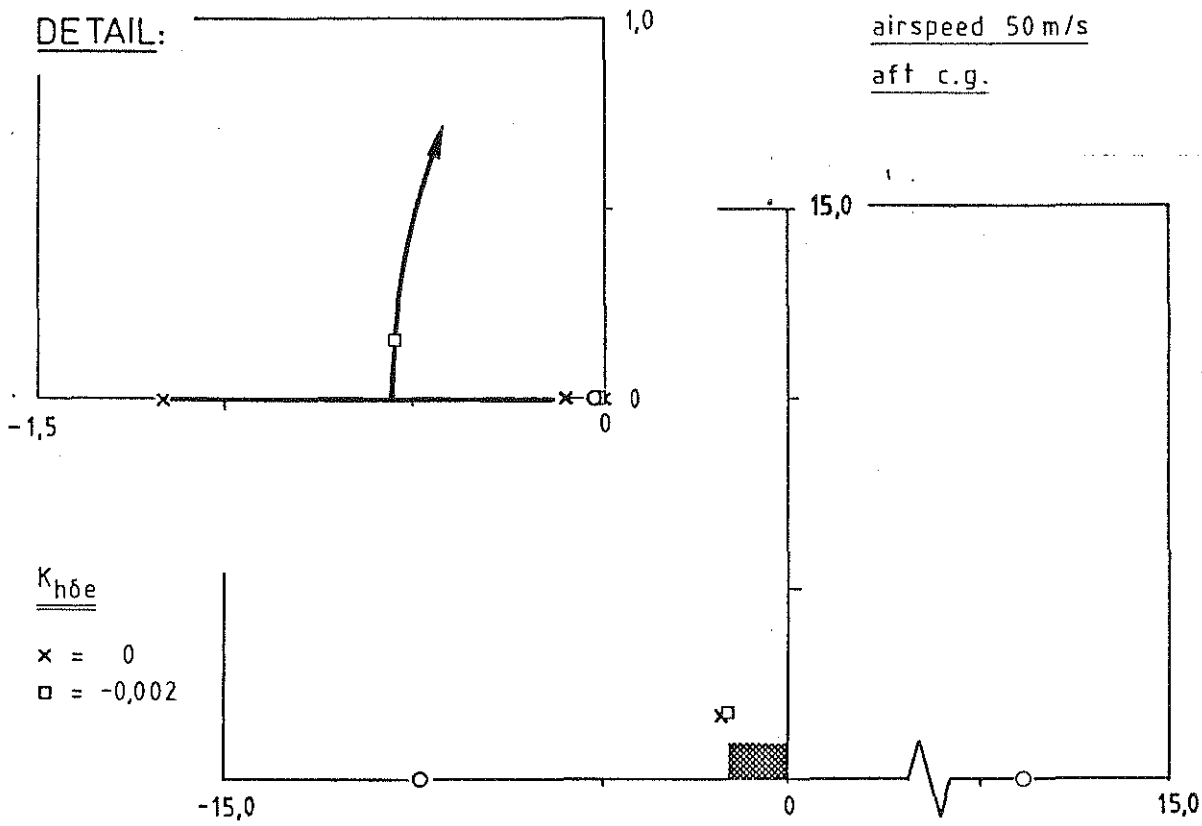

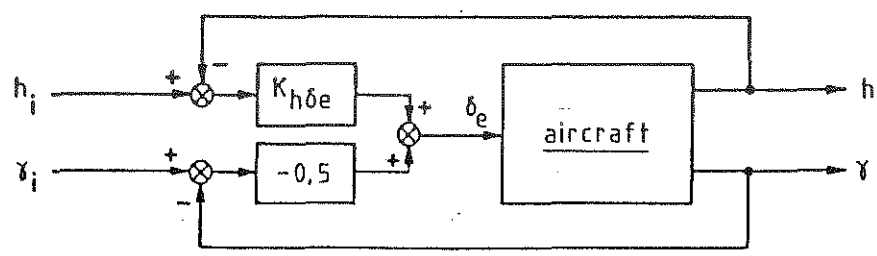

figure 4.2 (e): Root locus for feedback of altitude on elevator

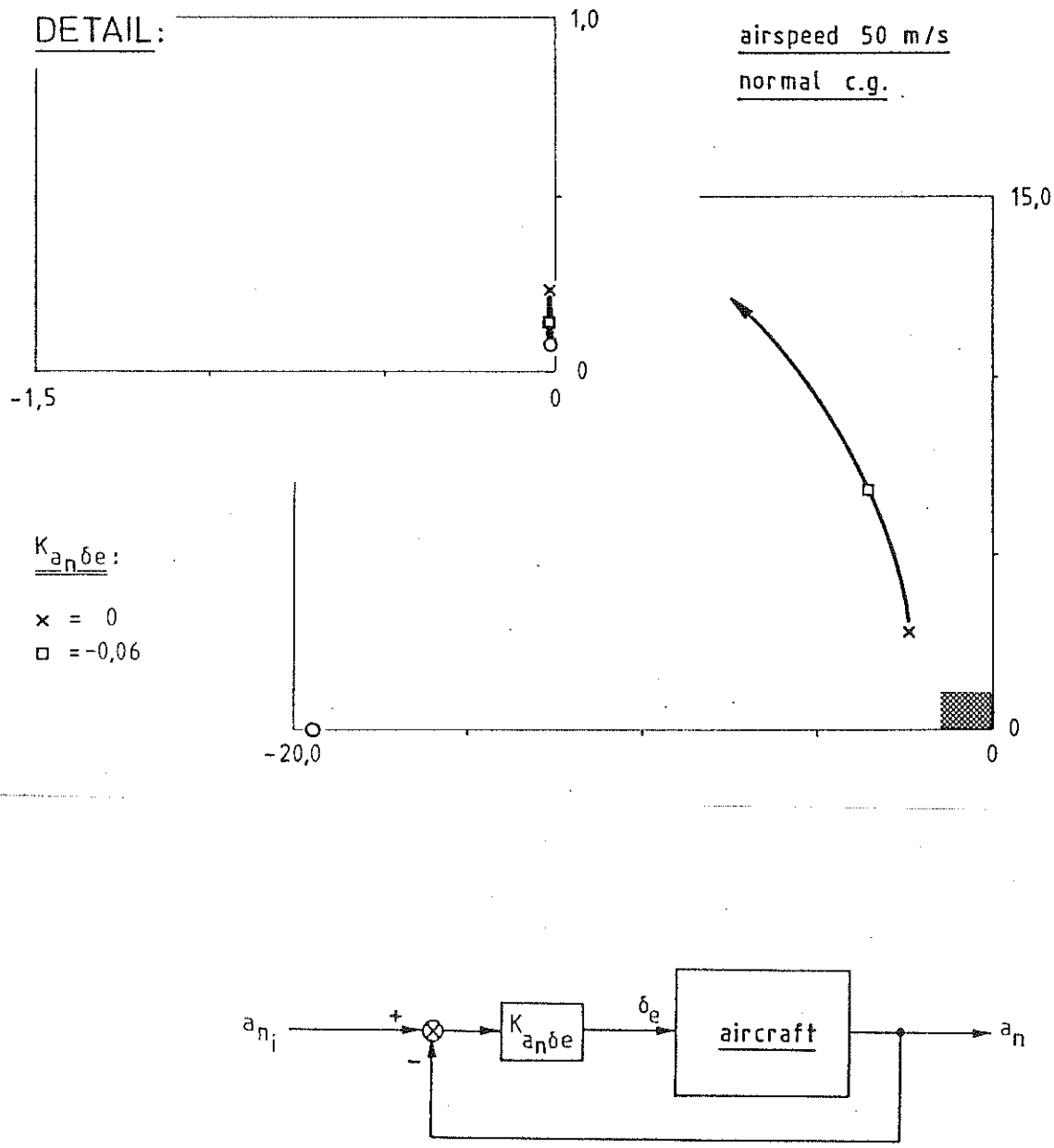

figure 5.1 (a): Root locus for feedback of normal acceleration on elevator

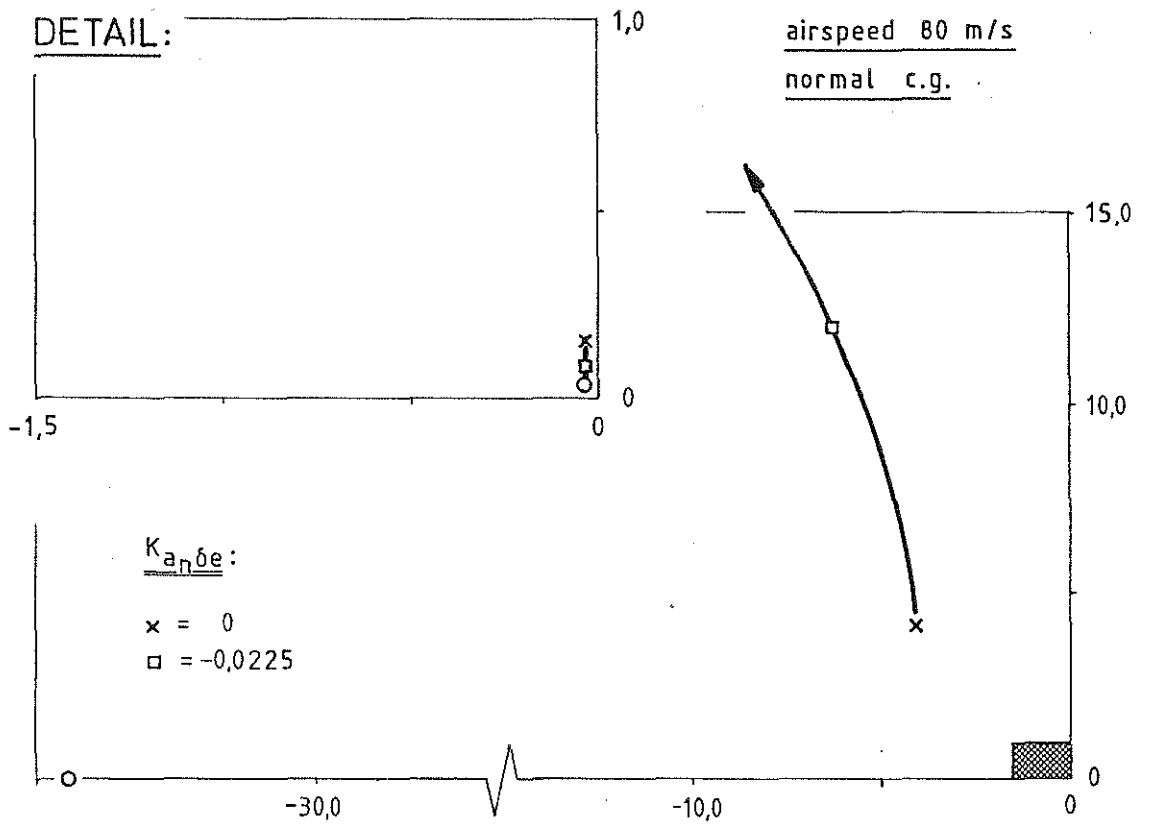

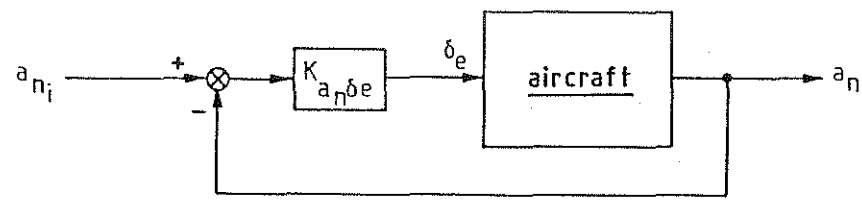

figure 5.1 (b): Root locus for feedback of normal acceleration on elevator

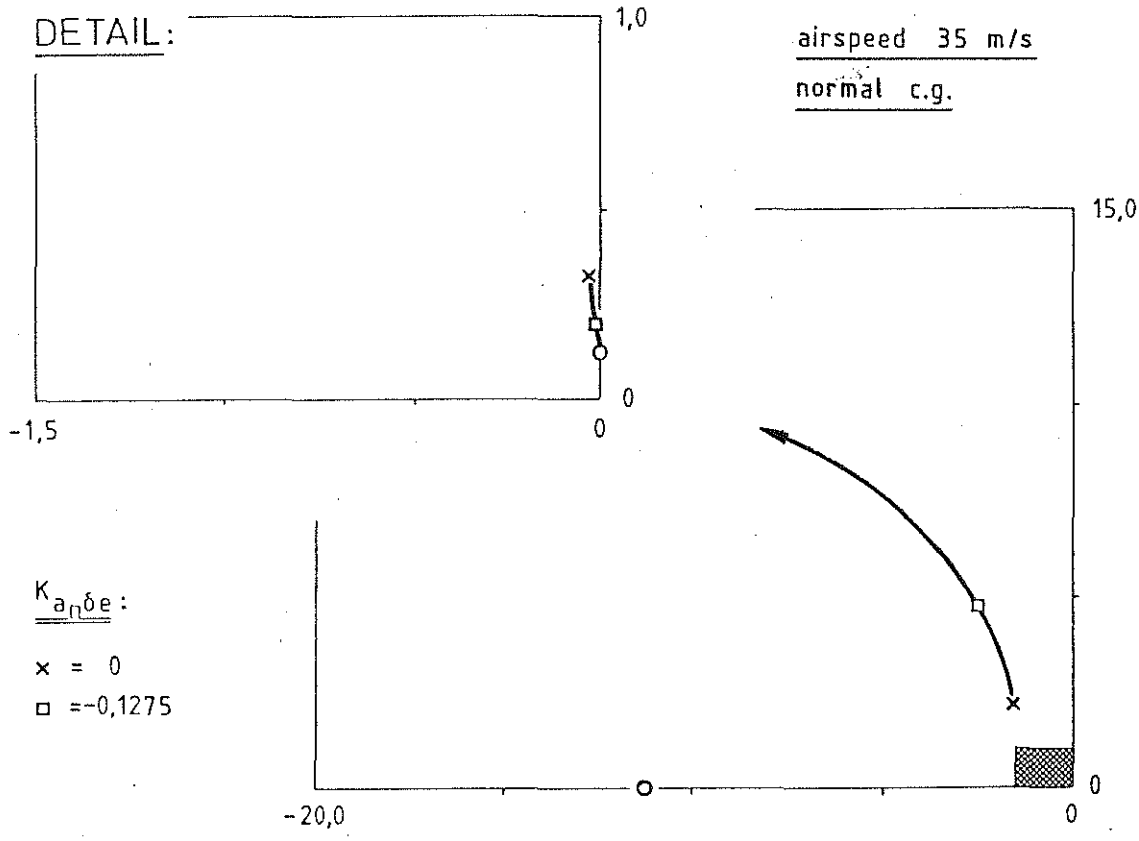

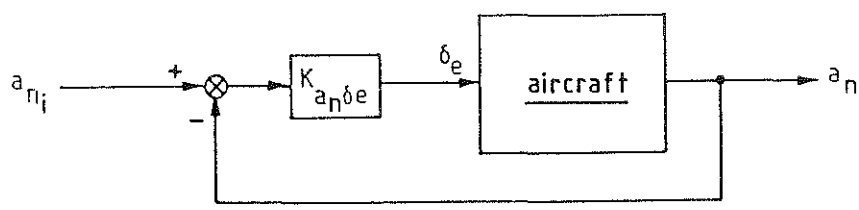

figure 5.1 (c): Root locus for feedback of normal acceleration on elevator

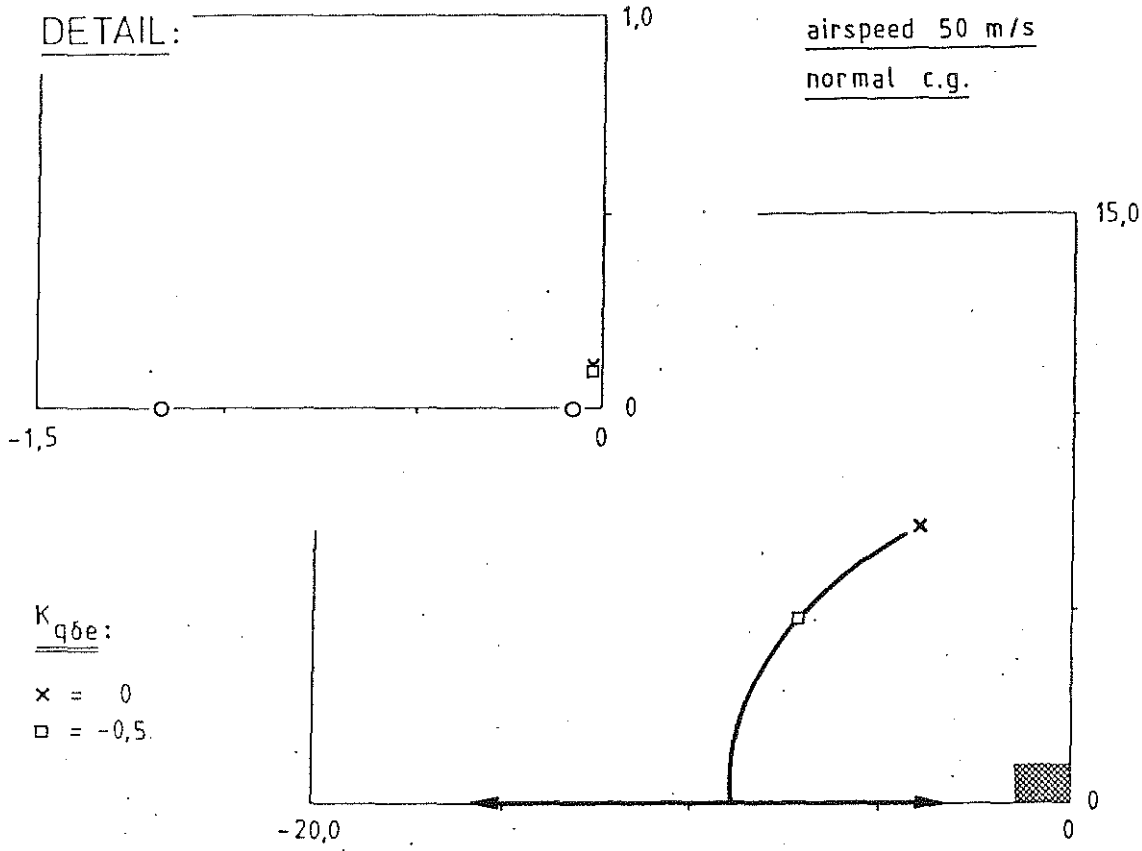

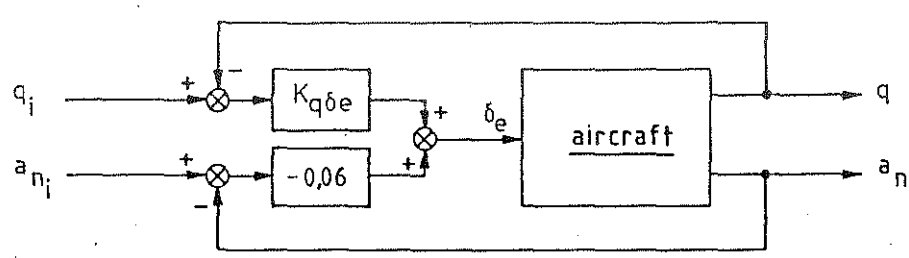

figure 5.2 (a): Root locus for feedback of pitch rate on elevator

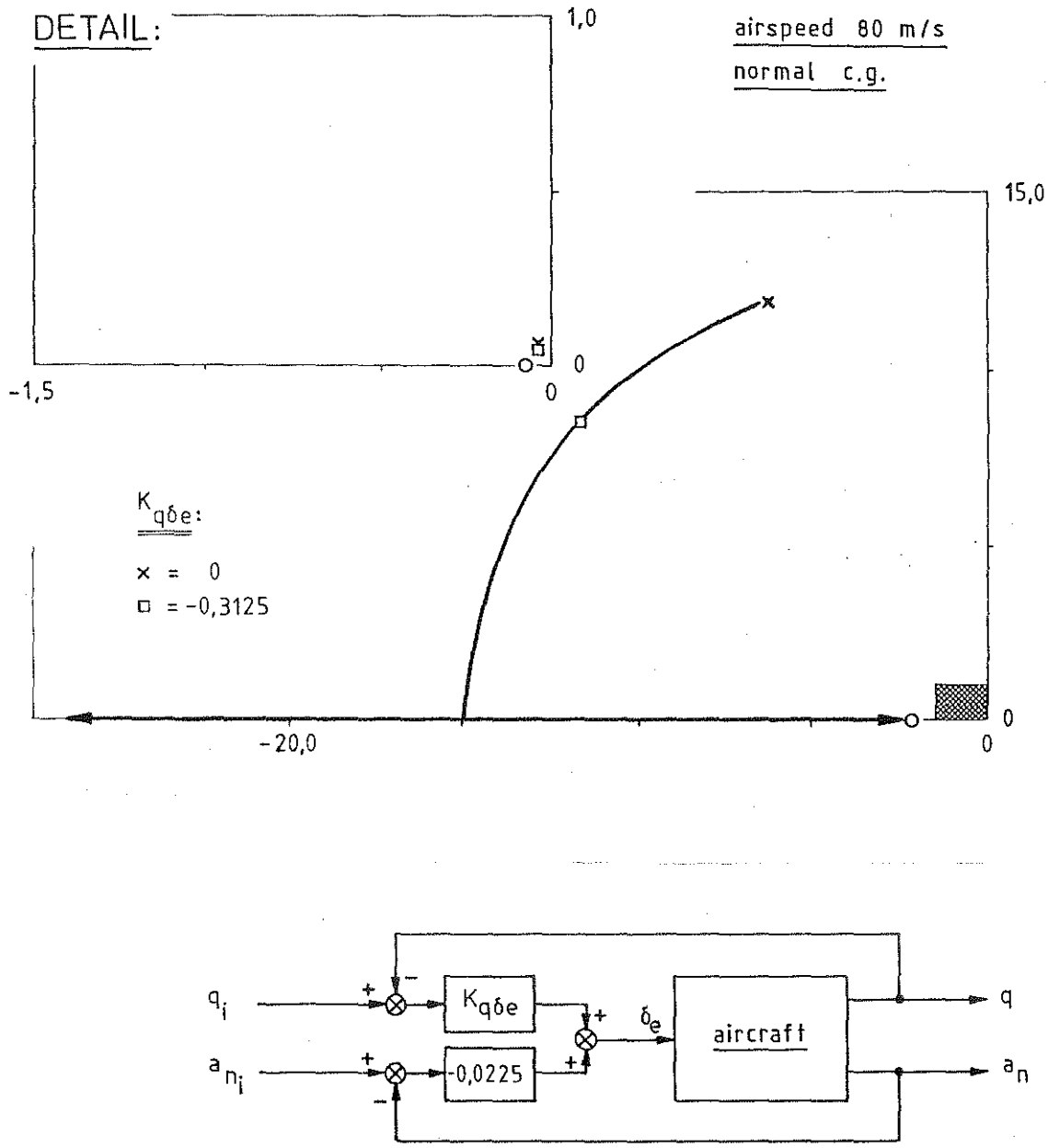

figure 5.2 (b): Root locus for feedback of pitch rate on elevator

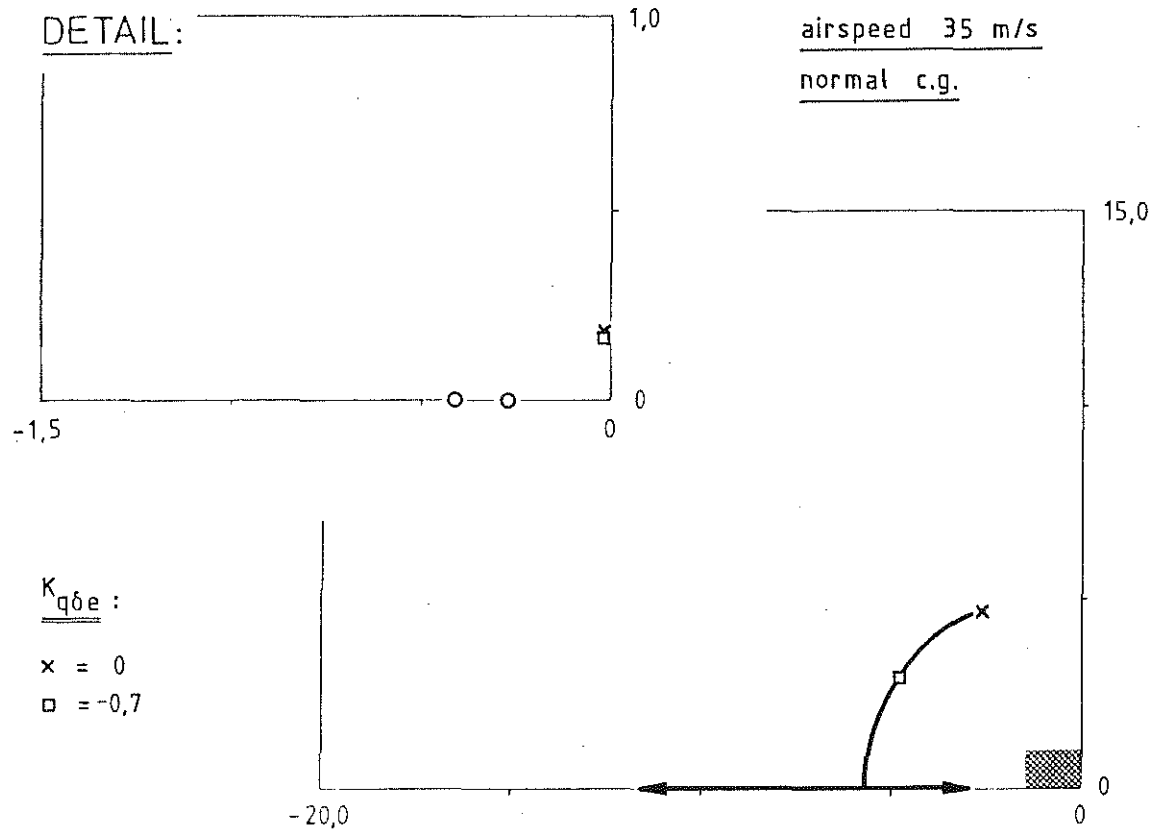

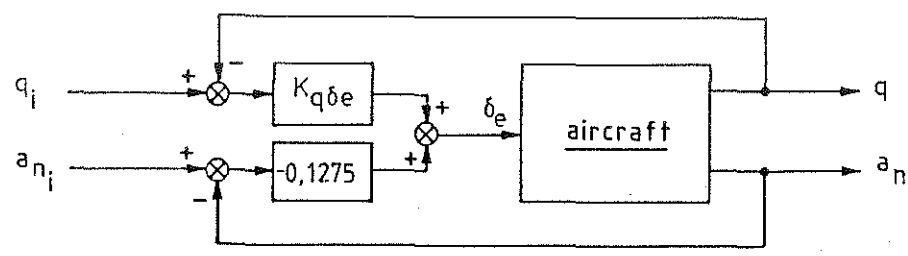

figure 5.2 (c): Root locus for feedback of pitch rate on elevator

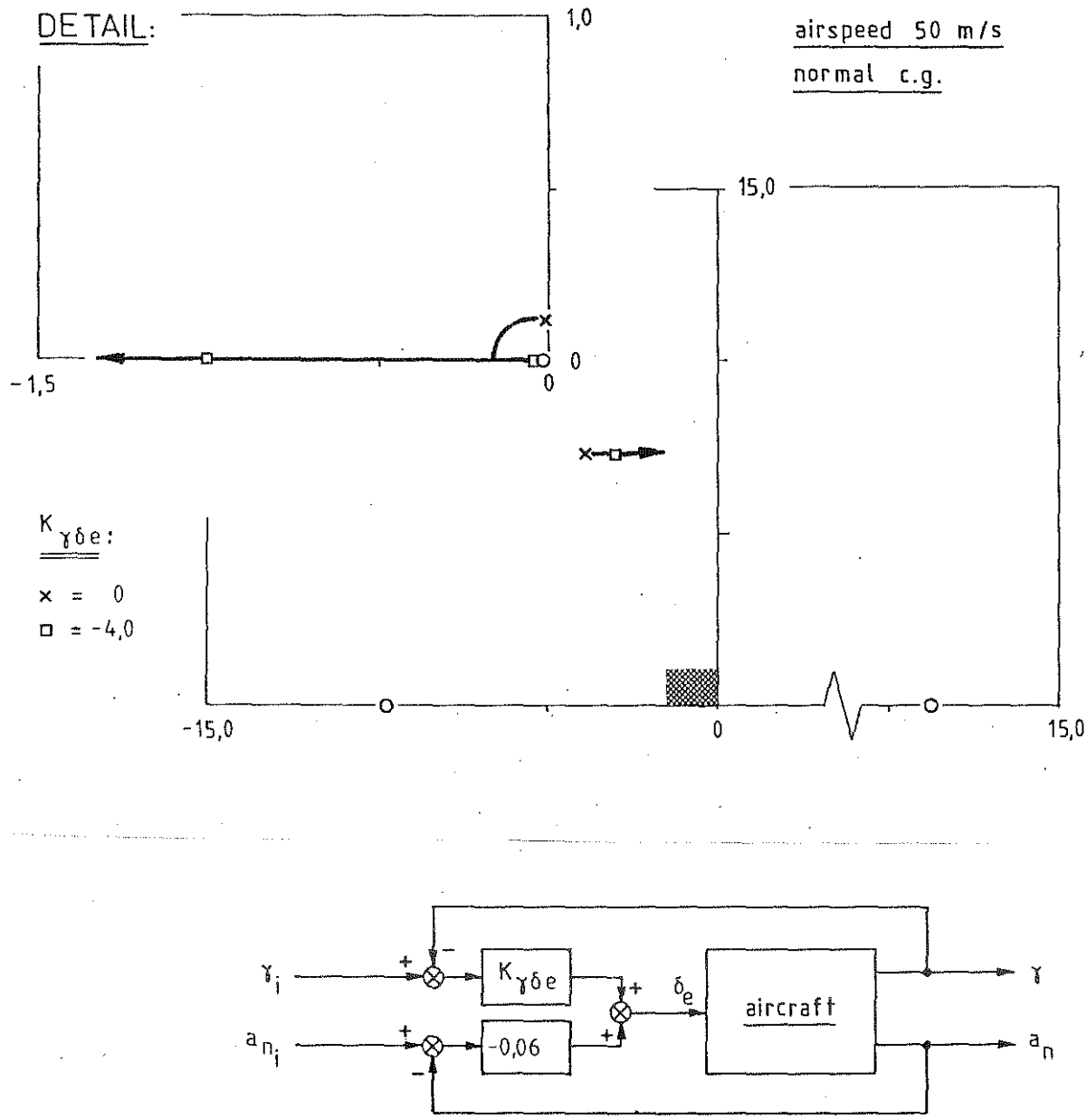

figure 5.3 (a): Root locus for feedback of flight path angle on elevator

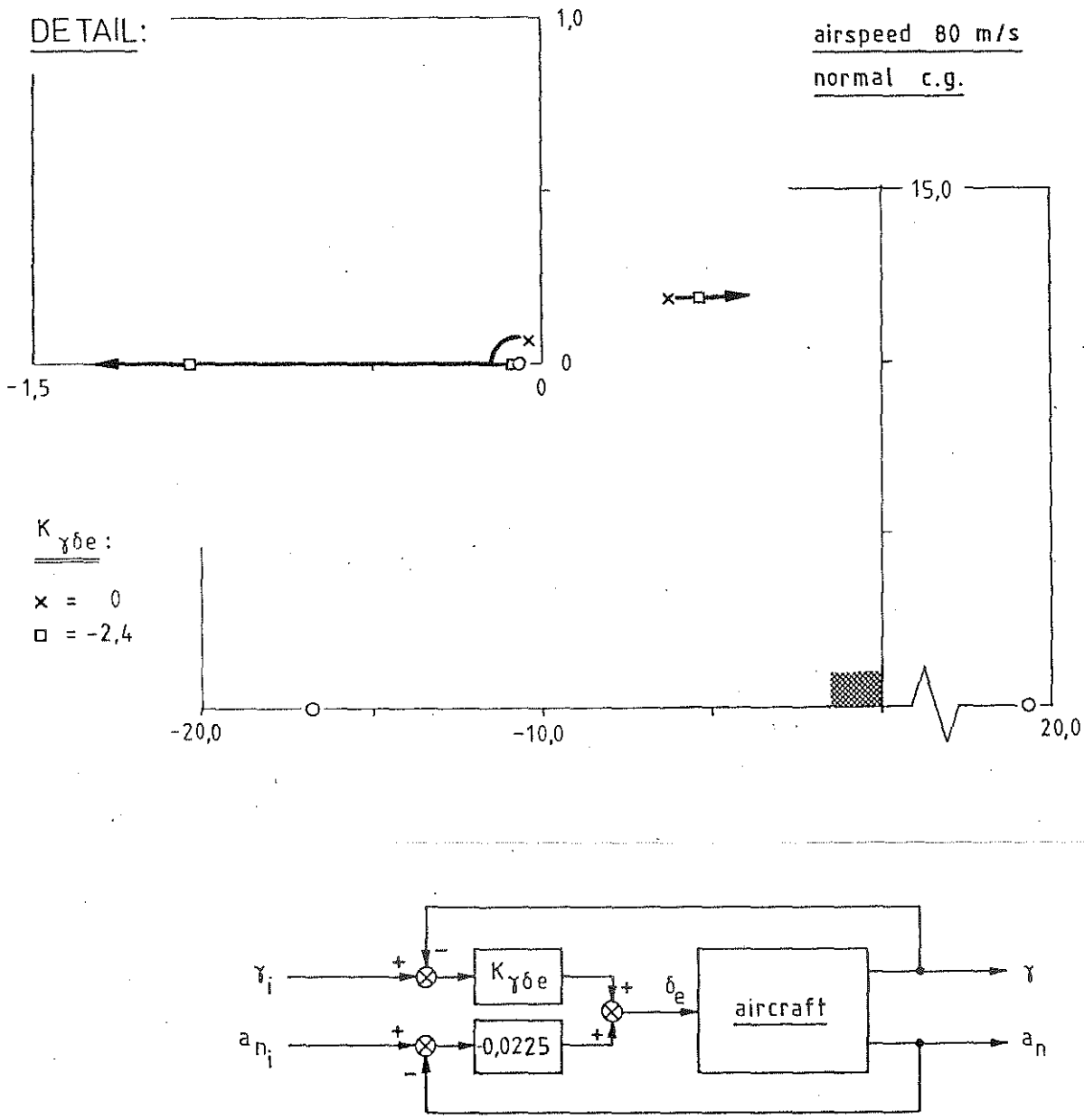

figure 5.3 (b): Root locus for feedback of flight path angle on elevator

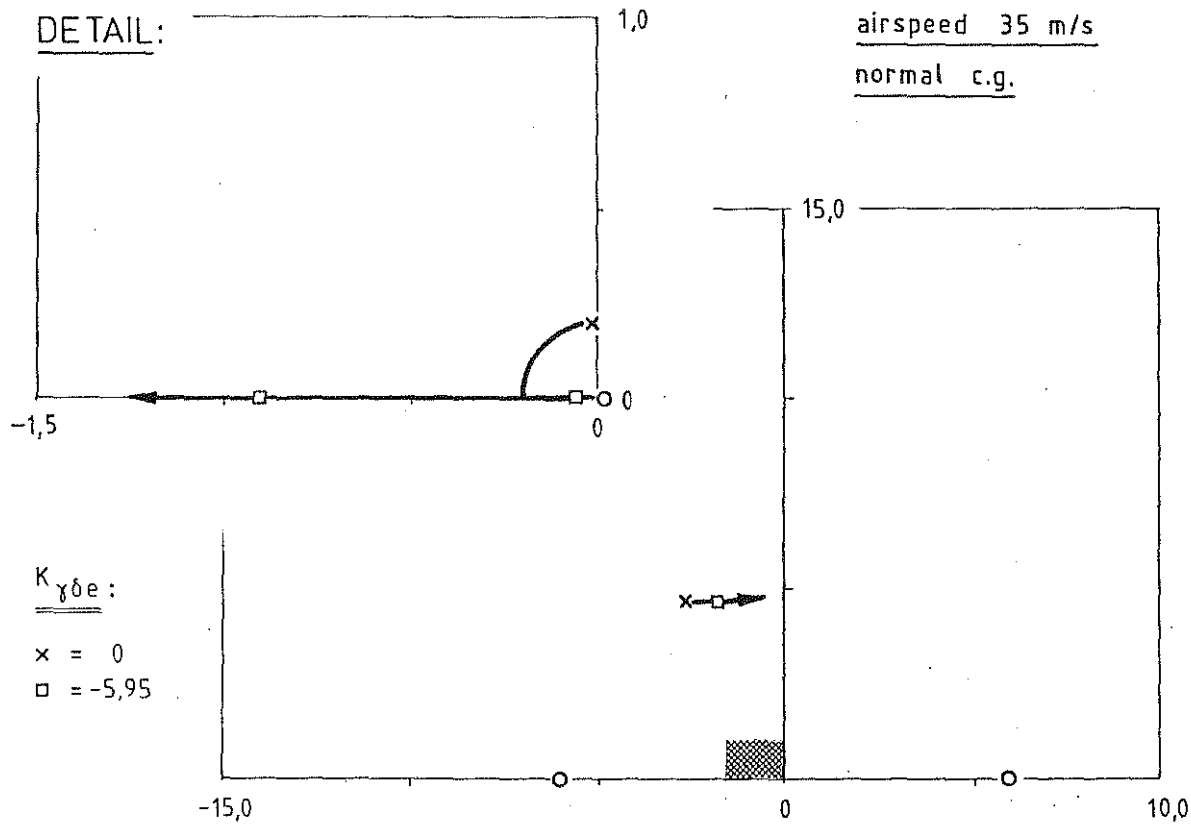

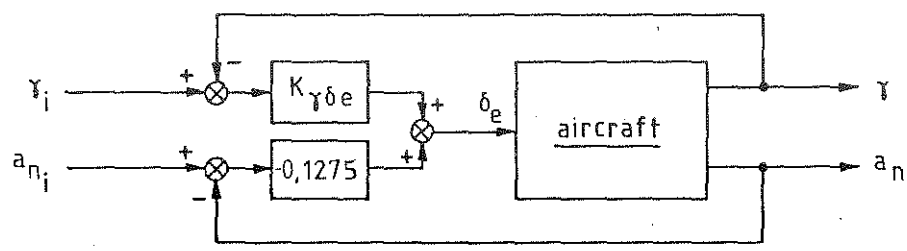

figure 5.3 (c): Root locus for feedback of flight path angle on elevator

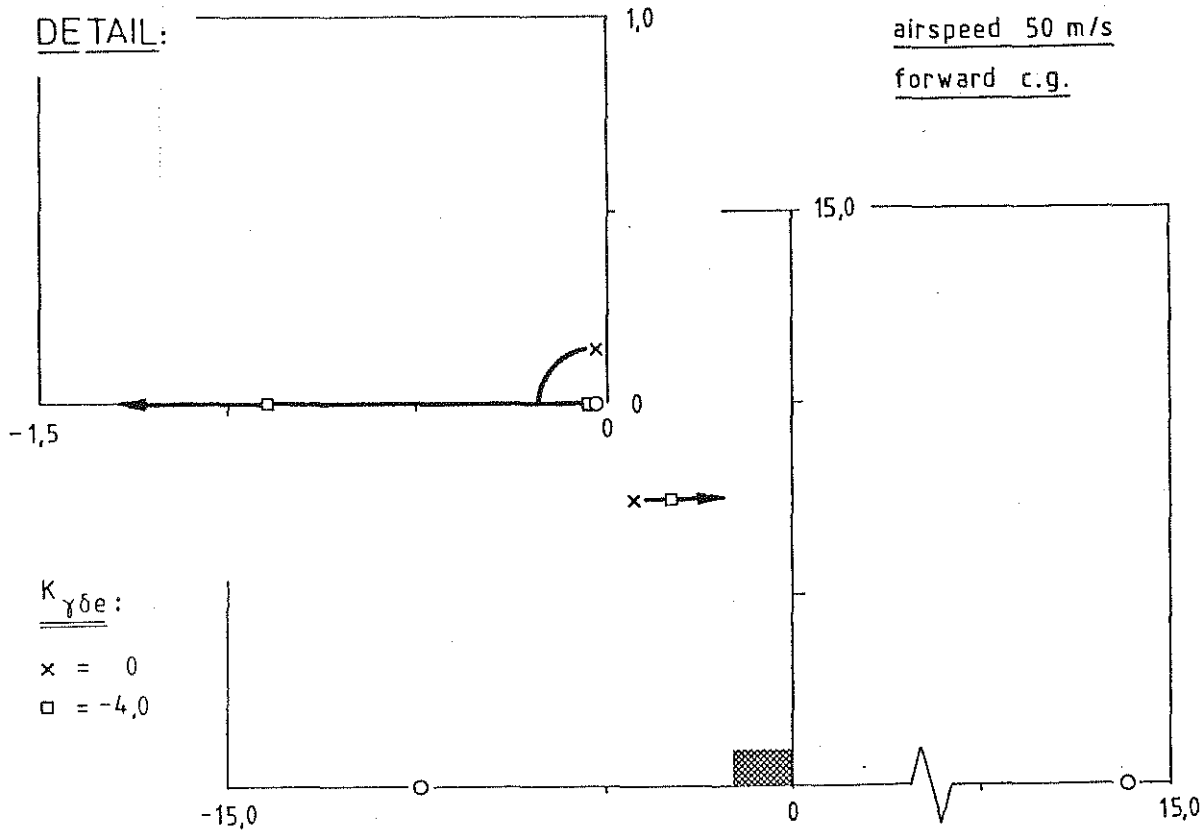

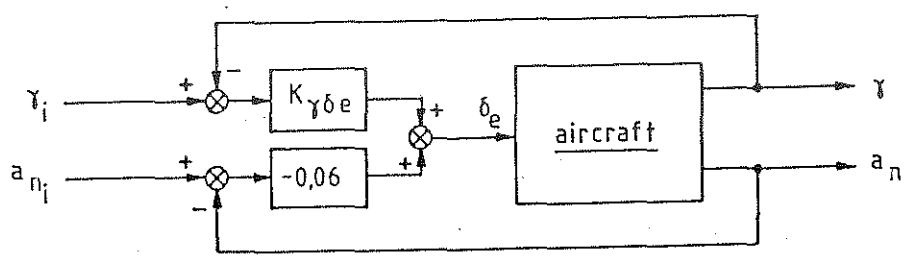

figure 5.3 (d): Root locus for feedback of flight path angle on elevator

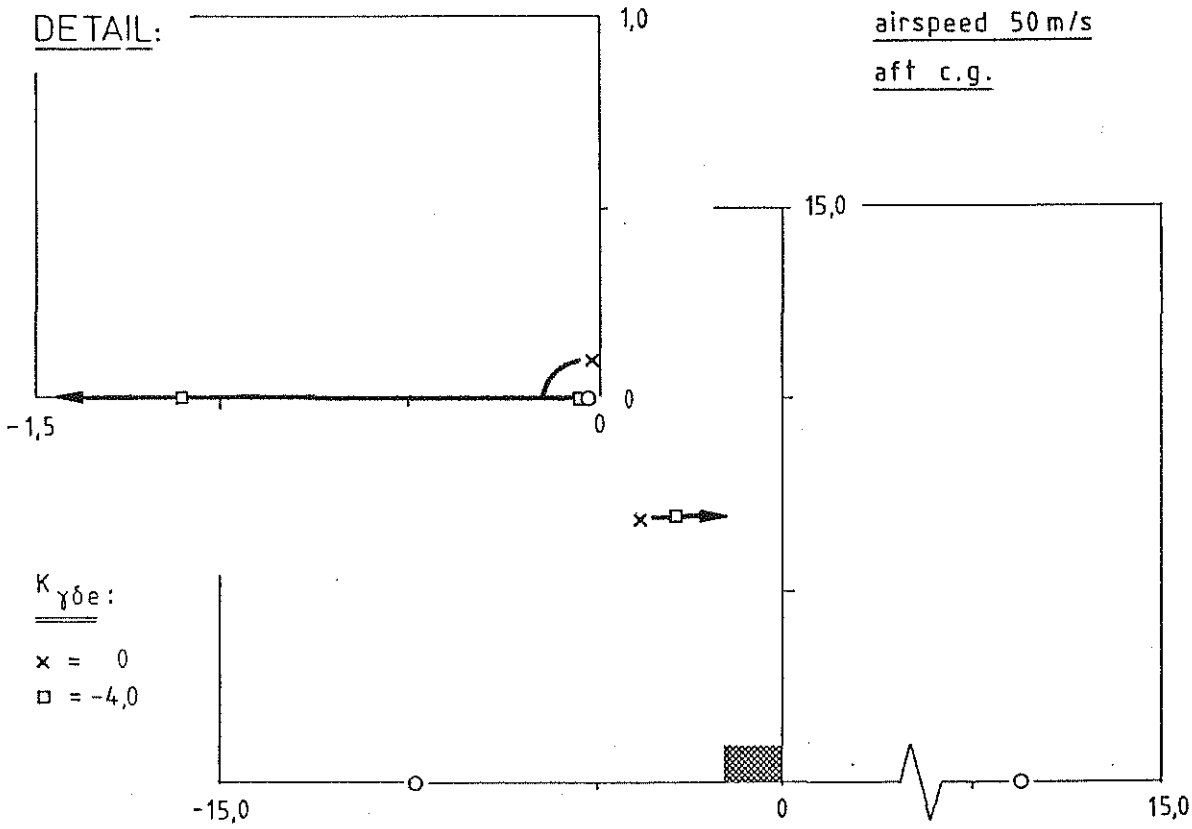

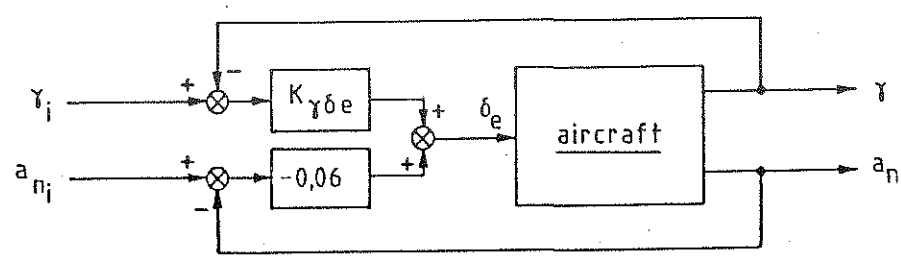

figure 5.3 (e): Root locus for feedback of flight path angle on elevator

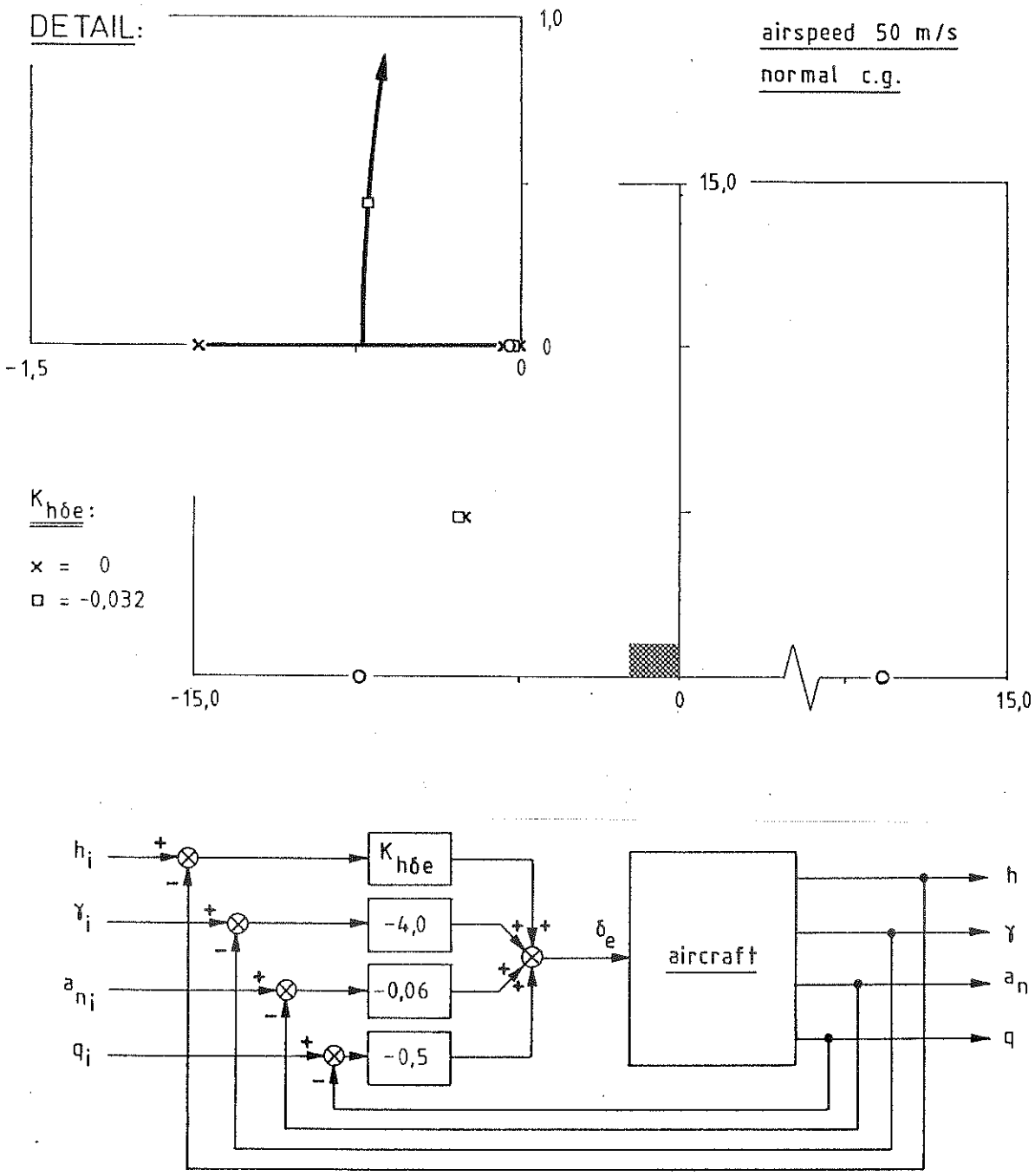

figure 5.4 (a): Root locus for feedback of altitude on elevator

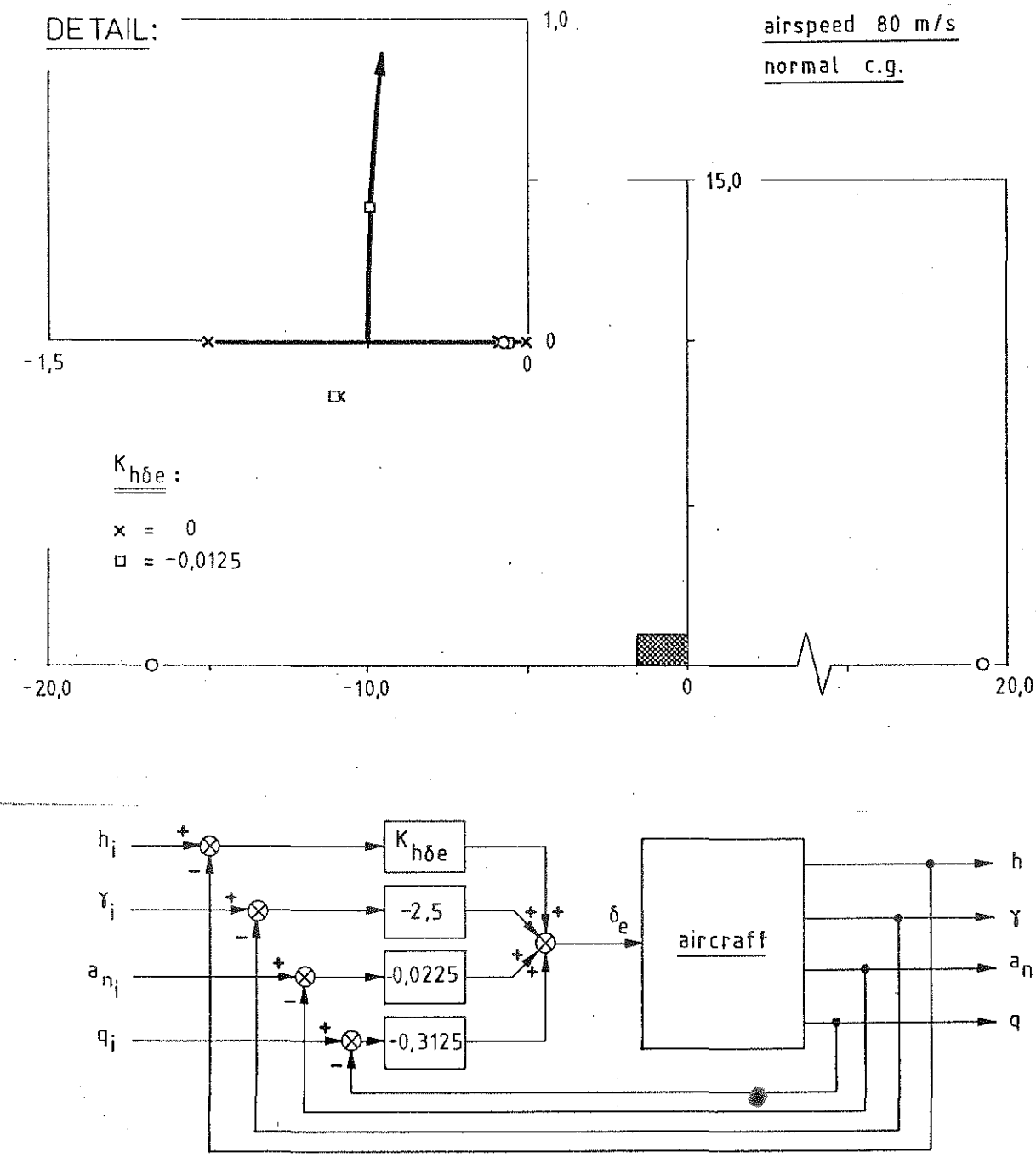

figure 5.4 (b): Root locus for feedback of altitude on elevator

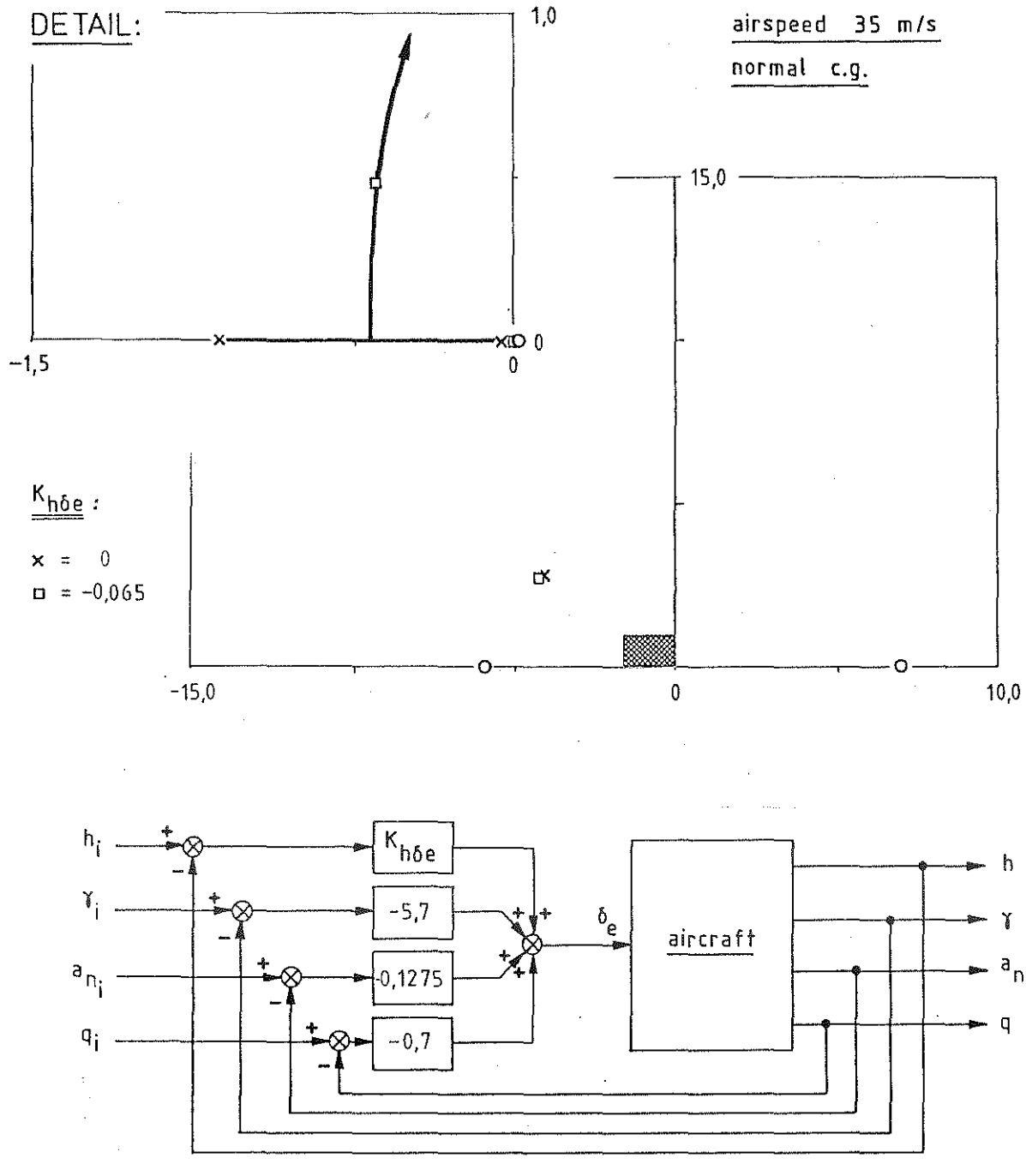

figure 5.4 (c): Root locus for feedback of altitude on elevator

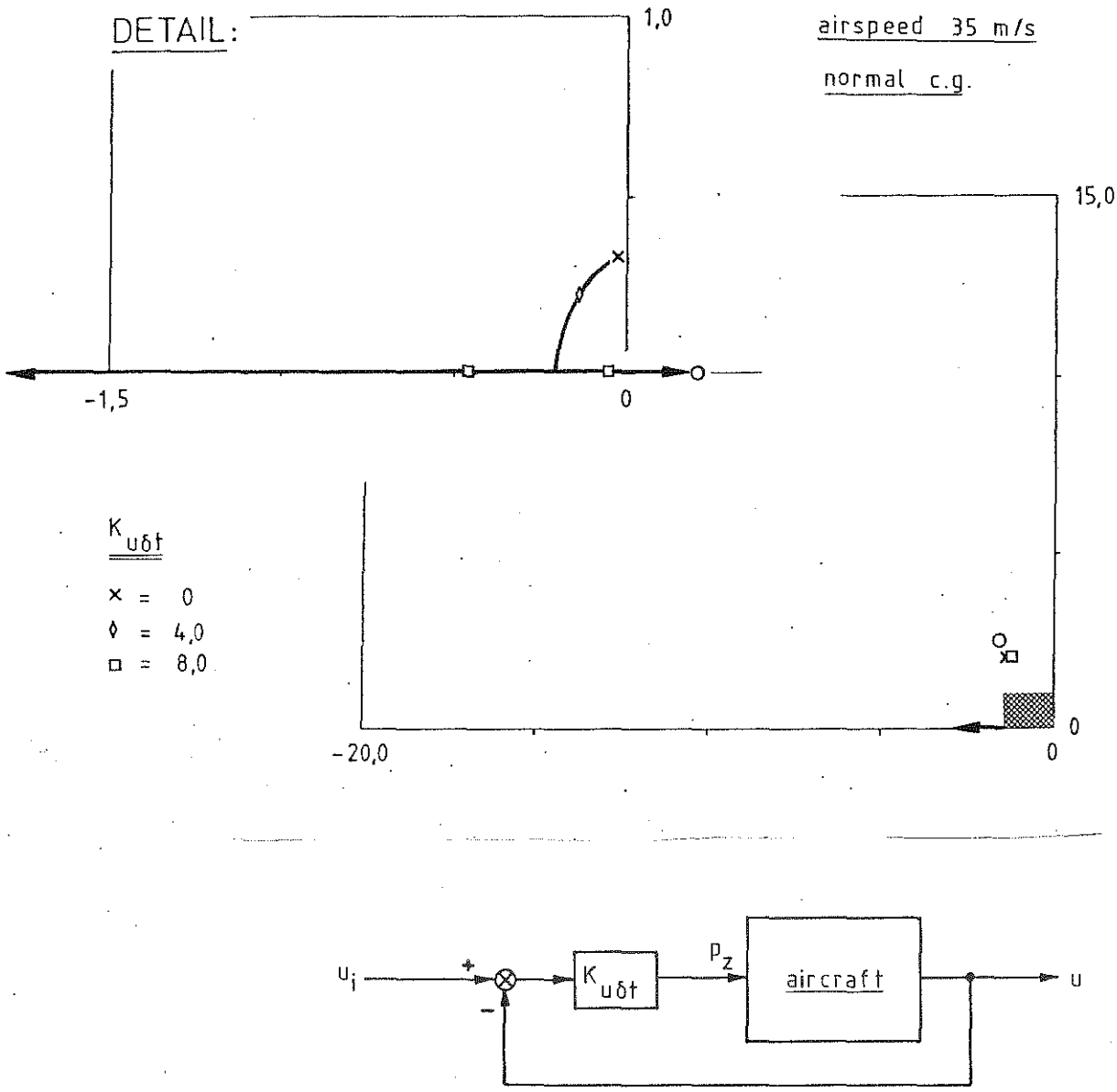

figure 6.1: Root locus for feedback of airspeed on throttle

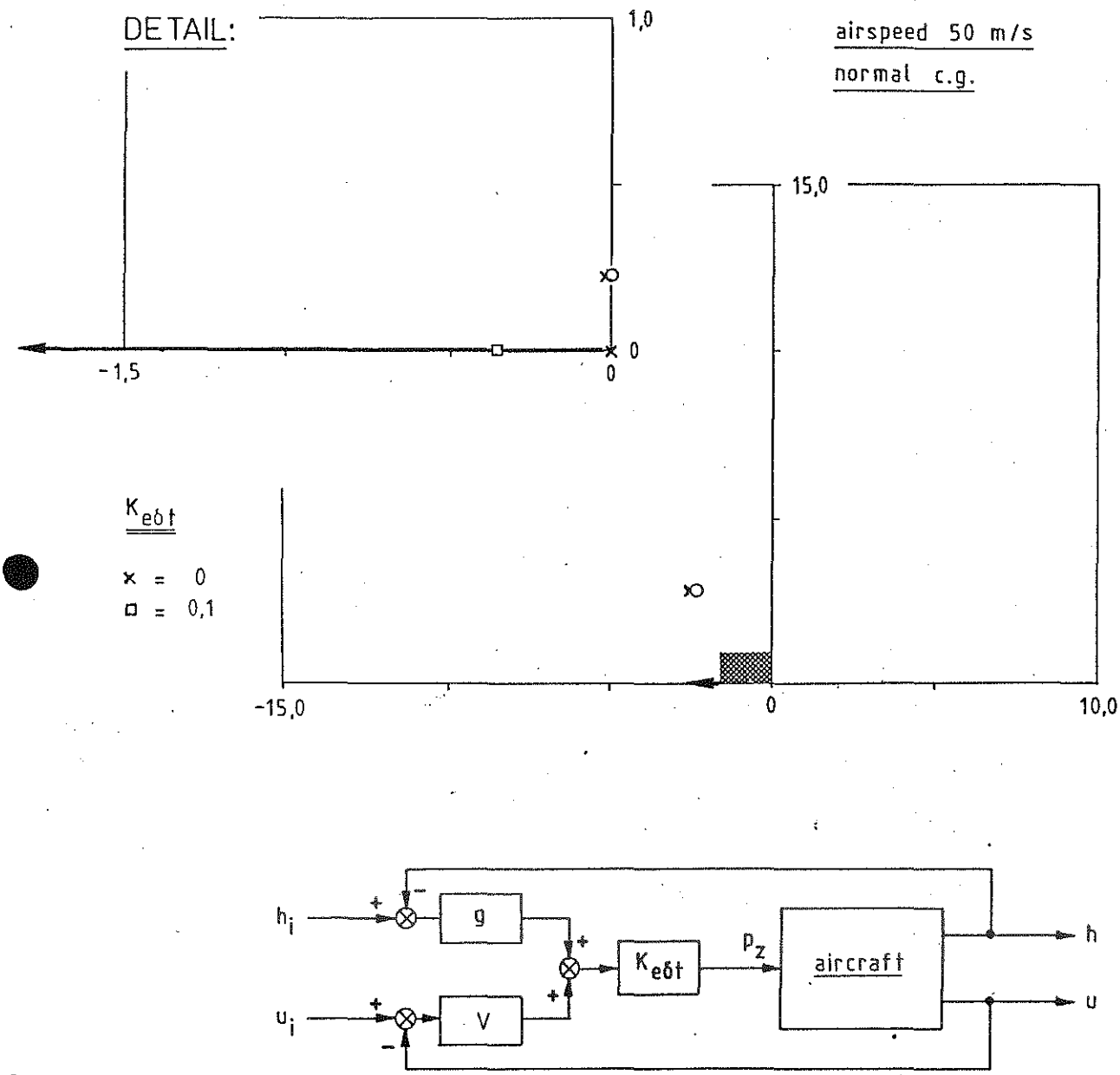

figure 6.2 (a): Root locus for feedback of specific energy on throttle

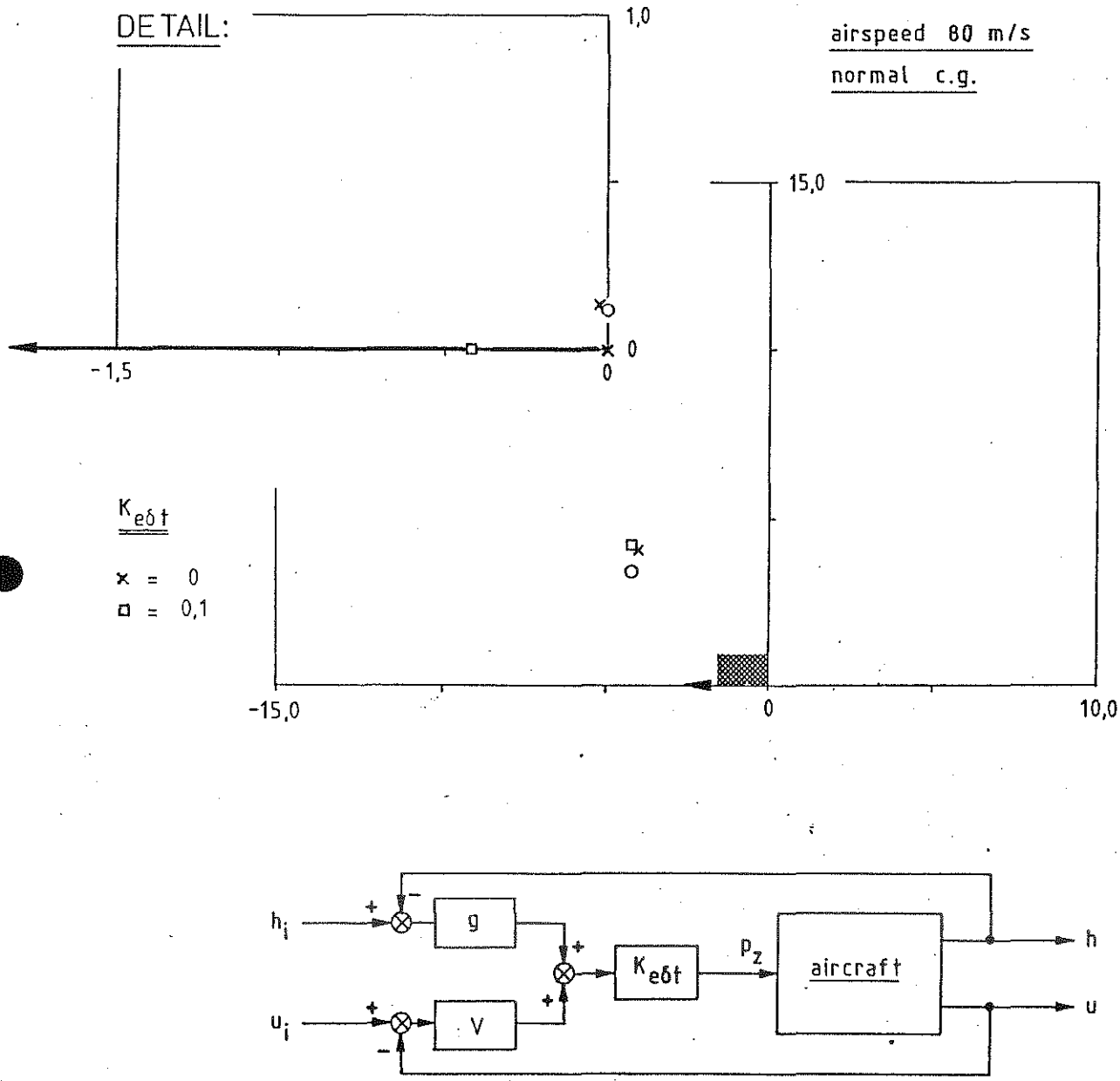

figure 6.2 (b): Root locus for feedback of specific energy on throttle

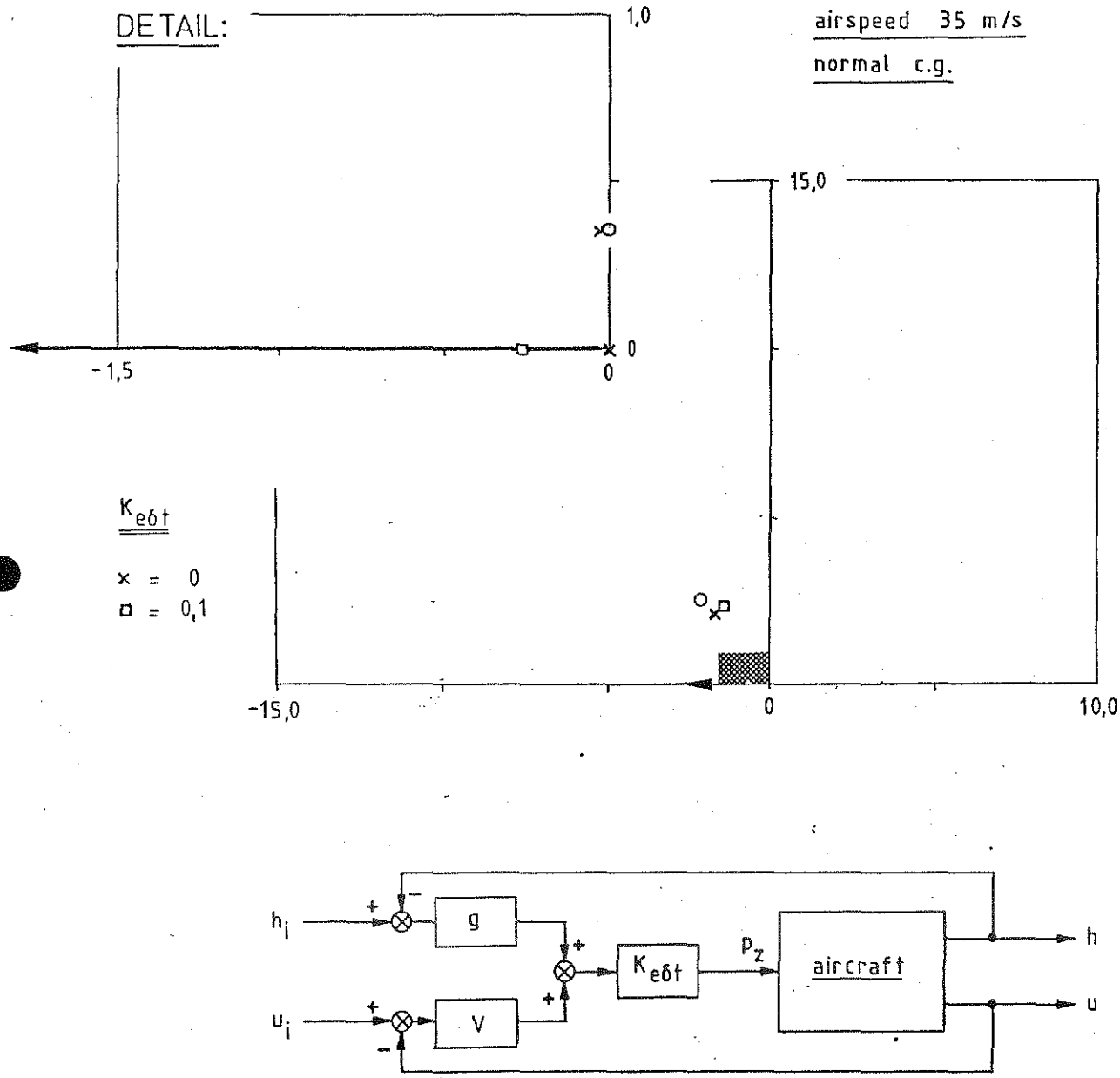

figure 6.2 (c): Root locus for feedback of specific energy on throttle

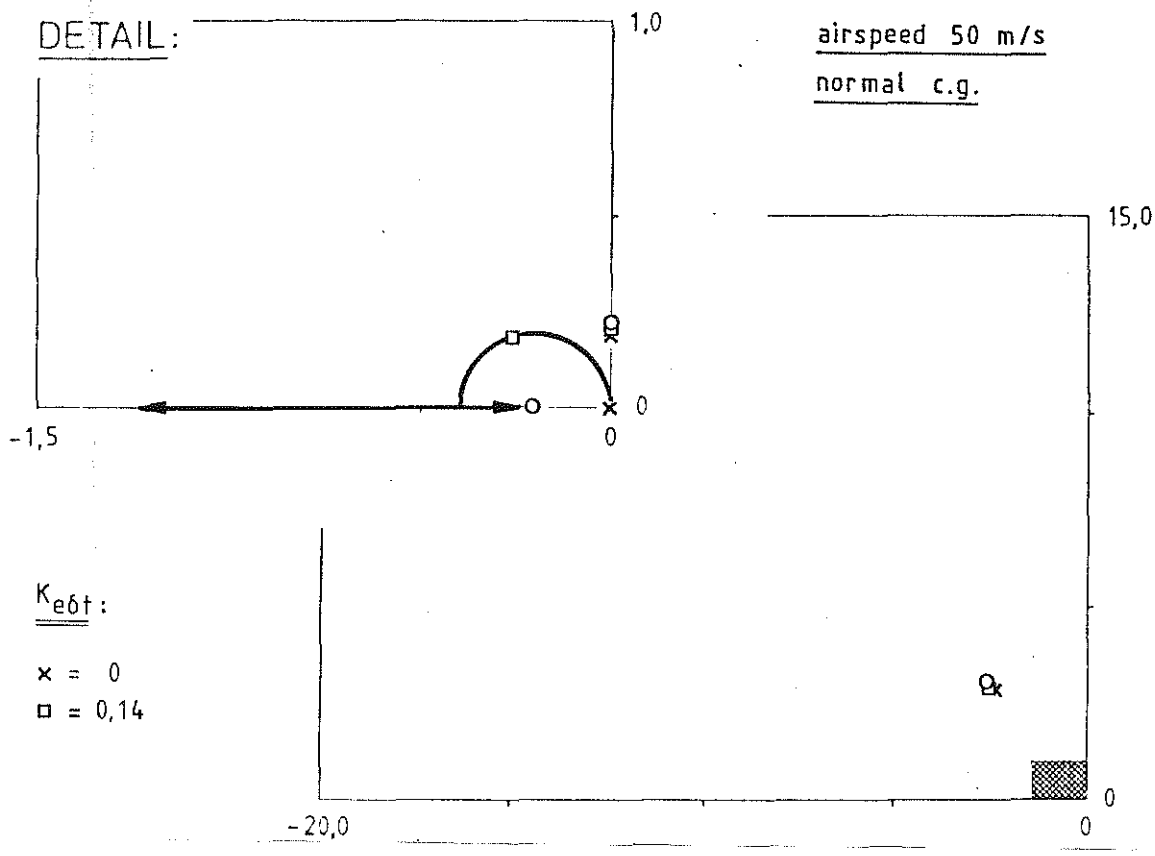

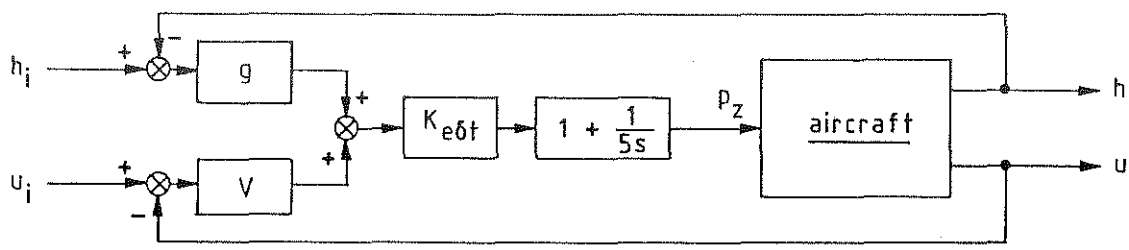

figure 6.3 (a): Root locus for proportional-integral feedback of specific energy on the throttle

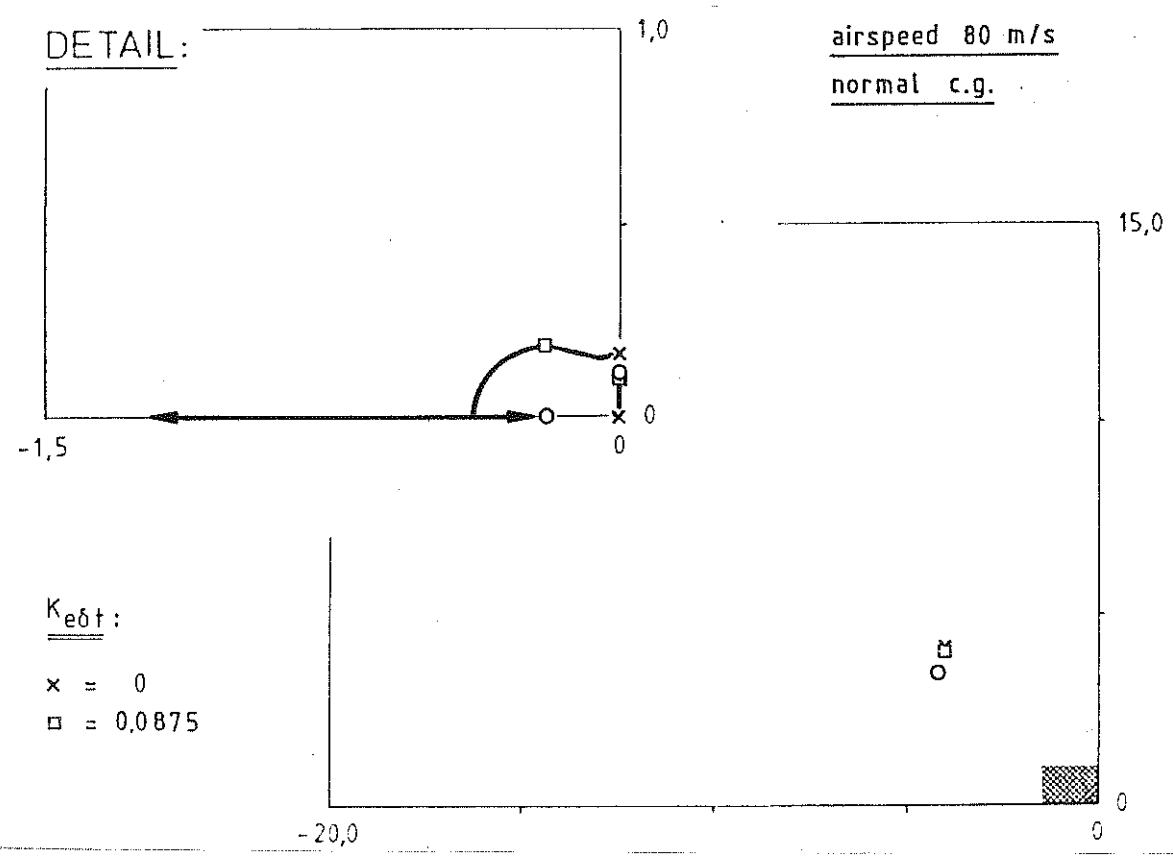

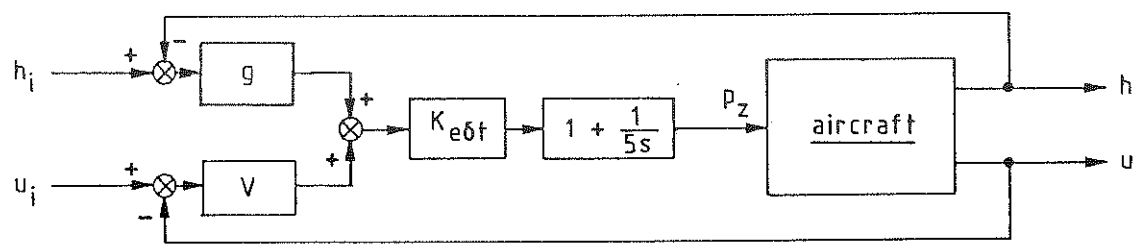

figure 6.3 (b): Root locus for proportional-integral feedback of specific energy on the throttle

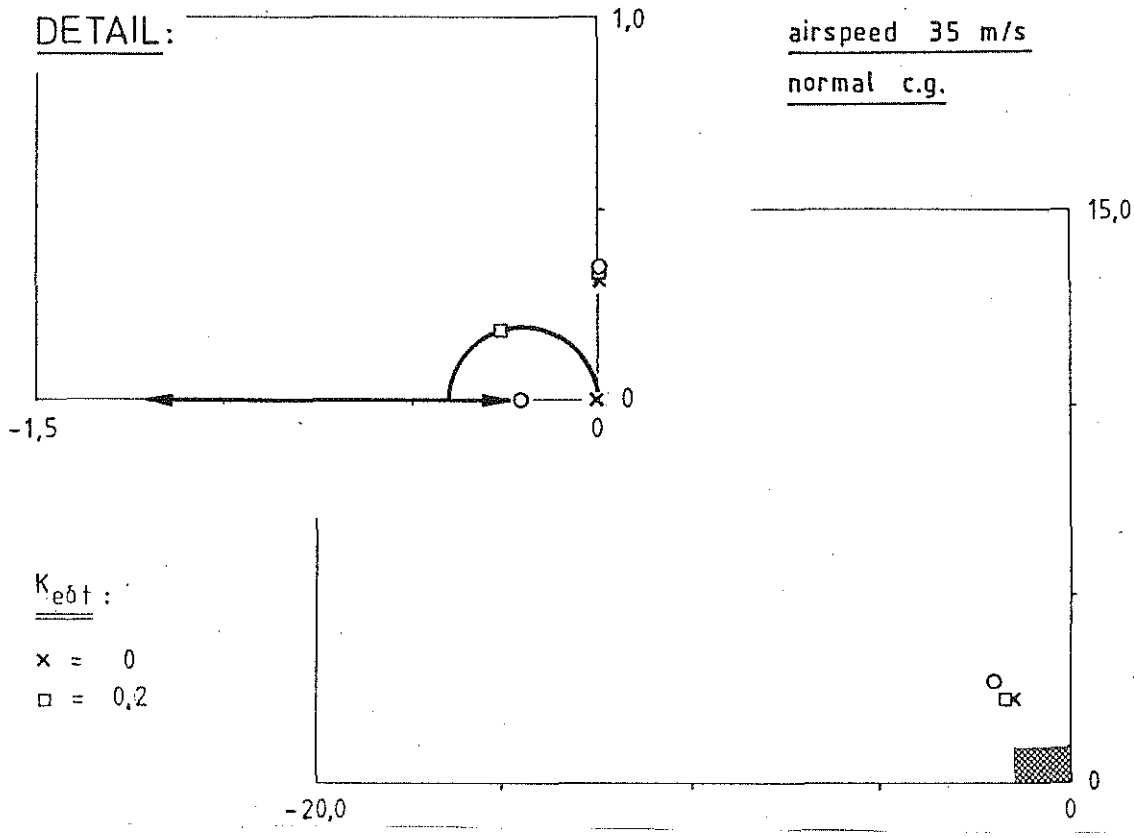

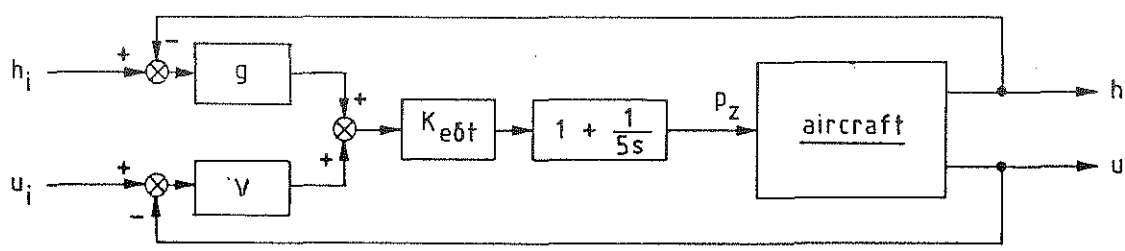

figure 6.3 (c): Root locus for proportional-integral feedback of specific energy on the throttle

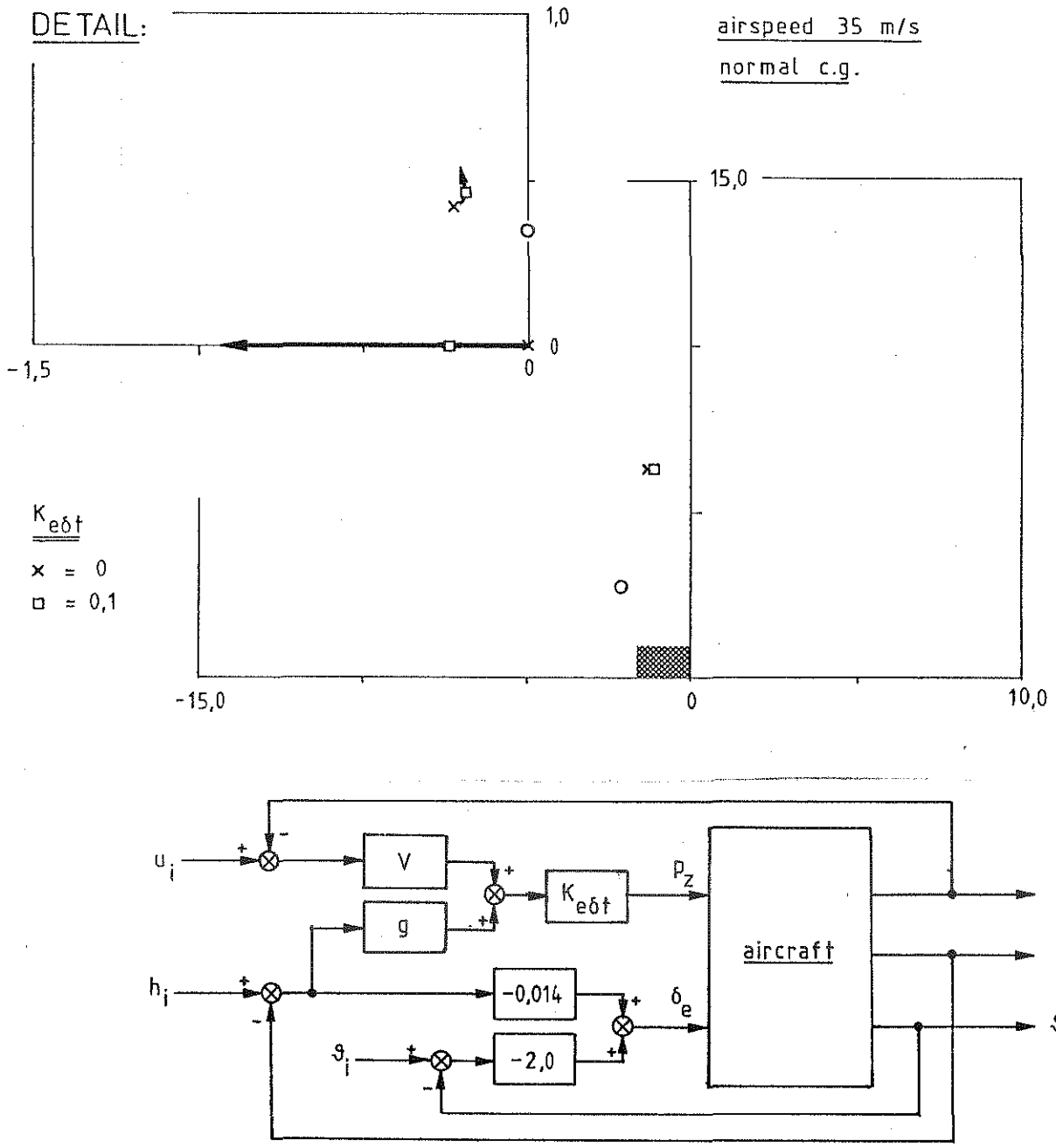

figure 7.1: Root locus for feedback of specific energy on throttle

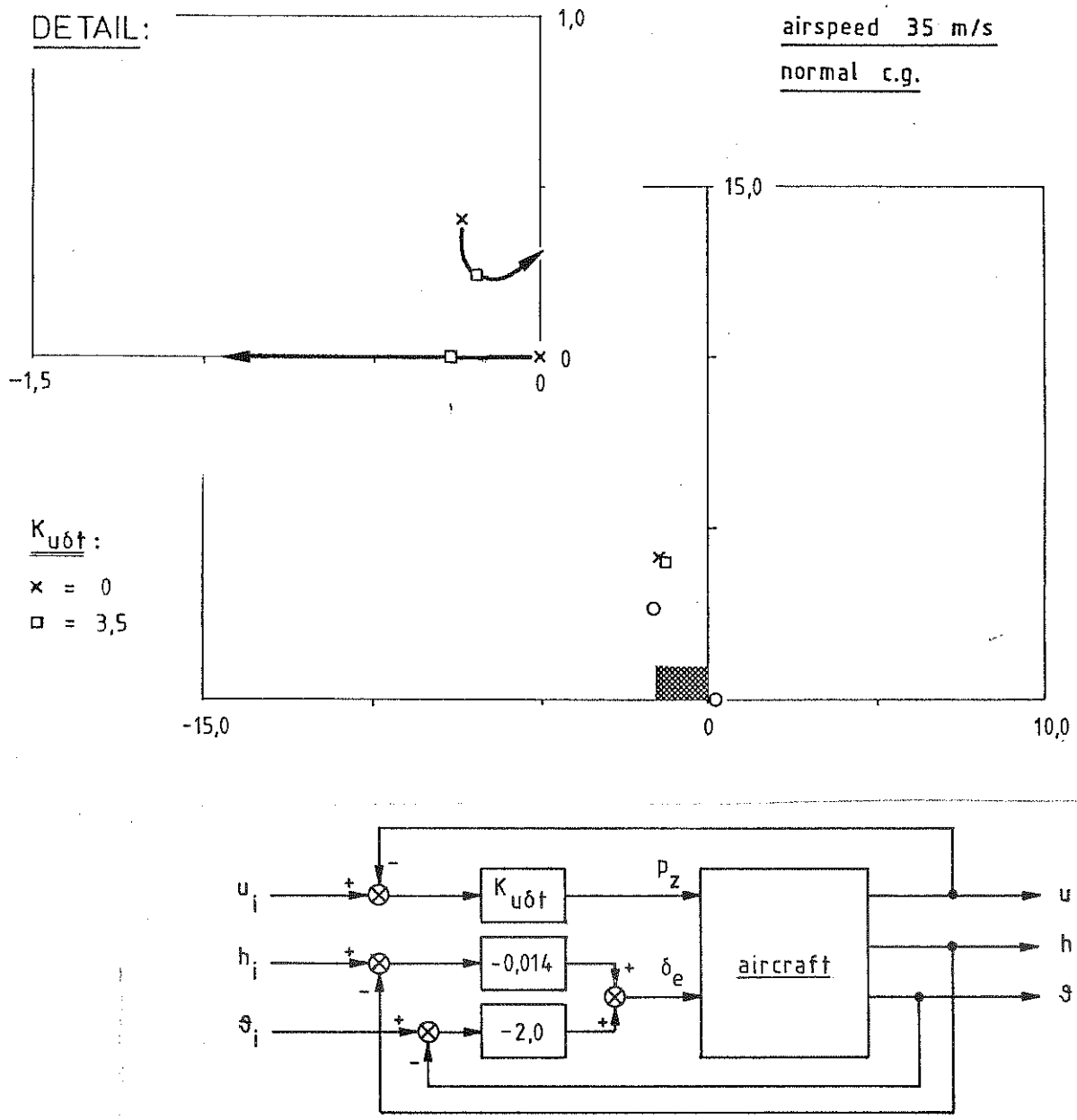

figure 7.2: Root locus for feedback of airspeed on throttle

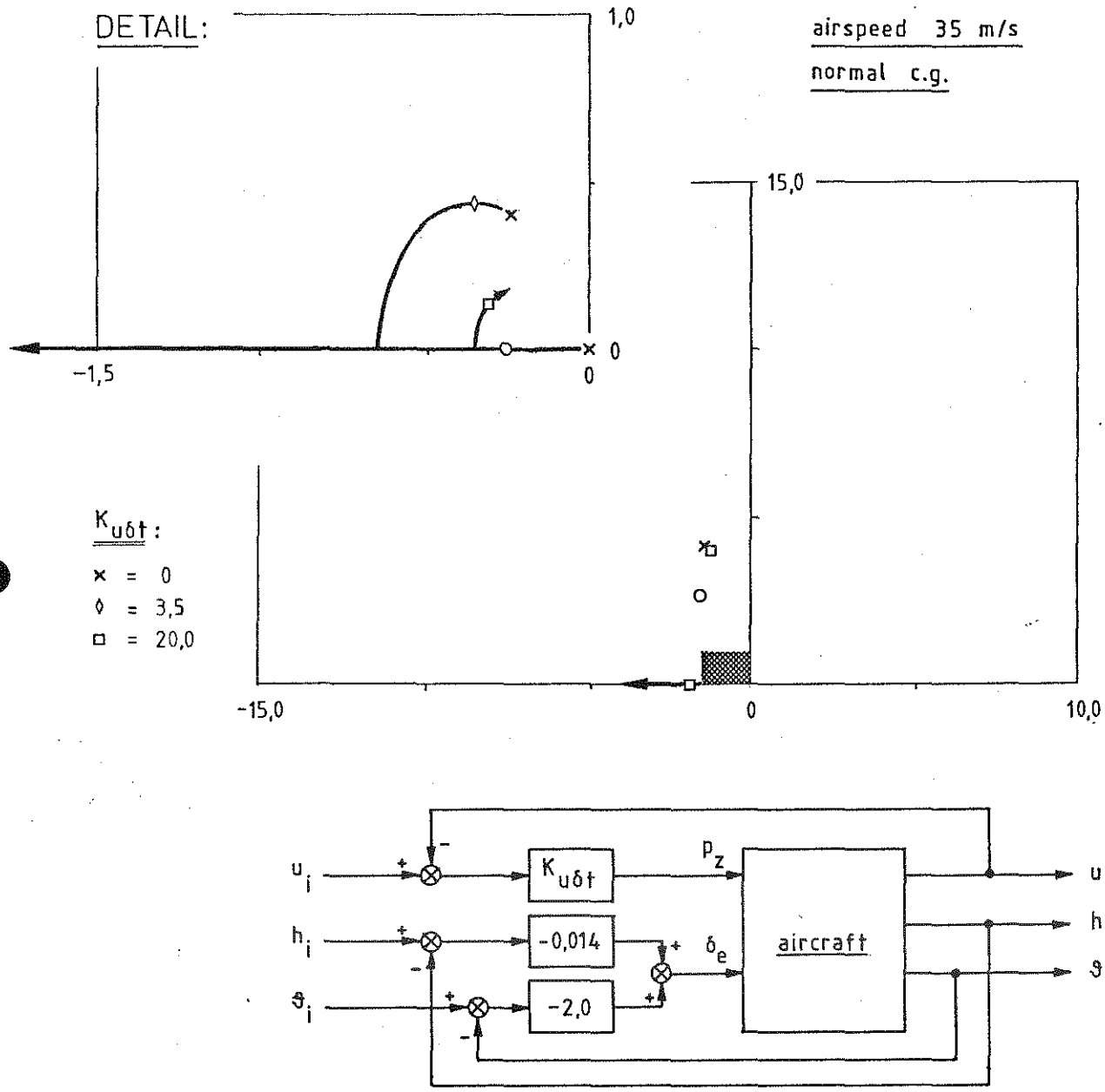

figure 7.3: Root locus for feedback of airspeed on throttle with $z_{\delta t}$ removed from the throttle input vector

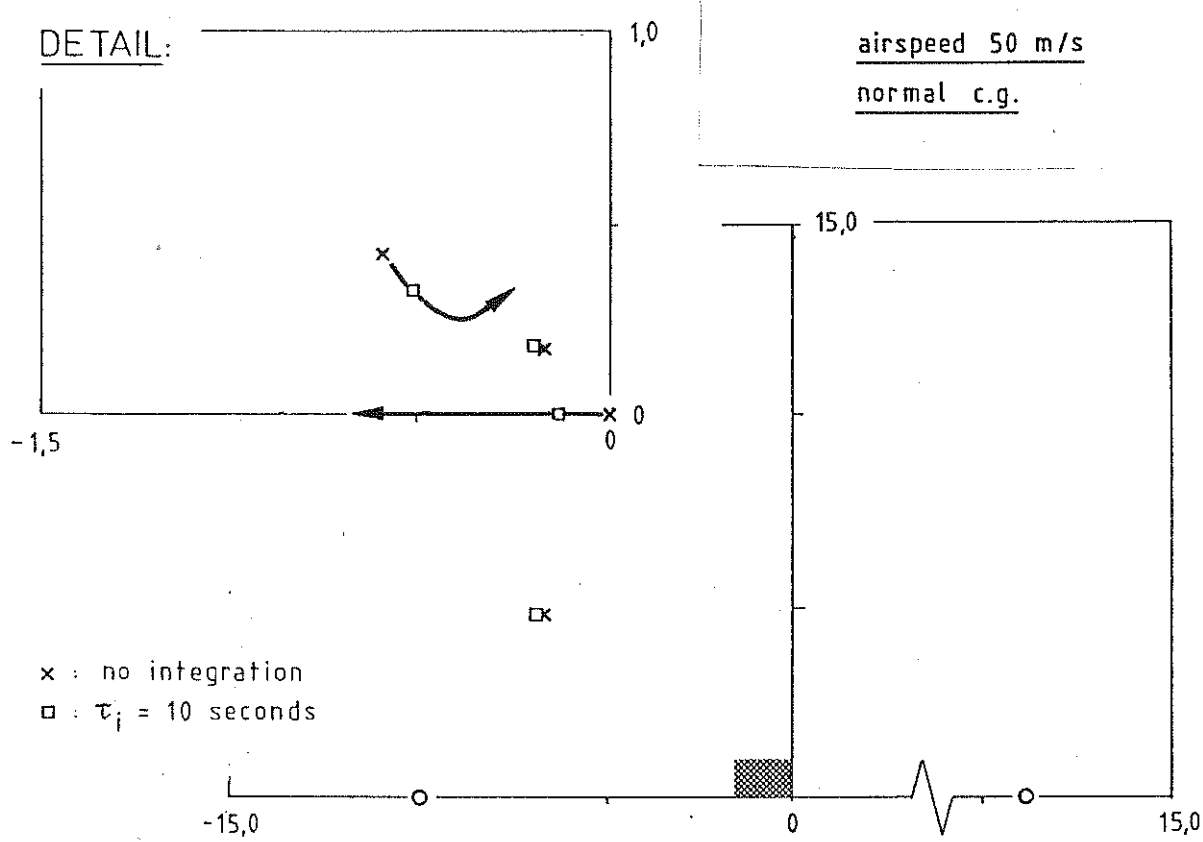

feedback on elevator as in figure 5.4 (a), with:

$K_{h\delta e} = -0.04 \cdot (1 + 1/\tau_i s)$

$K_{\gamma\delta e} = -5.0$

$K_{a_n\delta e} = -0.06$

$K_{q\delta e} = -0.5$

PI-feedback on throttle as in figure 6.3 (a) with:

$K_{e_{\delta t}} = 0.1$

$\tau_i = 5$ seconds

figure 7.4: Root locus for adding integrating action to the feedback of altitude on elevator

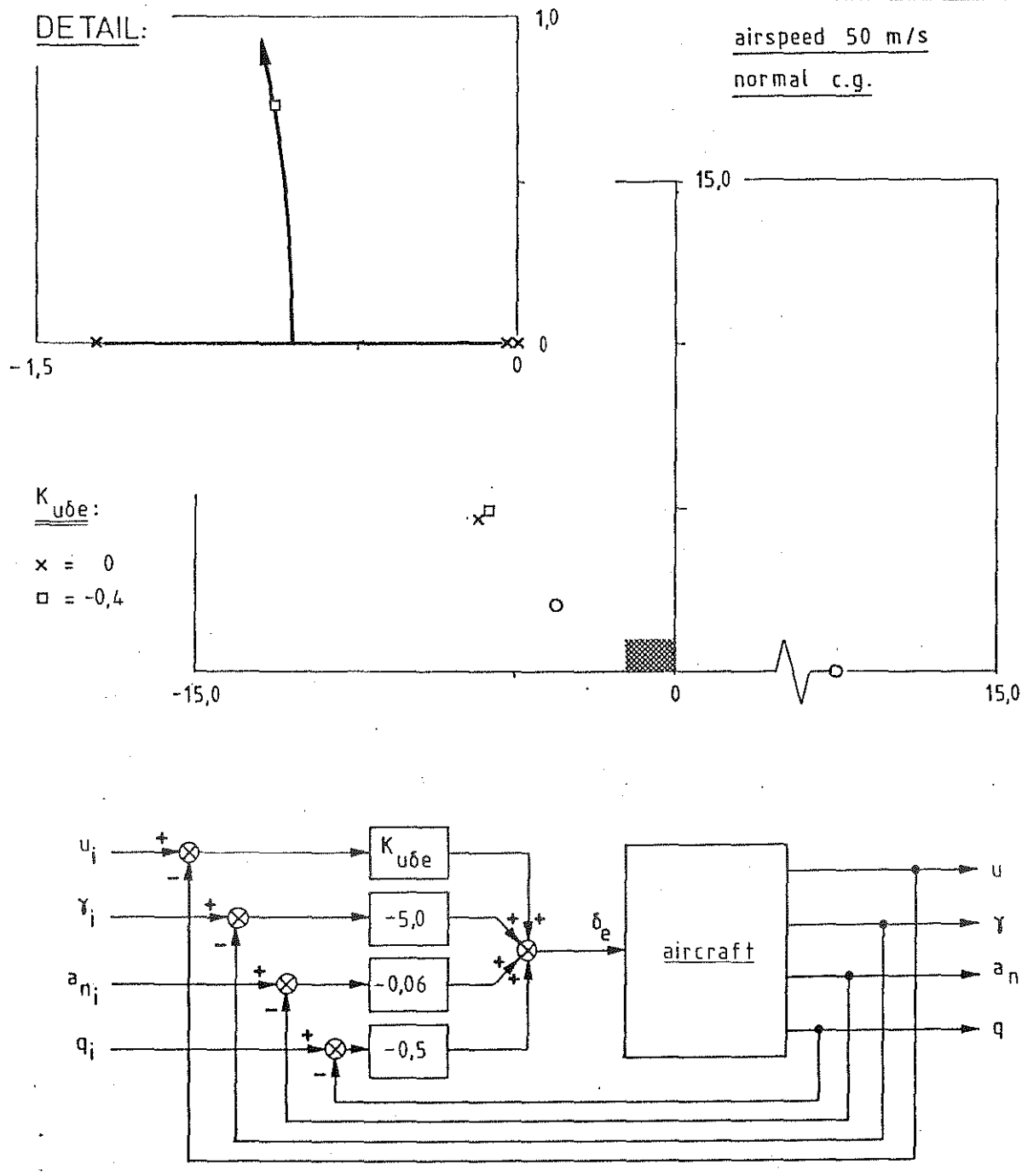

figure 7.5: Root locus for feedback of airspeed on elevator

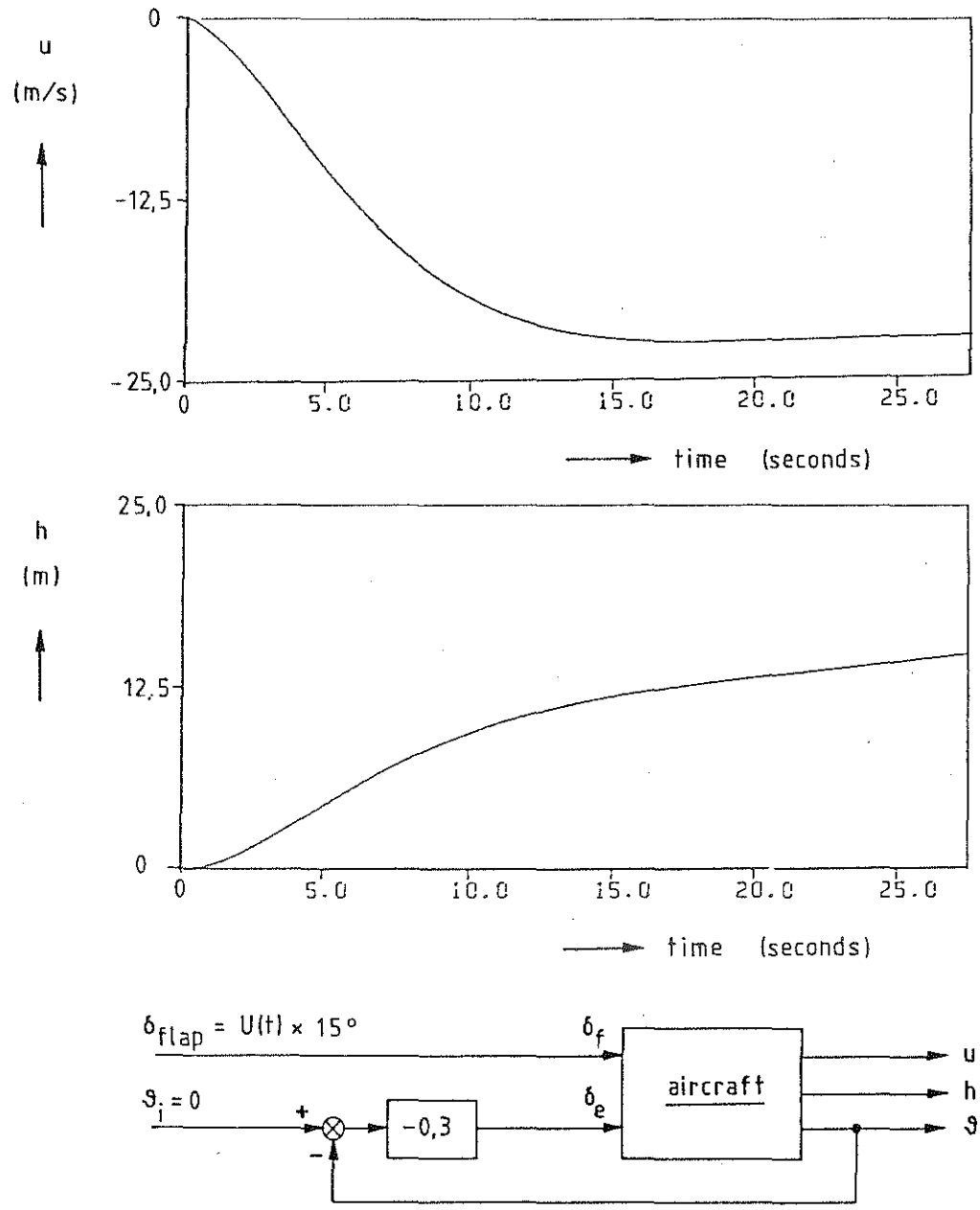

figure 8.1: Response of the 1968 Beaver model with modest phugoid damping to a step input on flap

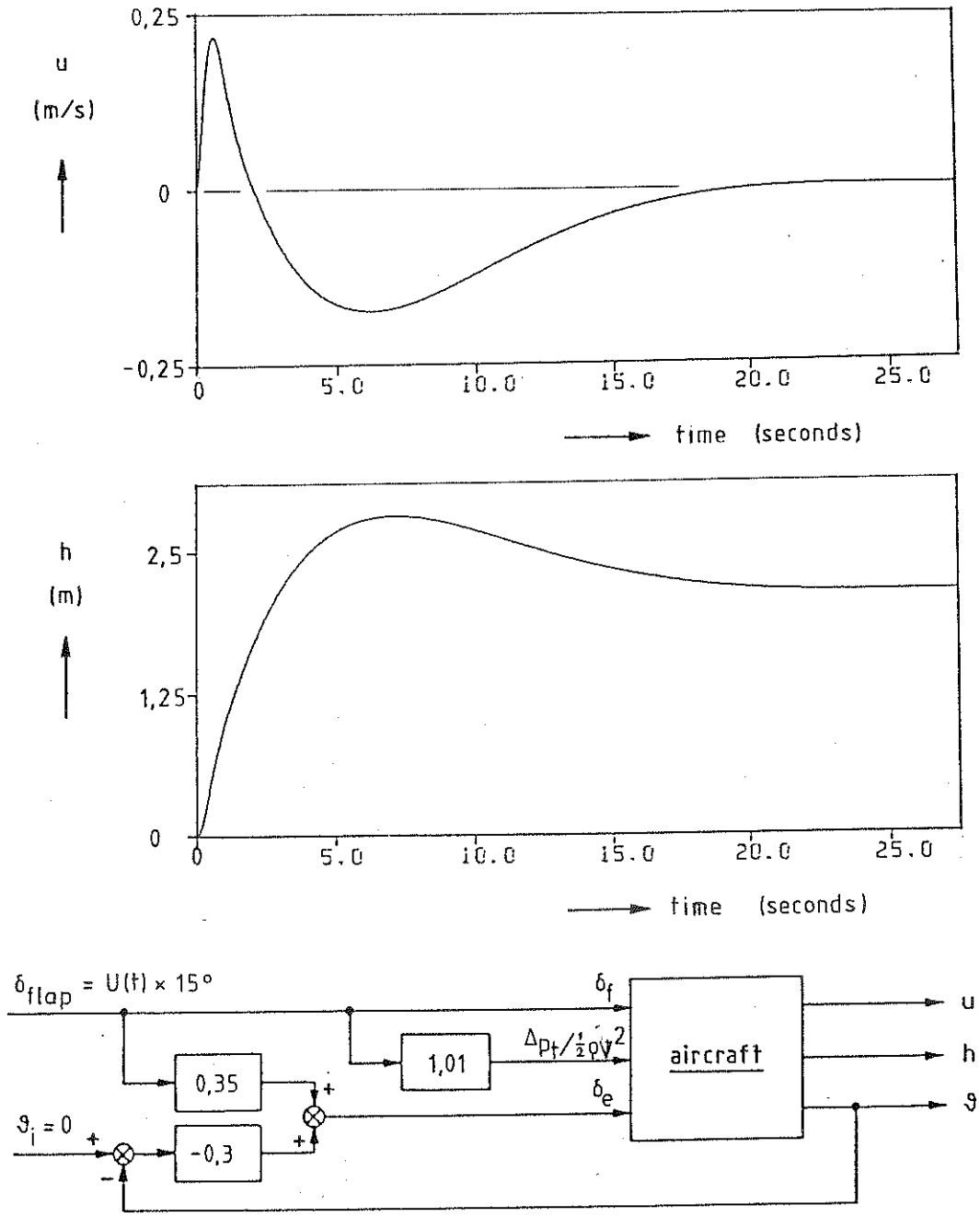

figure 8.2: Response of the 1968 Beaver model with modest phugoid damping with static compensation for flap effect to a step input on flap